Universidade de Aveiro
2008
Departamento de Engenharia Mecânica

Fábio Jorge Pereira Simões

Estudo da laminagem assimétrica na liga de alumínio 1050

Asymmetrical rolling of an aluminum alloy 1050

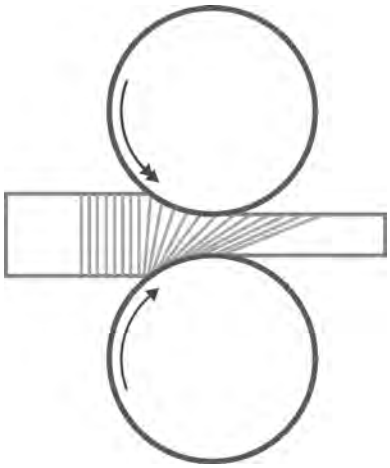

Universidade de Aveiro
2008
Departamento de Engenharia Mecânica

Fábio Jorge Pereira Simões

Estudo da laminagem assimétrica na liga de alumínio 1050

Asymmetrical rolling of an aluminum alloy 1050

Dissertação apresentada à Universidade de Aveiro para cumprimento dos requisitos necessários à obtenção do grau de Doutor em Engenharia Mecânica, realizada sob a orientação científica do Professor José Joaquim de Almeida Grácio, Professor Catedrático do Departamento de Engenharia Mecânica da Universidade de Aveiro, e do Professor José Manuel Ferreira Duarte, Professor Auxiliar do Departamento de Engenharia Mecânica e Gestão Industrial da Faculdade de Engenharia da Universidade do Porto.

Dissertation submitted to the University of Aveiro, Portugal, as the fulfillment of the necessary requirements for obtaining the PhD degree in Mechanical Engineering, and carried out under the supervision of Professor José Joaquim de Almeida Grácio, full professor of the Mechanical Engineering Department of the University of Aveiro, and professor José Manuel Ferreira Duarte, auxiliary professor of the Mechanical Engineering and Industrial Management Department of the Faculty of Engineering of the University of Porto.

FCT Fundação para a Ciência e a Tecnologia
MINISTÉRIO DA CIÊNCIA, TECNOLOGIA E ENSINO SUPERIOR Portugal

Bolsa de Doutoramento concedida pela Fundação para a Ciência e a Tecnologia (FCT), referência POSI/SFRH/BD/12649/2003

PhD scholarship granted by Fundação para a Ciência e a Tecnologia (FCT), reference POSI/SFRH/BD/12649/2003

dedicatória

dedico este trabalho à Diana, pelo que já passámos... e pelo nosso futuro!

o júri

presidente — Reitora da universidade de Aveiro

Doutor Frédéric Gérard Barlat
Full Professor, Pohang University of Science and Technology (POSTECH), South Korea;
Professor Catedrático Convidado da Universidade de Aveiro

Doutor Edgar Fernand Rauch
Investigador – Coordenador do Laboratoire GPM2 – Saint Marie d'Héres – France.

Doutor José Joaquim de Almeida Grácio
Professor Catedrático da Universidade de Aveiro.

Doutor José Manuel Ferreira Duarte,
Professor Auxiliar da Faculdade de Engenharia da Universidade do Porto.

Doutor Catalin Radu Picu
Professor Associado do Renssealaer Polytechnic Institute – Troy NY – USA.

Doutor Paulo António Firme Martins
Professor Catedrático do Instituto Superior Técnico da Universidade Técnica de Lisboa.

agradecimentos

Devo agradecer, em primeiro lugar, aos Professores José Grácio e José Duarte, pela oportunidade de desenvolver este trabalho de investigação, numa área cujo impacto no quotidiano é sobejamente reconhecido. A sua disponibilidade para o planemento de estratégias e discussão de resultados contribuiu decisivamente para o progresso do trabalho. O aconselhamento na fase de escrita da tese foi, sem dúvida, uma contribuição valiosa.

My thanks to Professor Frédéric Barlat, for the advices and support during the development of this work, including the chance of working at Alcoa Technical Center. This was one of the most valuable experiences I had in the last years. And also, I got the chance to see lots of snow...
Also my most sincere thanks to Doctor Jeong-Whan Yoon, who was one of the most supportive persons of this work. His friendship and suggestions were of outmost importance in critical stages of the investigation.

Aos meus colegas de investigação, Ricardo Sousa, Robertt Valente e Rui Cardoso, que me acolheram no grupo de investigação e sempre me apoiaram, quer com conselhos de ordem científica, quer com colaborações em trabalhos, mas sobretudo com um ambiente descontraído e indescritível. Desde as deslocações para a universidade, até aos almoços sempre interessantes, a boa disposição esteve sempre presente. Há coisas que não têm preço. Por isto, e para além da componente profissional, a minha passagem pelo Departamento de Engenharia Mecânica será sempre recordada com saudade.
Uma palavra especial também a duas pessoas: Gabriela Vincze, pelo apoio prestado em todo o trabalho, quer a nível de equipamentos, quer a nível de conselhos; e Prof. Francisco Queirós de Mello, pelo apoio e sugestões valiosas para a melhor prossecução dos trabalhos.

Aos professores, colegas de investigação e funcionários do Departmento de Engenharia Mecânica, um agradecimento sincero por me terem acolhido e integrado. Um ambiente de trabalho como este não é algo comum.

Agradeço também aos meus pais e à minha irmã, pelo apoio incondicional em todas as situações. Também à minha avó, por sempre torcer por mim!

Finalmente, o agradecimento mais significativo vai, sem dúvida, para a minha esposa, Diana, que partilhou este longo caminho comigo e sempre me apoiou, nos bons e maus momentos. Só nós sabemos as dificuldades que passámos, mas agora podemos olhar o futuro com outros olhos.

palavras - chave

ligas de alumínio, laminagem assimétrica, comportamento mecânico, textura cristalográfica

resumo

A investigação centrada na optimização do comportamento mecânico e formabilidade de chapas metálicas tem conhecido desenvolvimentos importantes ao longo dos últimos anos. A tendência de redução de peso dos componentes conformados, principalmente no que se refere à indústria automóvel, deve-se a questões não só de índole económica, mas também ecológica. Neste caso, um dos caminhos consiste em investigar novas ligas dentro dos aços já usados, possibilitando uma redução da espessura das chapas, mantendo ou melhorando a performance dos componentes. O caminho alternativo é o uso de outros materiais. Em alternativa ao aço, as chapas de alumínio apresentam potenciais vantagens em termos de peso e resistência à corrosão, mas a sua baixa formabilidade tem vindo a limitar o leque de aplicações.

A formabildade de chapas metálicas depende de um grande número de factores. O comportamento mecânico do material é apenas um deles. Neste trabalho pretende-se estudar o impacto da utilização de um processo alternativo para a produção de chapas, a laminagem assimétrica.

O processo de laminagem assimétrica pretende impôr tensões de corte ao longo da espessura da chapa, originando o desenvolvimento de componentes de textura específicos, designados componentes de corte, além de promover o refinamento de grão. Tais componentes de textura, não alcançáveis pelos processos tradicionais de fabrico, são apontados como benéficos para a melhoria substancial da formabilidade das chapas de alumínio. A diminuição do tamanho de grão resulta, também, num incremento da resistência mecânica. A principal meta é então a obtenção uma combinação optimizada entre formabilidade e resistência mecânica, não alcançável com os processos tradicionais de laminagem seguida de tratamentos térmicos. Neste trabalho, chapas de alumínio 1050 são sujeitas a laminagem assimétrica e posterior tratamento térmico, com o intuito de estudar o impacto do procedimento no desenvolvimento de texturas cristalográficas conducentes a uma melhoria na formabilidade da chapa, e no refinamento do grão, com vista a optimizar a resposta mecânica. São realizados ensaios experimentais para avaliação do impacto dos diversos parâmetros da laminagem no comportamento mecânico das chapas, e discutidas estratégias de optimização do processo de laminagem assimétrica.

keywords

aluminum alloys, asymmetrical rolling, mechanical response, crystallographic texture

abstract

Investigations focused on the optimization of the mechanical response and formability of sheet metal materials have experienced important developments over the past years. The reduction in weight of formed parts, especially on automotive industry, is sought not only because of economical factors, but also because of environmental issues. Because of this, some investigations are focused on the optimization of steel sheets, enabling a decrease in sheet thickness by increasing its resistance. The purpose is to obtain lighter components and yet as resistant as before, or more. An alternative way is to use other materials, such as aluminum alloys. These present a good potential for weight reduction, as well as advantages in terms of corrosion resistance, but their lower formability has imposed serious limitations to their widespread use.

Formability of sheet metals is related to a significant number of factors. The material's mechanical response is only one of them. The purpose of this work is to evaluate the influence of an alternative process for the production of sheets, the asymmetrical rolling. The asymmetrical rolling process intends to impose intense shear deformations across the sheet thickness, leading to the development of specific texture components, named shear texture components, as well as grain refinement. These shear texture components, not generated by conventional processing routes, are pointed out as beneficial for the improvement of the sheet's formability. The grain refinement will also improve the sheet's mechanical response. The main purpose is to obtain an optimized combination of strength and formability, not attainable by using conventional processing routes of rolling followed by annealing. In this work, 1050-O aluminum alloy sheets are asymmetrically rolled and annealed, aiming to study the effect of the rolling parameters on the development of shear texture components for improved formability, and grain refinement for optimization of the mechanical response. Mechanical tests are carried out, as a way to evaluate the effect of the asymmetrical rolling parameters on the sheets response. As closure, the results are discussed and optimization strategies for the asymmetrical rolling process are approached.

Table of Contents

List of Figures

List of Tables

Chapter 1 - Introduction

The importance of sheet metal forming industries in the main scope of industrial activities is nowadays not due to economic reasons only, but rather due to it's social and environmental impacts. Automotive and food packaging industries are two of the main branches of forming industries. Their growing importance lead to increased responsibility and awareness in social and, more recently, on environmental aspects. Since the beginning of the XX century, the development of the automotive industry lead the way to deep economic and social changes. Not being an initial concern, the environmental impacts of this industry first acquired importance by the oil crisis of the 1970's. From that time, increased efforts have been taken into reducing fuel consumption and gas emissions, first for economic reasons, then for environmental reasons. The reduction in weight of vehicles was identified as one of the ways to achieve this purpose. It was thus necessary to develop existing forming processes and materials. Increasing strength and reducing the thickness of sheets, while maintaining the desired formability, is the way to reduce vehicle mass while fulfilling all requirements.

1.1. Thesis motivation and objectives

The main purpose of the this work is to access the characteristics of asymmetrical rolling as an alternative mean to produce sheet metal with enhanced mechanical response. Being a derivation of the strip rolling process, already in use for many years in forming industries, asymmetrical rolling seems to have the potential to produce sheets with improved mechanical properties, namely an improved strength/formability compromise. This is especially important in the case of aluminum alloys, since their potential advantages in terms of weight reduction and corrosion resistance in vehicles are most of the times obliterated by their insufficient formability. Formability deficiency is related to a variety of reasons, ranging from springback problems to surface finish problems, but especially to their limited range of deformation before necking and consequent fracture and failure. These have been the reasons why steels are most widely used materials for the production of automotive bodies, for instance.

The main problems of aluminum alloys have been identified, as well as the majority of factors causing them. The crystallographic texture of aluminum is known to be one of the main factors controlling it's mechanical response, right after alloying. Grain size and morphology is also known to influence mechanical response. Optimizing texture, alloy content and grain structure has been the purpose of a large proportion of scientific production concerning metal forming in the last years.

Developing an alternative production method, having the potential to produce sheets with increased formability while meeting the requirements of productivity, safety and ecology is something many investigators have been seeking. As the primary sheet production method, rolling has significant impact on many of the material's properties. The type of deformation imposed leads to typical crystallographic textures, which in turn cause corresponding anisotropic response. Subsequent annealing treatments help tune textures to produce the desired formability / strength combination. But rolling followed by annealing was soon found not to be able to produce certain types of textures, found to be the best to achieve those purposes. {111}||ND texture components are produced in IF steels upon recrystallization. Given that such steels have high formability, these texture components were sought, as an attempt to increase forming limits of fcc metals as well. However, those texture components are not produced during conventional rolling, except in the sheet's surface where high friction conditions cause significant values of shear strain. This is why these texture components are designated “shear” texture components. Besides {111}||ND orientations (namely {111}<110> and {111}<112>), the {001}<110> and {112}<110> orientations are also shear texture components.

The main reason to study asymmetrical rolling is its ability to impose shear deformations on the sheet, which can promote the development of shear texture components throughout the entire sheet thickness. These texture components are said to enable an optimization of the sheet's properties [Kim, Lee, 2001]. Moreover, it is relatively easy to implement asymmetrical rolling mills to existing industrial facilities, thus minimizing costs.

1.2. Thesis organization

The thesis is divided in six chapters. After the current chapter, the thesis subjects are divided according to the following list:

- Chapter 2 describes the fundamentals of the conventional strip rolling of sheets, using an analytical approach. The main variables of the process and their influence on rolling power are analyzed. An analytical approach of the asymmetrical rolling is also proposed. The influence of the asymmetry factors is studied.
- Chapter 3 deals with the main issues regarding the formability of aluminum alloys, as well as the current state of the art concerning severe plastic deformation processes and especially asymmetrical rolling.

- Chapter 4 introduces the first rolling experiments performed. The main rolling variables are tested, having the sheet's mechanical response as the output. After this chapter, it is possible to identify the main issues and difficulties regarding asymmetrical rolling, providing valuable ground for the main set of experiments on chapter 5.
- Chapter 5 presents the main set of rolling experiments and the corresponding results. Texture analysis, tensile and shear testing, and also TEM observations are used to analyze the impact of the asymmetrical rolling process on AA1050-O sheets.
- Chapter 6 presents the conclusions derived from the studies, as well as directions for future steps on the investigation regarding asymmetrical rolling.

Chapter 2 - The strip rolling process

2.1. Introduction

Strip rolling is a particular case of rolling, in which the final metal part is intended to have a much greater dimension in width relatively to its thickness. The process promotes the reduction of the initial sheet thickness without significant amount of transverse deformation.

In this chapter, the strip rolling process will be briefly analyzed. The main concern is to identify the rolling process variables, their influence on rolling power, roll separation force and roll pressure distribution. This analysis will be later extrapolated for the case of asymmetrical rolling.

2.2. Strip rolling analysis

2.2.1. Basic concepts

The working rolls pull the sheet by friction to the gap between them, and the sheet is gradually compressed, decreasing in thickness as it advances, Figure 1. Due to geometric conditions, a sheet surface point at the entry of the rolls has lower velocity than the circumferential velocity of the rolls. As it advances, the sheet is pulled by friction and compressed. After the roll gap, the sheet surface velocity is greater than the roll circumferential velocity, since the sheet deforms in length as the thickness reduces.

$$\frac{V_{entrance}}{V_{exit}} = \frac{T_{exit}}{T_{entrance}} \quad (1)$$

Because of this, there is an intermediate point for which the sheet surface speed and the roll circumferential speed are equal. This is called the neutral point. Before the neutral point, the friction between the sheet surface and the rolls causes it to advance. After the neutral point, and since the velocity of the sheet is greater than the velocity of the rolls, the friction acts on the opposite direction. Thus, the balance of both sides causes the rolling process to work - Figure 1. The position of the neutral point varies with rolling conditions. When a larger reduction is imposed, the neutral point will move towards the exit side, causing an increase in friction and consequently an increase of the necessary rolling power.

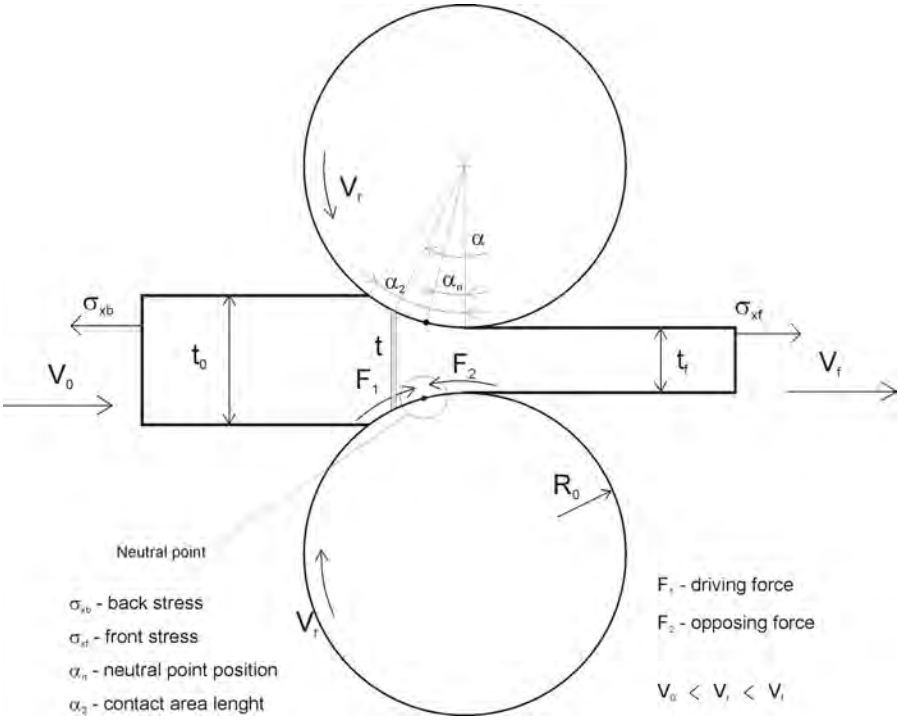

Figure 1: The rolling process and parameters. [Avitzur, 1983]

The maximum achievable reduction is limited by two factors: when the rolls start to slip over the sheet because the reduction imposed causes the neutral point to move towards the exit; and when the reduction imposed causes excessive pressure on the rolls, originating bending and flattening.

For the analysis of the rolling process, the independent process variables need to be identified. The list below contains the most important:

- E – modulus of elasticity of the rolls;
- m, μ – friction factor, or friction coefficient;
- R_0 – roll radius;

- t_0, t_f – sheet thickness at the entrance and at the exit of the rolls – can be replaced by the reduction ratio $r=t_f/t_0$;
- V_r – roll circumferential velocity;
- σ_0 – flow strength of the sheet;
- σ_{xf}, σ_{xb} – front and back tensions applied to the sheet.

The purpose will be to access the influence of the independent process parameters on the dependent ones, such as the entrance and exit velocity of the sheet (V_0, V_f) and the position of the neutral point. From these calculations it would be also possible to derive expressions for rolling pressure, torque and power.

2.2.2. The friction-hill curve. Influencing parameters

Using a free body equilibrium (or slab) analysis [Von Karman, 1925],[Siebel,1941], it is possible to derive the differential equations that describe the relationship between independent variables and dependent ones - Figure 2.

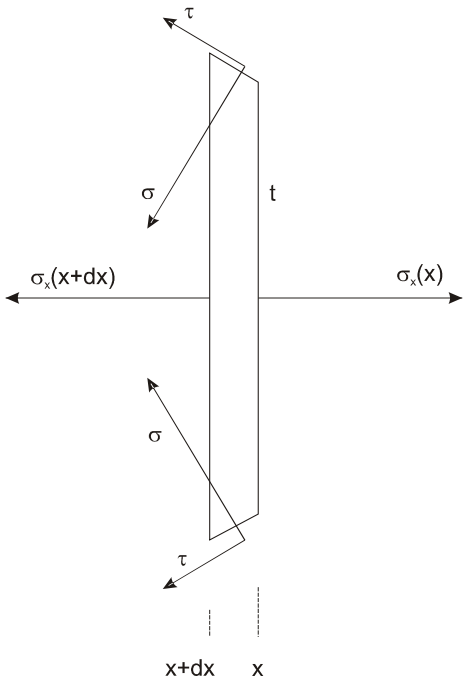

Figure 2: Slab analysis for determination of the equilibrium equation. [Avitzur, 1983]

In order to derive the balance equation on the slab, we consider the following conditions:

- friction stress τ, acting on the slab upper and lower surfaces;
- normal stress σ, acting also on the slab upper and lower borders;
- horizontal stresses $\sigma_x(x)$ and $\sigma_x(x+dx)$, as a result of the neighbor slabs.

Writing the equilibrium equation for the slab, the differential equation that describes stresses on the sheet from the entrance to the exit is obtained. After integration, and applying the friction (Coulomb model, $\tau=\mu\sigma$) and boundary conditions, it is then possible to derive the roll pressure distribution. Since there are many methods to solve the differential equation, an example of solution for roll pressure along the contact line between the sheet and the rolls is presented [Avitzur, 1983]:

For the exit side of the neutral point, the pressure distribution p is:

$$\frac{p}{2l/\sqrt{(3)}\sigma_0}=\left[1+\frac{2}{A^2}-\frac{\sigma_{xf}}{2l/\sqrt{(3)}\sigma_0}\right]e^{A\omega}-\frac{2}{A^2}(1+A\omega) \tag{2}$$

and for the entrance side of the neutral point,

$$\frac{p}{2l/\sqrt{(3)}\sigma_0}=\left[1+\frac{2}{A^2}(1-A\omega_0)-\frac{\sigma_{xb}}{2l/\sqrt{(3)}\sigma_0}\right]e^{A(\omega-\omega_0)}-\frac{2}{A^2}(1-A\omega) \tag{3}$$

where

$$A=\frac{2\mu}{\sqrt{(t_f/R_0)}} \qquad \omega=\tan^{-1}\left[\sqrt{(R_0/t_f)}\tan\alpha\right] \qquad \omega_0=\tan^{-1}\left[\sqrt{(R_0/t_f)}\tan\alpha_2\right] \tag{4}$$

The previous equations are plotted on Figure 3, where the abscissa is the relative distance along the x axis, and the ordinate is the roll pressure. Constant values of roll diameter R_0, rolling reduction $r = t_f/t_0$ and friction μ were used, and several values for front and back tension (σ_{xf}, σ_{xb}) are plotted as input parameters. Pressure and tension values are normalized relatively to yield stress by the factor $2/(\sqrt{3}\ \sigma_0)$. Note that the flow stress value is considered to be constant, which is in better agreement with hot rolling. In the case of cold rolling, the strain hardening effect is not negligible, and thus the flow stress at the exit side would be higher than at the entrance. Also note that the lines departing from the left side of the plot correspond to equation 3 (entrance side), and the right side curves correspond to equation 2. The curves derived from identical values of front and back tension always cross, and the crossing point is the neutral point.

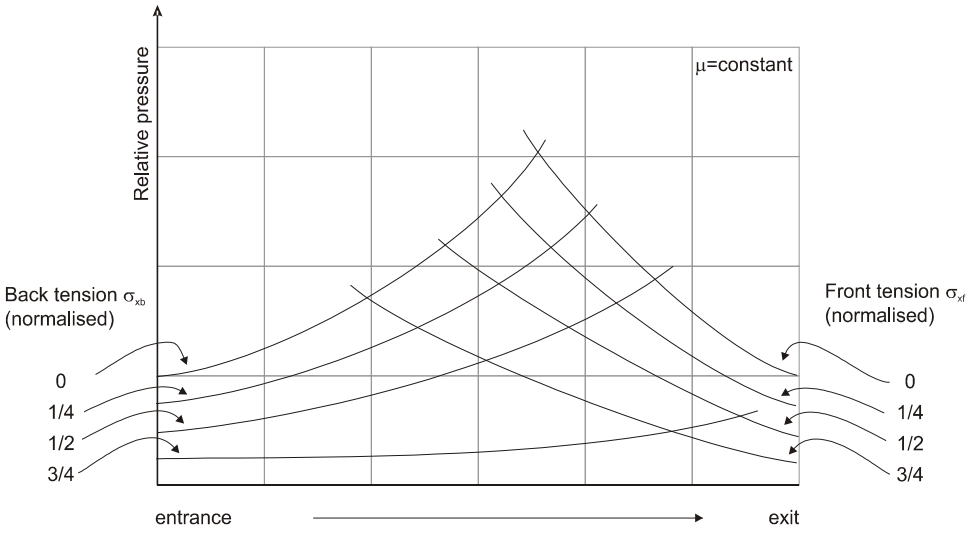

Figure 3: The friction-hill curve in rolling. Values for pressure, front and back tension are normalized by the factor $2\sqrt{3}\sigma_0$. [Avitzur, 1983]

Observing Figure 3, it is possible to conclude that imposing increasing values of front and/or back tensions causes the roll pressure to decrease. To calculate the roll separation force, the roll pressure expressions (2, 3) can be integrated along the contact arc between the sheet and the rolls. A good approximation of the roll separation force is derived from the area under the friction- hill curve. Since an increase in either the front or back tensions causes the roll pressure to decrease, it is immediate to conclude that the roll separation force will decrease as well. Figure 3 also shows that an increase in back tension will move the neutral point toward the exit, whereas an increase in front tension will move it toward the entrance.

Figure 4 shows the influence of friction conditions on the roll pressure distribution. As friction values decrease, the roll pressures decrease as well. The neutral point moves toward the exit. When the neutral point reaches the exit, the rolls will start to skid over the sheet, and rolling becomes impossible. Because of this, there is a minimum amount of friction required for rolling to take place.

The influence of thickness reduction is shown on Figure 5. As *r* values increase, the contact length between the sheet and the rolls increases. This causes the total amount of friction stress to increase, having a similar effect to the increase of friction coefficient.

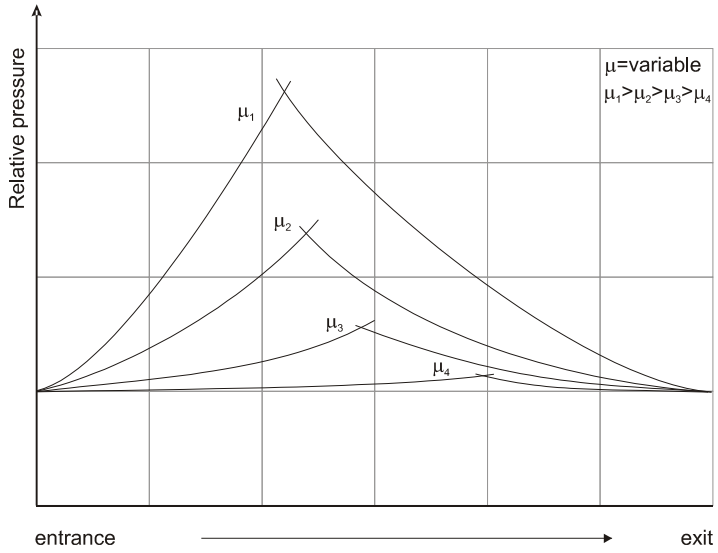

Figure 4: Influence of friction conditions on the roll pressure.[Avitzur, 1983]

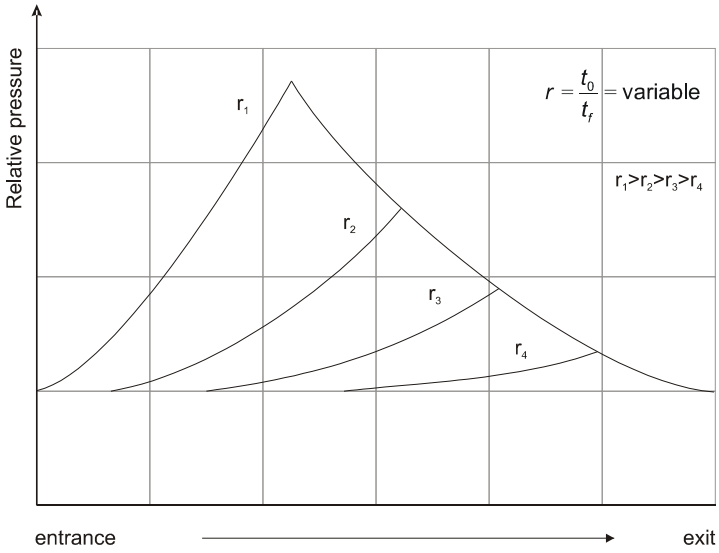

Figure 5: Influence of thickness reduction ratio on roll pressure.[Avitzur, 1983]

2.2.3. Rolling power and torque

The necessary rolling power can be derived from the torque, which in turn can be found by integrating friction stresses along the contact length. These friction stresses depend on the velocity field. At the entrance side, it was seen that the velocity V_0 of the sheet is smaller than the circumferential velocity V_r of the rolls. Here, friction contact between the sheet and the rolls will be responsible for rolling to take place. At the neutral point, sheet and roll velocities are equal. After the neutral point, the sheet's velocity V_f will be higher than V_r.

Because of this, at the exit side, friction will benefit the rolling process. The torque balance derived from the previous two zones will correspond to the necessary rolling torque. As a consequence, the torque will be greatly dependent on the position of the neutral point.

The following analysis is an upper bound approach [Avitzur, 1964], in which is the rolling torque and power are derived as a function of the neutral point position. The contact length α_2 (see Figure 1can be derived from the geometry by:

$$\alpha_2=\sqrt{\frac{t_f}{R_0}}\sqrt{\frac{t_0}{t_f}-1} \tag{5}$$

In the calculations, it is assumed that this length is small. Having into account the velocity distribution along the contact length, the rolling power *J* can be described by the following expression, as a function of the neutral point position α_n [Avitzur, 1983]:

$$J=\frac{2}{\sqrt{3}}\sigma_0 V_r(A(B+C)+D) \tag{6}$$

where:

$$\begin{aligned} &A=(1+\frac{R_0}{t_f}\alpha_n^2) \qquad B=\ln\frac{t_0}{t_f}+1/4\sqrt{\frac{t_f}{R_0}}\sqrt{\frac{t_0}{t_f}-1}+\frac{\sigma_{xb}-\sigma_{xf}}{2/\sqrt{3}\sigma_0} \\ &C=m\sqrt{\frac{R_0}{t_f}}\left[2\tan^{-1}\sqrt{\frac{R_0}{t_f}}\alpha_n-\tan^{-1}\sqrt{\frac{t_0}{t_f}-1}\right] \qquad D=m\frac{R_0}{t_f}(\alpha_2-2\alpha_n) \end{aligned} \tag{7}$$

From this expression it is possible to plot the required power as a function of the relative neutral point position α_n/α_2, having the friction value *m* as parameter - Figure 6. It is possible to observe that for high enough values of friction, there is a local minimum value for power, not considering negative values for the neutral point position.

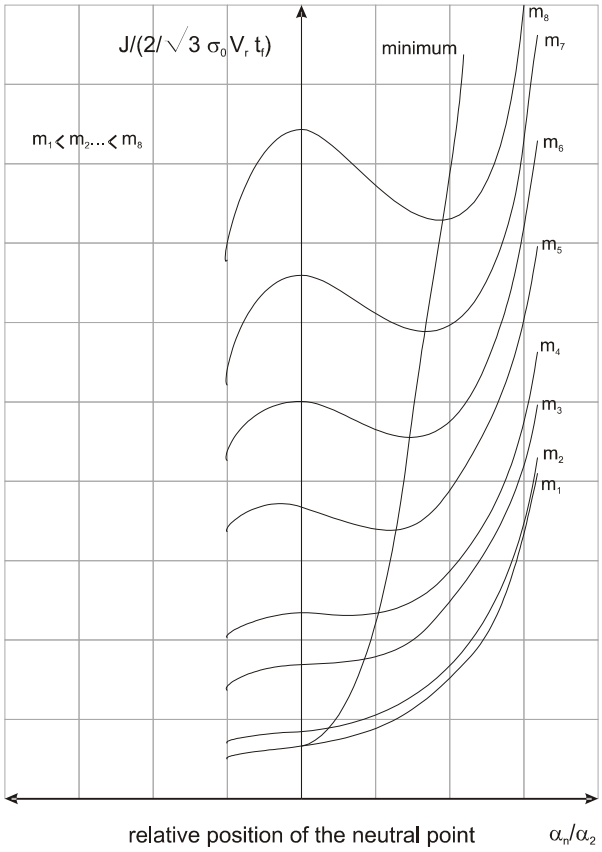

Figure 6: Power demand as a function of the neutral point position. When friction is high enough, there is a minimum value for power, considering the neutral point position to be positive.[Avitzur, 1983]

2.2.4. Symmetry disturbance

The analysis presented above assumes symmetry on the rolling process. The rolls are considered to have the same rotational speed, the rolls / sheet contact zones on the upper and lower sides are considered to have the same friction conditions. Consequently, pressure distribution and neutral point position are symmetric relatively to the mid-thickness plane of the sheet. Though these assumptions provide a valuable ground for the study of rolling, it is also important to be aware of the real conditions, and how these conditions affect the predicted results.

Since the upper roll is above the sheet, and the lower roll is under it, lubrication conditions are necessarily different. This leads to different friction conditions. There may be also differences in roll speeds, or speed fluctuations, eccentricity, and surface roughness. All of these factors disturb symmetry. For instance, if friction conditions are, for some reason, different on the upper and the lower contact zones, the neutral point position will be different on each one. The rolling pressure

distribution will be affected, which in turn, will affect the rolling torque. Even though the total torque (upper roll + lower roll) is nearly constant, the difference in friction may even cause one of the rolls to oppose the rolling action (negative torque).

Given a negative torque for the lower roll, its circumferential velocity at the contact zone will be smaller than the sheet's, thus opposing the rolling operation. Thus, there will only be an opposing force at the lower roll, causing the neutral point to be displaced toward the entrance. On the upper roll, and since we consider the total torque to remain nearly constant, the torque and hence the circumferential speed will have to be higher. The upper roll will be responsible for the entire rolling effort, compensating for the negative torque on the lower roll. So, its circumferential speed will be higher than the sheet's entrance speed throughout the entire contact zone, and the neutral point will be displaced toward the exit, Figure 7. The velocity differential will cause shear stresses to appear throughout the sheet thickness.

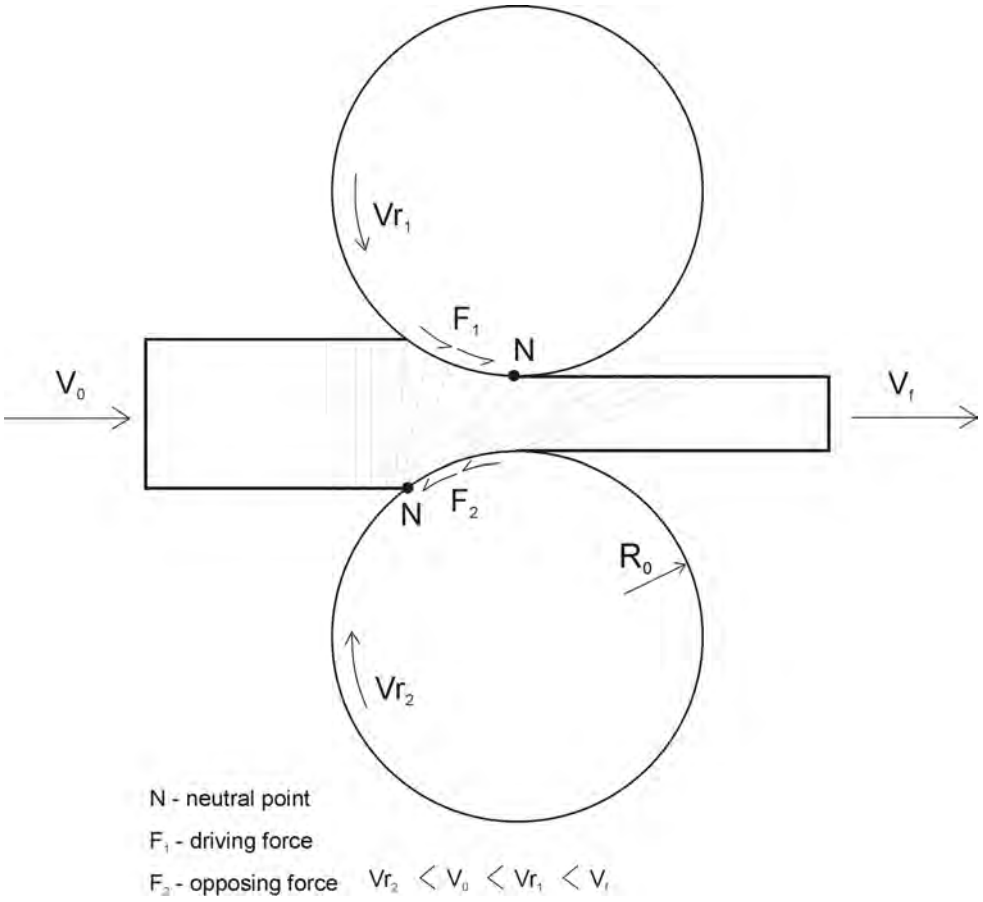

Figure 7: Symmetry disturbance by friction conditions. The neutral point position is no longer symmetric, causing shear stresses throughout the sheet thickness.

Consider the division of the system into 2 parts, the upper and lower half - Figure 8. Shear stresses at the mid-surface (S_1, S_2) will have to be considered, to maintain stress compatibility. We can then think about these shear stresses as front and back tensions applied to the lower and upper halves of the sheet, respectively. Having these conditions in mind, and since the presence of front or back tensions will decrease the roll pressure, we can reach the conclusion that asymmetrical conditions in rolling provide a decrease in the rolls separation force.

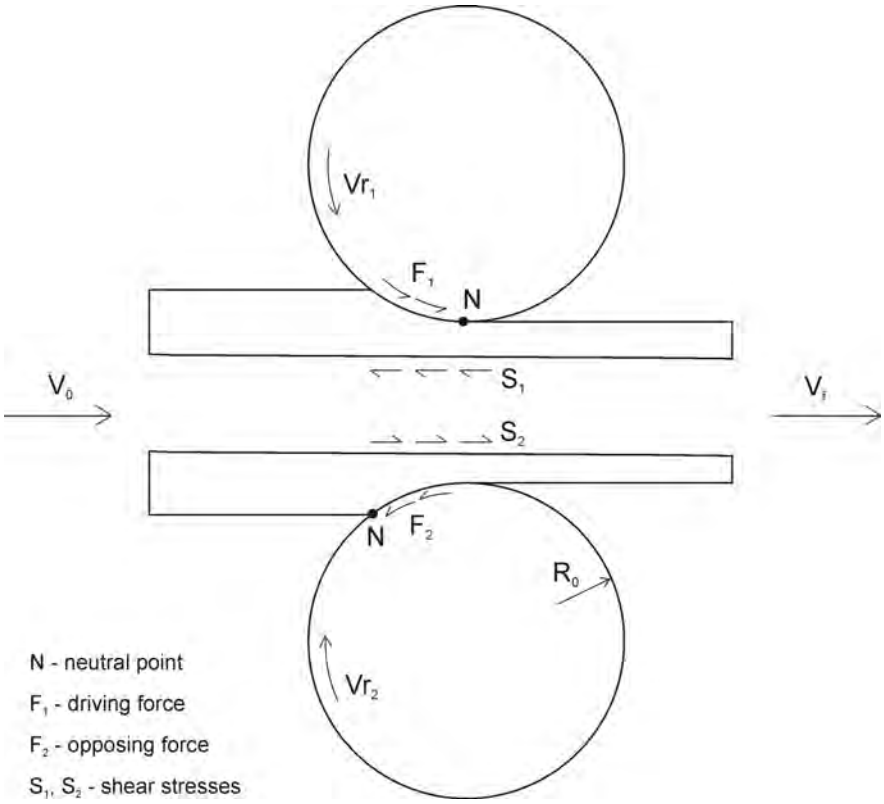

Figure 8: Asymmetric conditions in rolling. Division of the rolling system into 2 halves. The neutral point position is no longer symmetric. The load on the rolls is substantially reduced on asymmetric rolling.

2.3. The asymmetrical rolling process

Asymmetrical conditions cause instabilities on the rolling process, since the sheet tends to curve away from the faster roll at the exit, which can cause problems when it has to enter another rolling mill afterwards. But asymmetrical conditions may also be created intentionally, in order to lower the roll separation force or modify surface finish. Using different upper and lower roll speeds or diameters, or even using a stationary roll or dead block, it is possible to impose such conditions - Figure 9.

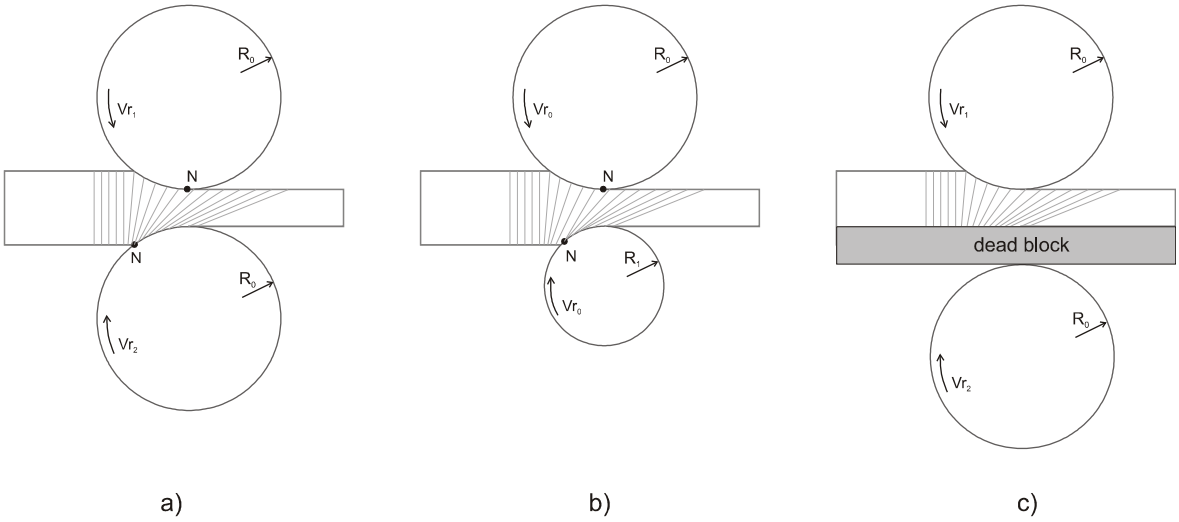

Figure 9: Asymmetrical rolling types: a) different roll speeds; b)different roll diameters; c) using a dead block.

Early analytical solutions for the asymmetrical rolling conditions were concerned about estimating its influence on rolling torque, roll separation force, and especially sheet curvature at the exit. Sachs [1947] first identified the region of cross shear, due to the fact that friction forces act on opposite directions in that zone. Johnson [1966] developed a model to predict strip curvature after asymmetrical rolling. Later studies used FEM analysis [Richelsen, 1994, 1997] in order to access the influencing factors in asymmetrical rolling.

The use of analytical methods provides a faster way to access the influence of asymmetric rolling factors (roll speed ratio, reduction per pass, friction) on the resultant sheet geometry and also on the required rolling power and roll separation force, avoiding the need to perform time-consuming FE simulations. Nevertheless, FE methods present their own advantages in terms of accuracy and flexibility.

The analysis of the asymmetrical rolling process presented here is the one used by Salimi [2002], which is derived from the slab method already used on the conventional rolling, with some modifications. He compared his analytical results with the experimental ones obtained by Hwang [1997], and a good approximation was observed. The results shown here are concerned only with rolling force and rolling torque as a function of rolling reduction, friction and roll speed ratio, despite the fact that strip curvature is the main motivation of Hwang's work.

Salimi uses the following assumptions: plane strain conditions, rolls behave as rigid bodies, and the sheet / rolls contact length is small, when compared to the circumference of the rolls. The rolls are considered to have different radii, and thus, different circumferential speeds. As seen previously,

the sheet's speed increases from the entrance to the exit of the rolls' gap, as its thickness decreases. There is a point (in fact, a small length) in the middle where the roll and sheet speeds are equal, called the neutral point. In this case, since the rolls have different speeds, the upper and lower neutral point locations are not symmetric.

The contact length is thus divided in three zones (figures 10 and 11): zone I is considered to be located from the entrance of the rolls up to the nearest neutral point. Zone II is the cross-shear zone, located between the two upper and lower neutral points. Zone III is the length between the second neutral point and the exit.

In Zone I, the sheet's speed is lower than the circumferential speed of each roll. The friction forces act forward, causing the sheet to enter the roll gap. In Zone III, since the sheet's thickness has decreased, its speed increases and becomes higher than the rolls' speeds. In this zone, friction is contrary to the sheet's movement. In Zone II, the upper roll runs slower than the upper face of the sheet (since the neutral point 1 is behind), and thus friction acts on the opposite direction of the sheet's movement.

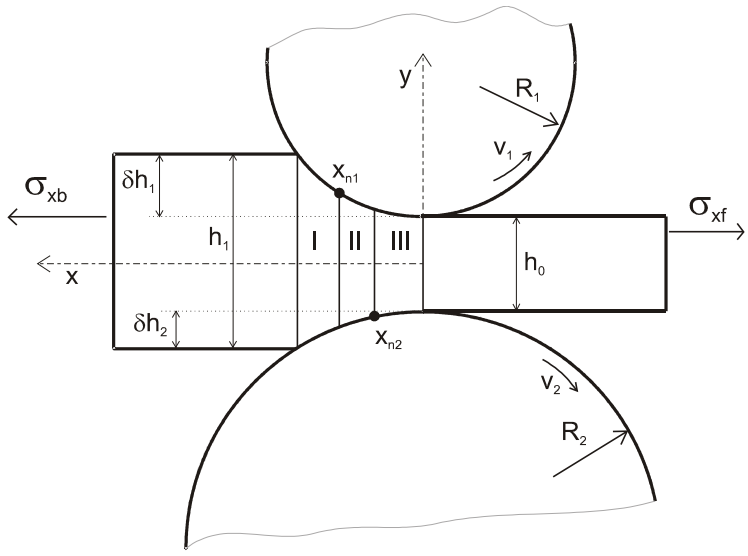

Figure 10: Geometry definition at the contact zone [Salimi, 2002].

But on the lower side, the roll speed is still higher than the sheet's speed (the neutral point 2 is still ahead). So, friction forces are forward, promoting the sheet's entrance. For this zone, friction forces act on opposite directions on the upper and lower sides of the sheet, causing shear stresses -Figure 11.

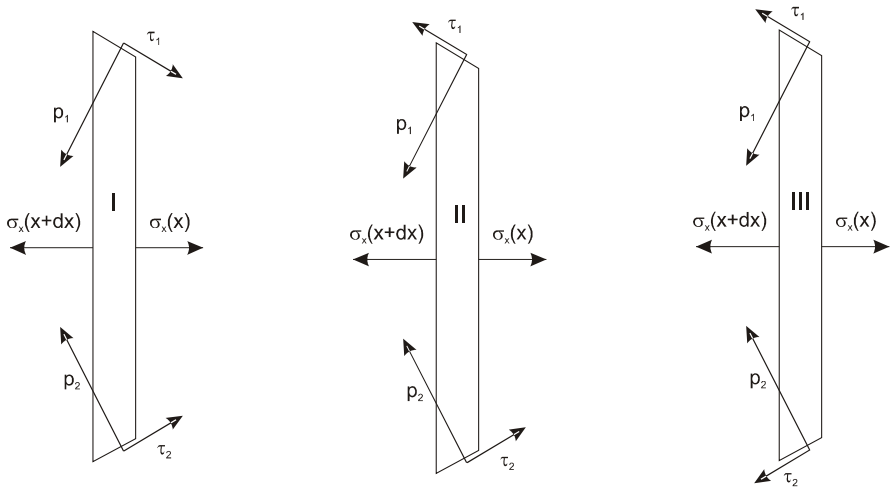

Figure 11: Slab analysis for asymmetrical rolling [Salimi, 2002].

By writing the equilibrium conditions of three zones, it is possible to obtain a differential equation describing the roll pressure p as the material passes trough the roll gap. By integration, the solution of this equation can be obtained, for each zone. The general solution is [Salimi, 2002]:

$$p = Ax - B\ln(x^2 + h_0 R_m) - \frac{E}{\sqrt{h_0 R_m}}\tan^{-1}\frac{x}{\sqrt{h_0 R_m}} + C_i \tag{8}$$

where:

$$A = R_m\left(\frac{m_1}{R_1^2} + \frac{m_2}{R_2^2}\right)\frac{\sigma_0}{\sqrt{3}} \qquad B = \left(\sqrt{1 - m_1^2 c_1^2} + \sqrt{1 - m_2^2 c_2^2}\right)\frac{\sigma_0}{\sqrt{3}}$$

$$E = R_m h_0 A - \tau_e R_m \qquad R_m = \frac{2R_1 R_2}{R_1 + R_2} \qquad m_1; m_2 - \textit{friction factors for roll 1 and roll 2} \tag{9}$$

$$\tau_e = \tau_1 + \tau_2 \rightarrow \textit{Zone I} \qquad \tau_e = \tau_1 - \tau_2 \rightarrow \textit{Zone II} \qquad \tau_e = -\tau_1 - \tau_2 \rightarrow \textit{Zone III}$$

Values for A, B and E are related to zones I, II and III. They will be added subscripts 1-3 for proper identification. The constant Ci is derived from the boundary conditions on each zone. This means that there will be three equations describing pressure distribution along the three zones, pI, pII and pIII, in which there will be three different C formulas, C1, C2 and C3. As a reference, those formulas are presented next.

$$C_1 = \sigma_{xb} - B - A_1 l + B\ln(l^2 + R_m h_0) + \frac{E_1}{\sqrt{R_m h_0}}\arctan\frac{l}{\sqrt{R_m h_0}} \tag{10}$$

$$C_3=\sigma_{xf}-B(1-\ln(R_m h_0)) \tag{11}$$

$$C_2=(A_2-A_3)x_{n2}+\frac{E_3-E_2}{\sqrt{R_m h_0}}\arctan\frac{x_{n2}}{\sqrt{R_m h_0}}+C_3 \tag{12}$$

where, considering $v_1 \leq v_2$, values for A_2 and E_2 are:

$$A_2=-R_m\left(\frac{m_1}{R_1^2}-\frac{m_2}{R_2^2}\right)\frac{\sigma_0}{\sqrt{3}} \qquad E_2=R_m h_0 A_2-R_m \tau_{e2} \qquad \tau_{e2}=(m_2-m_1)\frac{\sigma_0}{\sqrt{3}} \tag{13}$$

Formulas for C_2 have the position of the neutral point x_{n2} as unknown. Both x_{n2} and x_{n1} could be obtained by considering the boundary condition $p_I = p_{II}$ at x_{n1}. Adding the integral of roll pressure distribution along the three zones, the total roll separation force can be obtained. The rolling torque can be calculated by integrating the friction stresses along the contact length on the upper and lower rolls, multiplied by each roll radius. Multiplying torque by the rolls angular velocities we obtain the necessary rolling power. Using this analytical approach, it is possible to plot the total rolling force and rolling torque as a function of the reduction per pass, friction conditions and roll speed ratio. Results from this model are shown next.

Figure 12 shows the influence of the roll speed ratio on the total rolling force. Analyzing the figure, it is possible to confirm that:

- the total rolling force decreases as the speed ratio increases;
- the total rolling force increases when higher reduction values are imposed.

These conclusions were already predicted in the previous section. Figure 13 shows the influence of the same variables on the rolling torque. By observing the figure, it becomes clear that the rolling torque decreases as roll speed ratio increases. Reduction in thickness has the contrary effect, it causes the torque to increase significantly. This may lead to the conclusion that asymmetrical rolling is easier to perform than conventional rolling, since the rolling force and torque decrease. It should be noted, though, that if in the case of roll separation force such statement is true, in the case of rolling torque it can be deceiving.

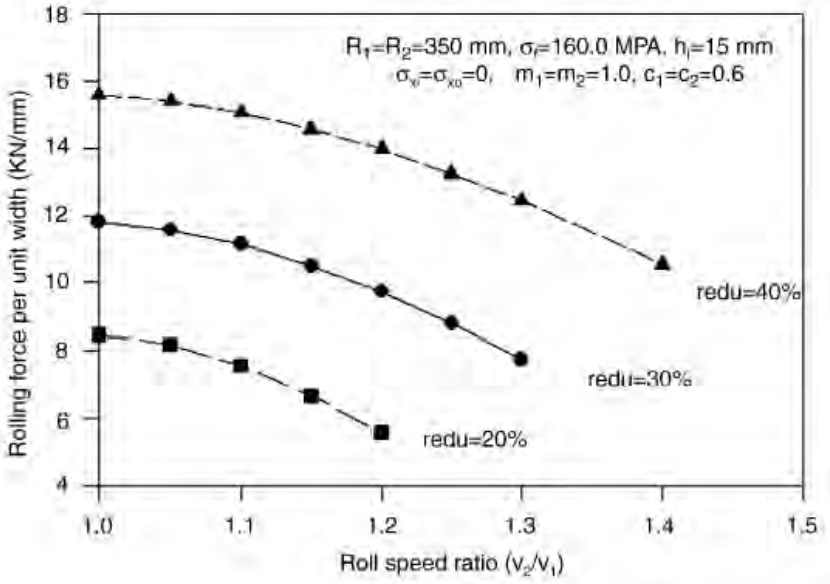

Figure 12: Influence of roll speed ratio on total rolling force, for various thickness reduction values [Salimi, 2002].

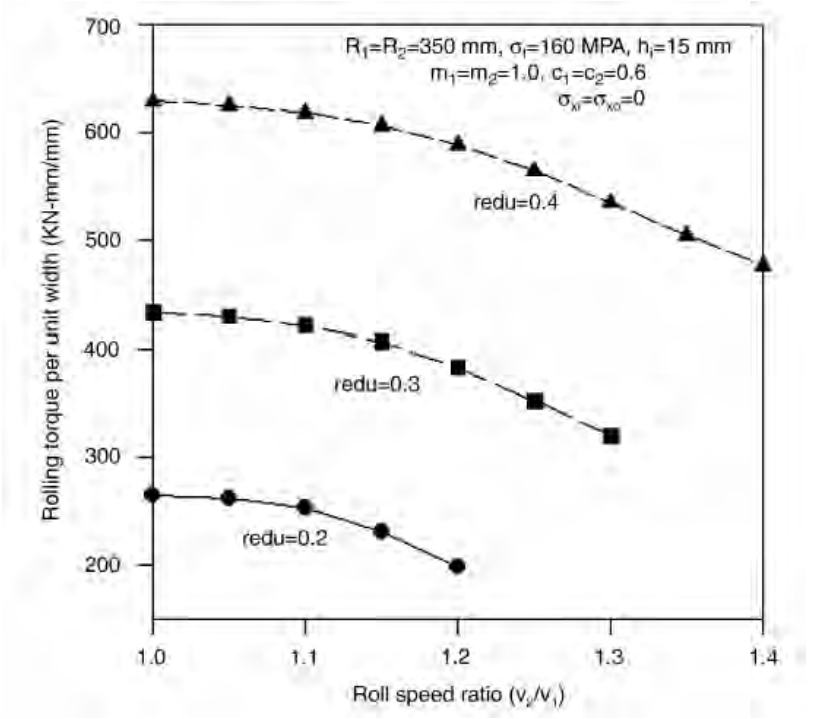

Figure 13: Influence of roll speed ratio on rolling torque, for several values of reduction in thickness [Salimi, 2002].

The necessary rolling torque derives from the balance between friction stresses acting on the upper and lower rolls, Figure 14. In case of symmetric conditions, the friction stresses between the entrance and the neutral point oppose the rolls movement, whereas the friction stresses acting from the neutral point to the exit promote it. In imposed asymmetric rolling conditions, the neutral point position is different on the upper and lower rolls. If the upper roll has greater speed, its neutral point will be offset towards the exit. Similarly, on the slower roll the neutral point will be positioned towards the entrance. For this roll, the contact length in which the roll circumferential speed is higher than the sheet surface is smaller than the length in which that speed is smaller. The torque balance, in this case, is negative, and the slower roll is actually opposing the rolling action, in order to maintain its speed. This means that the upper (faster) roll will have to provide the hole rolling torque. The rolling torque decreases in asymmetrical rolling, but it will have to be supplied by one engine only.

In the beginning, the study of asymmetrical rolling was focused on its detrimental effects on sheet geometry, and rolling efficiency. But later, asymmetrical rolling was recognized as an opportunity to modify the sheets' properties, by taking advantage of the shear stresses created. Imposing shear stresses on the sheet's plane has two purposes: modification of texture and grain refinement.

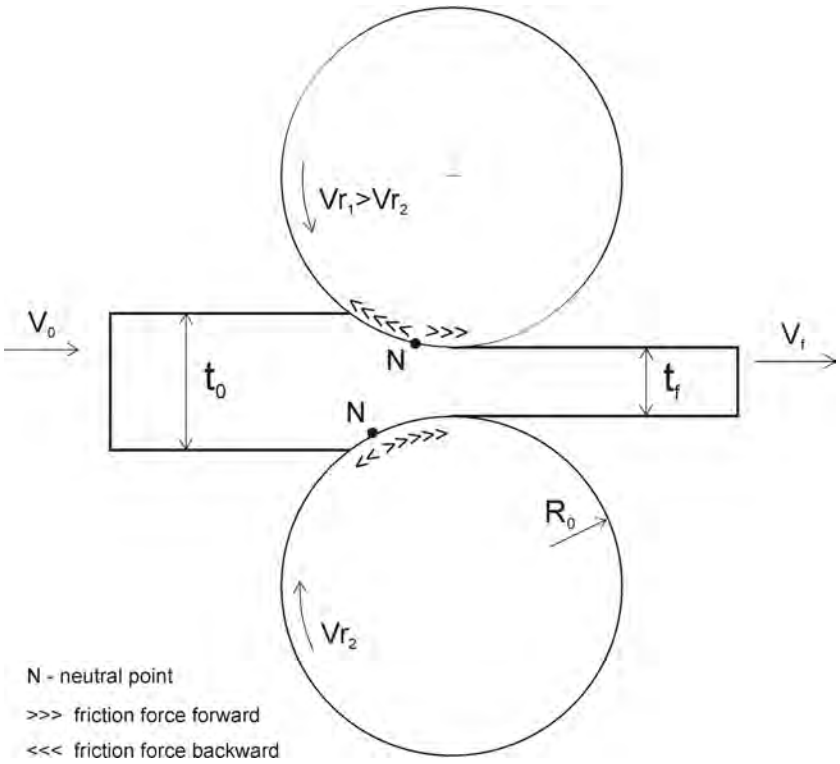

Figure 14: Friction and torque balance in asymmetric rolling.

Chapter 3 - State of the art

3.1. Conventional rolling of aluminum sheet

Rolling is one of the most widely used forming processes, especially because it is economic and flexible. The majority of products formed by rolling are thin sheets, whose primary consumers are the transportation (especially automotive and aerospace) and packaging industries.The origins of the rolling process go back to the 16th century, but it was only during the industrial revolution of the 18th century, with the onset of the steam machine, that large production rolling mills were first built. During the last century, and because of productivity demands, the rolling process was progressively optimized, especially because of automotive industry.

3.2. Applications of sheet aluminum alloys on formed parts

Rolled products, i.e. sheet, plate and foil constitute almost 50% of all aluminum alloys used [alumatter, 2007]. Aluminum sheets have a set of attractive properties which explains their widespread adoption in components requiring corrosion and crack resistance, high energy absorption, all combined with low density and full recycling capability. By using alloying elements and heat treatments or strain hardening, the range of achievable properties is vast. It is possible to have alloys with yield stresses ranging from 20MPa (1xxx series) to 500MPa (7xxx series) – see Appendix B. Current applications of rolled aluminum alloys include tankers, kitchenware, foil, beverage cans, automotive trim and chassis parts, airframes and even armor plates and missiles.

For the automotive industry, the use of aluminum alloys is still not significant. The majority are cast components such as cylinder heads, gear box housings and wheels. Since the 1970's, due to the oil crisis, an effort has been carried out by many car manufacturers toward the use of formed

aluminum sheets in car frames and body panels, aiming for weight reduction and thus better fuel efficiency.

3.3. Formability of aluminum sheets

Forming of aluminum sheets soon raised significant problems. The manufacture of car body panels and frames requires the sheet to have good formability and adequate strength. The term “formability” refers to a wide set of factors, ranging from intrinsic material properties to extrinsic factors such as forming conditions. In general, it is a measure of the material's ability to accommodate the strains occurring during a forming process and to produce a part that meets the requirements on mechanics, dimension and appearance [Li, Ghosh, 2004].

Extrinsic factors usually have greater influence on formability, as defined above. Despite this, only the material aspects are of concern in this work, and thus formability is considered here as the ability to deform up to high strains before failure by excessive reduction in thickness. There are several ways to access the formability of a sheet, from the simple measurement of uniform and total elongation during a tensile test, to the more complex determination of its forming limit diagrams, FLD [Keller, Backofen, 1964], [Goodwin, 1968], [Campos *et al*, 2006], using formability tests such as Erichsen, Swift, Nakazima, LDH (Limit Dome Heigth) and Fukui [Duarte, 1997].

Aluminum alloy sheets present reduced formability when compared to steels sheets, the traditional body panel materials. The maximum achievable strain during forming is usually higher on steels, whereas aluminum alloys tend to exhibit earlier necking and consequently, failure. Typical tensile elongation for aluminum alloys is lower than 30%, whereas for drawing steels this value is about 50%. Similar trend is observed on a plane strain condition, where aluminum fails after 25% elongation and steel strains up to 45% [Li, Ghosh, 2003].

From the set of macroscopic parameters influencing formability, two of the most important are strain hardening and strain rate hardening or strain rate sensitivity. They are in turn related to microstrucutural properties such as crystallographic structure and texture, grain size and morphology and precipitates / alloying elements. Aluminum alloys also introduced difficulties related to their low elastic modulus. This causes the part to display higher elastic deformation after unloading (springback), causing final parts to diverge from their expected dimensions, as well as difficulties on tool conception.

3.3.1. Strain hardening and strain rate hardening

Strain hardening is the ability to increase resistance with increasing strain. For materials following the Ludwik hardening law $\sigma = K\varepsilon^{n}$, it is defined as:

$$\theta = \frac{\partial \sigma}{\partial \epsilon} \qquad or \qquad n = \frac{\partial \ln \sigma}{\partial \ln \epsilon} \tag{14}$$

θ is usually referred to as strain hardening rate, σ is the tension, ε is the strain and *n* the strain hardening index. During deformation, if a region is subjected to increased or localized strain, that region will strain harden, and hence transmit strain to the neighbor areas, which are less resistant. This way, the material is able to delay strain localization by spreading deformation, promoting more uniform thinning [Li, Ghosh, 2004].

Strain rate hardening is the ability to resist strain localization (or necking) by accommodating any strain rate changes. When the material is subjected to thinning, there will be regions where strain rate increases. If the material has positive strain rate hardening, those regions will respond with increased resistance, and thus force slower strain rate regions to sustain the deformation, delaying failure by excessive thickness reduction [Mahmudi, 1996]. On the other hand, if the material has negative strain rate sensitivity, it will tend to produce strain localization, leading to earlier failure. Strain rate hardening can be defined as:

$$m = \frac{\partial \ln \sigma}{\partial \ln \dot{\epsilon}} \tag{15}$$

In the above equation, *m* is usually referred as strain rate sensitivity index and $\dot{\varepsilon}$ is the strain rate. This definition is useful because *m* is constant for materials following the Cottrell-Strokes strain rate hardening law, $\sigma = F(\varepsilon)^{m}$, where $F(\varepsilon)$ is a function of strain. A typical example is the Swift law.

Positive strain rate sensitivity is desirable when considering industrial processing, since the material will deform in a stable manner, delaying strain localization. When strain rate is increased, by increasing forming speed for instance, the material will respond with increased resistance and extension, thus providing improved productivity.

High values for strain rate sensitivity, ranging from 0.01 to 0.02, combined with high values for strain hardening rate can be observed on deep drawing steels, enabling them to have very good necking resistance, and hence, good formability [Shi, Meuleman, 1992]. Aluminum alloys tend to have lower strain rate sensitivity values, usually negative. Moreover, the increase in alloying elements and tempering treatments have a detrimental effect on this parameter. Other phenomena also tend to occur, as described next.

3.3.2. The Portevin-Le Châtelier phenomenon

When strain rate sensitivity is negative, the material responds to tension with strain localization phenomena, usually in significant number, leading to narrow deformation bands on the surface. The sheet's tensile curve becomes serrated, because of inhomogeneous strain distribution. Deformation bands leave traces on the sheet surface, rendering it unsuitable for many applications, due to its poor superficial quality, or causing early failure. This is the so-called Portevin-Le Chatelier, or PLC phenomenon [Hähner, 1997],[Duarte,1997].

The occurrence of PLC is a consequence of the interaction between solute atoms on the structure and dislocations [Picu *et al*, 2005], designated by dynamic strain aging, or DSA. It is known to be dependent on temperature and strain rate, as well as solute distribution [Picu *et al*, 2006] and grain size. It can be observed on many types of materials, including aluminum, copper and nickel alloys, steels and even h.c.p. materials such as zinc, as long as there are solute atoms to interact with dislocations.

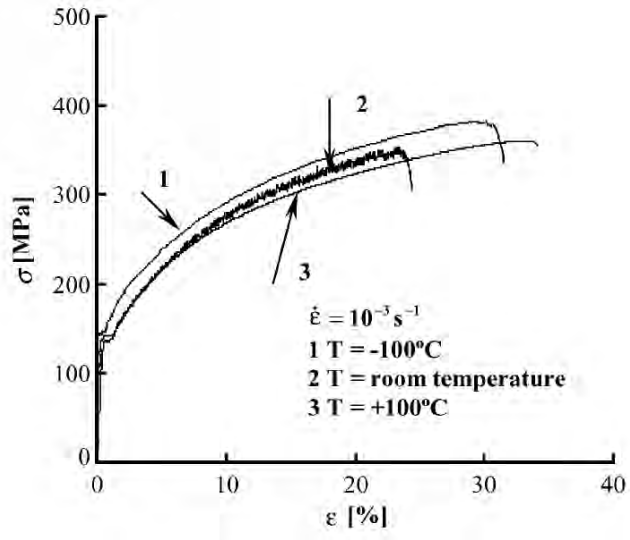

Figure 15: Fig.1. Typical true stress–true strain curves at three temperatures within and outside the PLC range. The curves are serrated within the domain in which the SRS is negative and smooth outside. The ductility is reduced within the domain. [Picu, 2005]

The PLC phenomenon can be minimized, and even eliminated by imposing the right conditions of temperature and strain rate. It has been found that there is a window of temperature and strain rate for which the PLC phenomenon occurs, causing serrated flow and decreased ductility Figure 15.

3.3.3. Springback

When a sheet is bent and deformed plastically, besides the permanent plastic deformation there will also be a residual amount of elastic stress that causes the sheet to return towards its undeformed configuration, when the bending moment is removed. This is called springback.

In all sheet forming processes, springback is more or less present, not only on deep drawing and bending, but also in but flanging and hemming. It affects part geometry and can have significant effects on productivity. Since springback consists of an elastic deformation, it depends on the elastic modulus of the material. More precisely, it increases as the strength–to–modulus ratio increases.

The increase in strength, combined with the lower Young's modulus (nearly 1/3 of steel), originates significant springback issues in aluminum alloys - Figure 16. High strength and dual phase steels were developed as a response to aluminum alloys, because their very high tensile strength enables thickness (and hence, weight) reduction on the components while maintaining the required resistance and good formability. But the increasing strength also lead to increasing springback issues. This is why the study of springback is of such industrial and scientific relevance nowadays.

3.4. Microstructural aspects related to formability

The effort towards the widespread adoption of aluminum alloys motivated many studies, aiming to improve sheet properties and response. The microstructural features, - crystallographic texture, grain structure and size, precipitation structure - which constitute the base for the material's macroscopic response, are the main focus of these studies. The resulting strain hardening response, strain rate sensitivity, among other properties, will help to determine the respective influences of those features.

3.4.1. Crystallographic texture

The set of preferred grain orientations in space, or crystallographic texture, is known to be the main source of anisotropic response of a material. Individual crystallites tend to deform by slip in preferred orientations, causing the mechanical response to be strongly depend on the direction of solicitation.

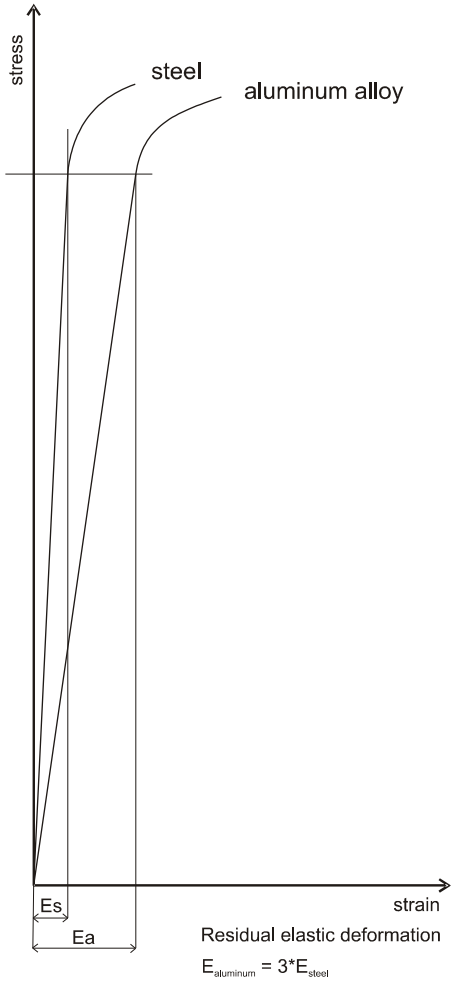

Figure 16: Springback comparison between steel and aluminium alloys. Since aluminium alloys have on third of the elastic modulus of steels, residual elastic deformation on parts is much higher.

3.4.1.1. Schmid law

To move a dislocation, and thus cause plastic deformation, a critical stress must be applied to overcome the resistance to dislocation movement (glide).For an applied stress, σ, the resolved shear stress acting upon a dislocation is:

$$\tau_b = \sigma \cos\varphi \cos\lambda \tag{16}$$

The resolved shear stress must exceed a critical value before shear can occur. The above equation is in fact a yield criterion for crystallographic slip, and it is named Schimd law. This condition would define the proportional limit, or yield stress. The microstructure of the metal defines τ_b.

The link between the two (for single crystals) is the Schmid factor, cos φ cos λ, which typically has values between 0.2 and 0.4. In a polycrystalline sheet of metal, each individual grain, or crystal, deforms on up to five slip systems, with the activity on each defined by the resolved shear stress, just as for the single crystal. However, the deformation of the individual grains is constrained by that of its neighbors. Thus, the discrete nature of slip is the fundamental origin of plastic anisotropy: slip activity is related to the way a crystal is oriented relative to the axes of deformation [Kocks *et al*, 1998].

3.4.1.2. Texture and mechanical properties

Texture is the distribution of crystal orientations within a sample. It can be described by the relation between two reference systems, the crystal reference system and the sample (macroscopic) reference system. The most usual way to describe an orientation of a crystal relatively to the sample (macroscopic reference system) is to say that one of its reference directions is parallel to the sample's normal direction, and another reference direction is parallel to the sample's rolling direction – see Appendix A.

The processing routes usually generate typical texture components. Rolling of aluminum sheets originates typical β fiber textures (Brass: {011}<112>; S:{123}<634>. Cu: {112}<111>). These textures evolve to cube ({001}<100>) and Goss ({011}<001>) textures after recrystallization.

In order to achieve good forming capability, sheet must be able to deform as far as possible before failing by excessive thickness reduction. The measure of this capability is usually given by the ratio between the sheet's deformation in width and its deformation in thickness, for a given set of conditions - the *r* value, or Lankford coefficient. The average value of *r*, r_m, is calculated from three values at specific directions from the rolling direction, usually 0° (RD itself), 45° and 90° (transverse direction):

$$r_m = 1/4(r_0 + 2r_{45} + r_{90}) \quad (17)$$

The variation of *r* values along the set of directions is described by:

$$\Delta r = 1/2(r_0 - 2r_{45} + r_{90}) \quad (18)$$

Higher r_m values mean increased deformation before rupture, and hence, better formability. If *r* values present significant variations, that is to say if Δr is high, then the final part may fail sooner than expected, or present "ears", which constitute a waste of material. Figure 17 shows a aluminum cup after deep drawing. Ears are visible in the rolling direction (marked) and also in the transverse direction. These are due to the differences in *r* values when considering the various directions. The sheet has higher *r* values on the rolling and transverse directions, and much lower *r* value on the 45° direction.

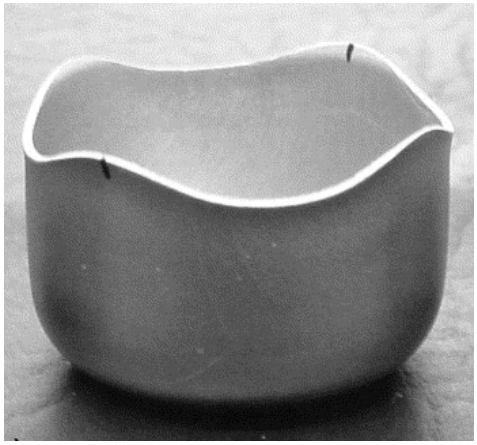

Figure 17: Typical appearance of a deep drawn cup with ears under 0° and 90° to the rolling direction (marked; AA1200-O). [Engler, 2007].

Texture is closely related to *r* values. In fact, different preferred orientations are known to cause the material to have higher or lower *r* values depending on the directions considered. For instance, rolling texture components (Brass, S, Copper) increase *r* values at 45° from rolling direction, whereas recrystallization texture components (especially Cube) reduce it significantly - Figure 18. To be able to control texture composition on sheets is very important, since it is then possible to reduce earing and increase formability. In the case of the deep drawn cup of Figure 17, and observing the *r* value evolution for each texture component shown on Figure 18, the sheet probably has strong Cube texture, since the cup height at 45° from the rolling direction is the lowest.

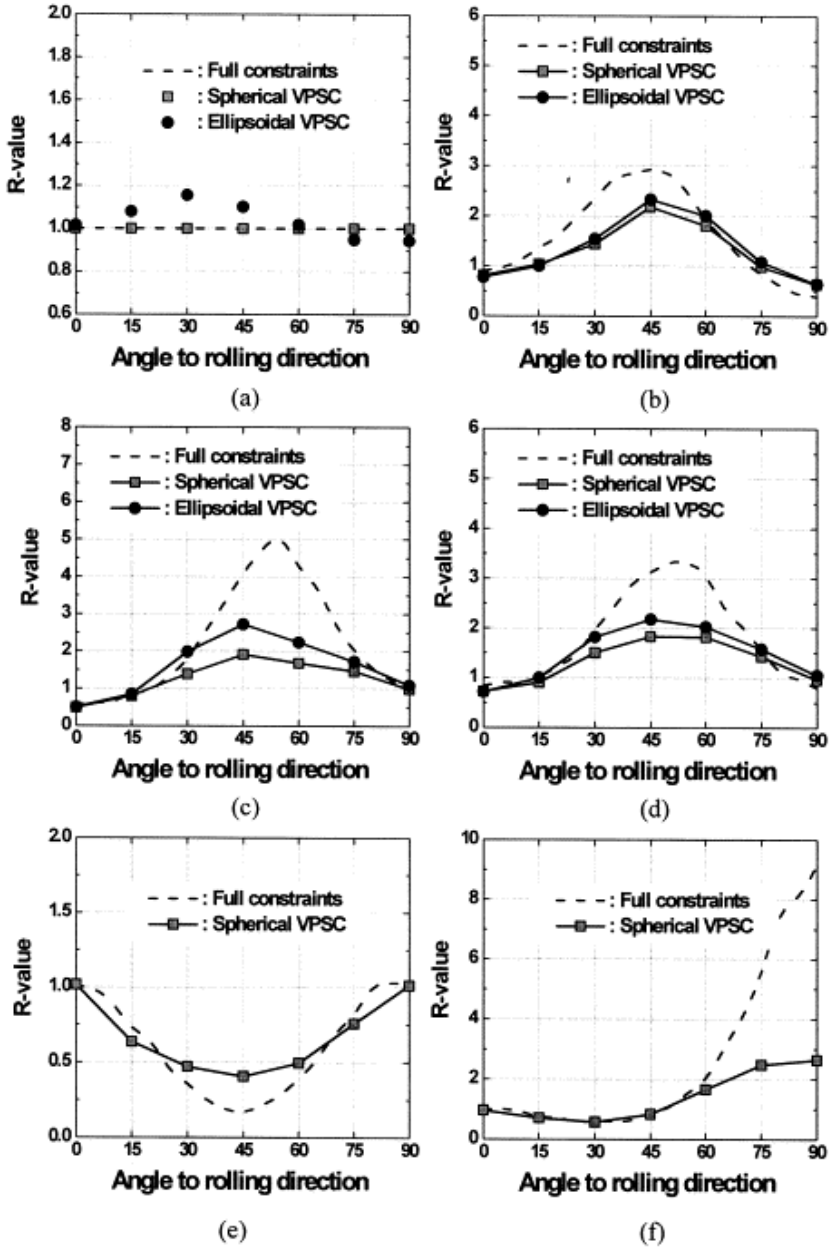

Figure 18: Comparison of r-value directionality predicted by the Taylor (full constraints) and the VPSC models for six texture components. (a) Isotropic; (b) Copper; (c) Brass; (d) S; (e) Cube; (f) Goss. See [Choi et al, 2000] for further details.

3.4.2. Grain size

In polycrystalline materials, a number of mechanical properties are known to be grain size dependent. The dependence of strength on the grain size of metals has received a great deal of attention since the early work of Hall and Petch [Hall, 1951][Petch, 1953]. They concluded that the strength of all polycrystalline materials is related to the grain size, *d*, through the equation which states that the yield stress, σ_y, is given by:

$$\sigma_y = \sigma_0 + k_y d^{-\frac{1}{2}} \tag{19}$$

where σ_0 is termed the friction stress and k_y is a constant of yielding [Hall, 1951][Petch, 1953]. It follows from (19) that the strength increases with a reduction in the grain size and this has led to an ever-increasing interest in fabricating materials with extremely small grain sizes.

The Hall-Petch equation is based on the principle that when a material is subjected to stress, dislocations are formed within the grains. These dislocations move up to grain boundaries, since they constitute obstacles to their motion. When a sufficient number of dislocations pile up at grain boundaries, they cause stress in that region. When the stress reaches a sufficient level, is causes dislocations to appear at the neighbor grains. After this, generalized yielding throughout the material occurs.

The amount of stress required to cause dislocations to propagate to neighbor grains is dependent on the length of the dislocations mean free path (which is directly related to grain size), much like the crack propagation stress is related to its length in fracture mechanics (there is a critical stress above which a crack will grow and this stress is proportional to the inverse of the square root of the length of the crack). If the grain size is smaller, the dislocation mean free path decreases, and the stress required to propagate the dislocations to the neighbor grains increases. This causes yield stress to increase as well.

Grain size affects dislocation formation, movement and accumulation and thus it affects the material's strain hardening. If grain size is large, a larger number of dislocations tend to form inside the grain. As the number of dislocations increases, the probability of interference also increases. Dislocation accumulation tends to block the movement of newer dislocations, causing plastic flow to become more difficult as well. So, strain hardening benefits from larger grain sizes.When the grain size decreases, it becomes harder for dislocations to form and move inside the grains. Eventually, for grain sizes small enough, dislocations have no space to form inside the grains, and thus they cannot originate plastic deformation. For grain sizes down to a few manometers (usually $<$10nm), the deformation mechanism switches to grain boundary shear. This may lead, under the appropriate conditions of strain rate and temperature, to super plasticity [Valiev *et al*, 1997].

3.4.3. Alloying elements and precipitation structure

Pure aluminum has a tensile strength of about 60MPa, which limits its use to low demanding applications. By adding alloying elements, it is possible to achieve up to 500 MPa (see Appendix B). From the existing alloys, the 5XXX, containing Mg as the major alloying element, and the 6XXX series, containing Mg and Si are the most widely used in forming industries. For instance, the 5XXX series alloys are used in beverage packaging (in the can ends, whereas the can body is usually made of an AA3XXX – [alumatter, 2007-2]). The heat treatable Al-Mg-Si alloys of the 6XXX series are often chosen for automotive body materials, since they show a good combination of formability, corrosion resistance and weldability.

Figure 19: Stages in the drawing and ironing of a beverage can. [alummater, 2007-2]

When deformed, pure aluminum tends to form dislocation cells, lowering the overall energy and reducing strain hardening. By adding alloying elements, it is possible to create strengthening mechanisms to obtain improved response.

In the case of the 5XXX series alloy, the Mg is easily dispersed in the Al matrix, replacing Al atoms, because it has high solubility in aluminum. But the addition of Mg causes distortion of the crystal structure, since the atomic radius of Mg is 0.160nm, whereas Al has 0.142nm. During deformation, dislocations tend to be trapped by the solute atoms, increasing the yield stress. As the stress level increases and dislocations start moving, their movement is always affected by the presence of Mg atoms. Because of this, dislocations are prevented from arranging into cells and lower their energy (dynamic recrystallization), and thus, strain hardening increases in comparison to pure aluminum. This is the reason why these alloys are said to be work hardenable. Their strength comes from the amount of strain imposed on the crystal structure. The addition of Mg also causes undesired effects, such as the PLC effect, already discussed (see page 46).

The 6XXX series aluminum alloys have a different strengthening mechanism. The alloying elements are Mg and Si. These form precipitates (Mg_2Si) given the right processing conditions are met. The alloy is heated above the *solvus* temperature, in order to dissolve the alloying elements; then the alloy is quenched and the rapid cooling causes these alloying elements to become trapped inside the aluminum matrix, forming a superssaturated solid solution; afterwards, the elements in the solid solution start to decompose and form precipitates. This latter stage can occur artificially by supplying heat, or naturally, at room temperature. During aging, alloying elements trapped inside the Al matrix evolve trough stages, before becoming coherent precipitates. Generally, these stages are [Miao, Laughlin, 1999] [Gracio *et al*, 2004]:

α (superssaturated solid solution) --> GP zones β' --> β' --> β

Guinier–Preston, or GP-zones have been first recognized as microstructural elements in aluminum alloys since the work of Guinier and Preston [Preston, 1938]. The zones are formed by "natural aging" at room temperature, and in early stages of the industrially important "artificial aging" at temperatures in a range 100–180°C. GP zones are early localized concentrations of atoms, in this case spherical, but with unknown structure. β'' are needle shaped coherent precipitates that cause some distortion of the crystal structure, accommodated by localized strain. These evolve to β' semi-coherent precipitates, who cause larger distortion of the crystal structure, this time accommodated by dislocations at the interface. β is the final stage, in which the precipitate acquires a different crystallographic structure, incoherent with the original Al structure.

The knowledge and control of the precipitation sequence enables the control of the mechanical properties of these alloys. These are generally classified in terms of aging condition. Even at room temperature, precipitates will evolve. If the alloy is allowed to develop precipitates at room temperature for a given period, the aging is called "natural" - Natural Aging, NA. If the formation of precipitates is accelerated by means of heat treatments, the aging is "arfificial" - Artificial Aging, AA. The aging level is usually divided in the following states:

- Under-aged (UA) - refers to a state in which GP zones are starting to form from the atoms in solid solution. Since GP zones are coherent with the crystal structure, they provide a reduced level of strengthening. It is possible to obtain a good formability but reduced strength by using an under-aged alloy.
- Naturally aged (NA) - to take advantage of the additional strengthening provided by semi-coherent precipitates, maintaining good formability, additional aging treatment can be used – the naturally aged (NA) condition. In this state, semi-coherent precipitates (in minor concentrations) and GP zones (at their peak concentration) provide a more efficient obstacle for dislocations, and hence, increased strengthening. This state can be obtained by letting the alloy age at room temperature, and it is the most used one in forming industries, because of its good combination of strength and formability.

- Peak aged (PA) - when further strengthening is required, the development of incoherent precipitates can be achieved rapidly by heat treatments. The size of the precipitates is influenced by time and temperature. Hence, it is possible to obtain a peak-aged condition, in which the precipitates have the right size and morphology to provide the maximum strengthening.
- Over aged (OA) - if the precipitates are allowed to grow excessively, the reverse effect occurs, and a decrease in strength is observed.

Figure 20 shows the evolution of mechanical response and hardness of a 6022 alloy when subjected to annealing at different times. The effect of the various aging conditions can be observed.

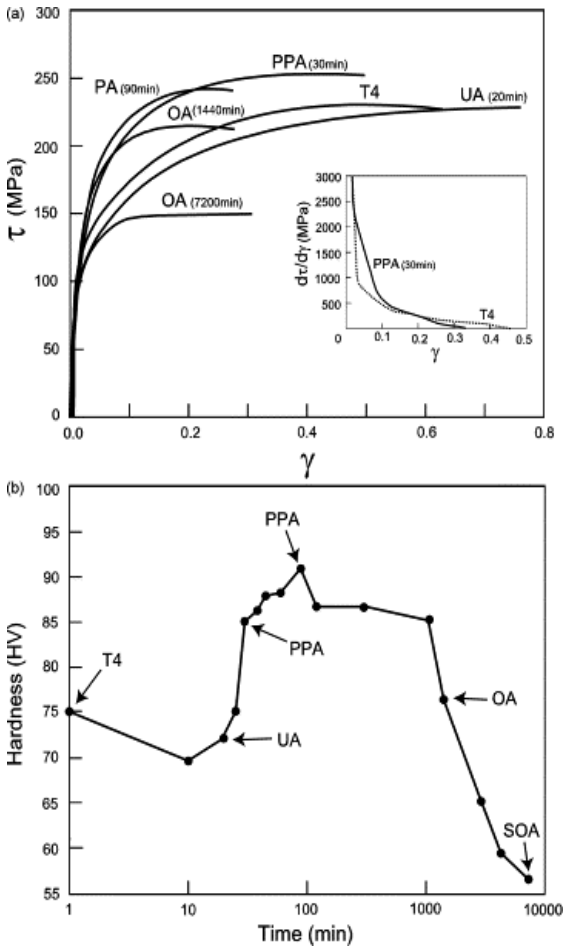

Figure 20: Monotonic shear stress vs. shear strain curves at 90° from the rolling direction for naturally aged (T4), under-aged (UA), pre-peak-aged (PPA), peak-aged (PA), over-aged (OA) and strongly over-aged (SOA) 6022 alloy (a), and corresponding isothermal aging curve at 200 °C (b). From [Gracio et al, 2004].

3.5. Optimization of properties

Limitations for the widespread use of aluminum alloys in forming industries originated strategies aiming to optimize sheet's properties, especially the formability / strength combination. Aside from alloying, crystallographic texture and grain size and morphology are the main factors influencing the formability of sheets. Strategies towards the optimization of these parameters are presented next.

3.5.1. Texture optimization strategies

Over the past years, manufacturers attempted to produce sheets with controlled volume fractions of texture components, in order to obtain balanced properties. Rolling texture components were combined with recrystallization texture components, because they act on opposite ways. For instance, the copper texture component, typical from the rolling process, yields high values of *r45*, whereas the cube component, which is formed during recrystallization, lowers *r45* dramatically – see Figure 18.

It is known that crystallographic texture is one of the main factors influencing plastic anisotropy [Bunge, 1982]. Low carbon steels exhibit high *r* values, and thus very good deep drawability. {111}||ND textures (also called γ fiber - Figure 21) appear on these materials after recrystallization - Figure 22. This indicates that these texture components seem to improve formability. Aluminum alloys are generally processed by rolling, originating β fiber textures – Copper, Brass, S. These textures evolve to cube texture and Goss after recrystallization, causing *r* values to decrease, especially *r45*.

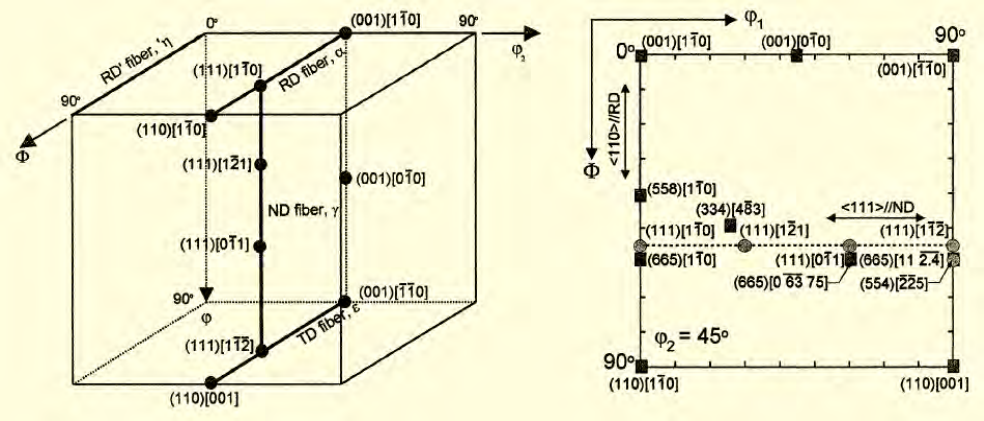

Figure 21: Tri-dimensional view and φ_2=45° ODF section of Euler space, showing locations of some orientations and fibres [Hong, Lee, 2002].

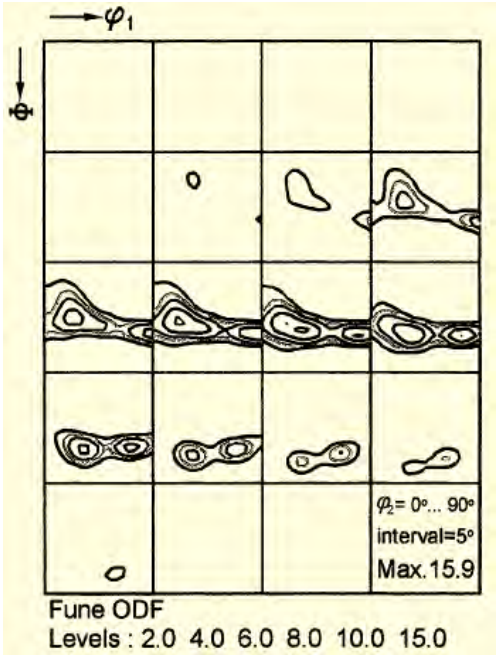

Figure 22: ODFs of 95% cold-rolled and recrystallized IF steel sheets. φ_2 values start from 0° in top left section and increase by 5° with moving to right section [Hong, Lee, 2002].

{111}||ND texture components are difficult to achieve in Al alloys using conventional processing methods, though some good results have been obtained [Engler *at a*l, 2001]. Because of this, there was an attempt to develop alternative sheet manufacturing processes. It was observed that shear deformation gives rise to shear texture components, namely {001}<110>, {111}<110> and {111}<112>, among which {111}||ND components can be found. These components are said to be the most favorable for improving formability in sheets [Kim *et al*, 2002].

3.5.2. Grain refinement strategies

As stated before, grain size affects not only the strength, but also the strain hardening behavior of the material. Smaller grain sizes are usually sought because they cause, in general, an increase in yield stress, as well as superior surface quality on formed parts, preventing defects such as “orange peel”[1] to occur. On the other hand, an excessive decrease in grain size - to the range of <500 nm- also causes a decrease in strain hardening, leading to practically no plastic deformation capability [Wang, 2004].

1 Orange peel refers to surface morphology of sheets having large grain sizes. This large grain size causes the surface to become textured like an orange peel.

Extreme reduction in grain size, down to nanometer level, was first recognized by Gleiter [Gleiter, 1989] to be a strategy with great potential for many materials. Since then, nanocrystalline materials were found to display increased strength/hardness and improved toughness, though reducing elastic modulus and ductility. They also have enhanced diffusivity, higher specific heat, enhanced thermal expansion coefficient (CTE), and superior soft magnetic properties in comparison with conventional polycrystalline materials.

Materials are usually classified in terms of grain size (d) according to the following scale:

- $d>10\mu m$ – conventional grain size;
- $1<d<10\ \mu m$ – fine grain size;
- $100nm<d<1\ \mu m$ – ultra-fine grain size;
- $d<100nm$ – nanocrystalline grain size.

Conventional thermo-mechanical processing of metals can lead to grain sizes of about 15 to 20 μm. For further grain refinement, other strategies must be employed. These strategies are usually divided into 2 main groups: synthesis of small clusters into ordered structures, or breaking down polycrystalline materials into smaller units (grains). Examples from the first group are inert gas condensation and electrodeposition. From the second group, the most common strategy is severe plastic deformation (SPD).

3.5.2.1. Synthesis methods

Inert gas condensation: In short terms, inert gas condensation consists of evaporating a material inside a vacuum chamber, using a variety of methods (such as resistive heating, radio-frequency, heating, sputtering, electron beam heating, laser/plasma heating, or ion sputtering) [Gleiter, 1989]. The evaporated material is then condensated into a collector trough the interaction with the inert gas in the chamber atmosphere, and a fine powder is obtained. This powder is then compacted, originating a solid 3D crystallite, with grain size in the order of a few nanometers. This was the first process used to achieve nano structured materials. Still, materials produced by inert gas condensations can be prone to porosity,flaws or impurities, which greatly affects their mechanical properties [Youngdahl *et al*, 1997]. In fact, the theoretical gain achieved by decreasing the grain size may be lost because of processing defects, leading to poor results in terms of mechanical response.

Electrodeposition: A base material is subjected to an electrical potential while placed inside a chamber having atoms of the material to be deposited in the atmosphere. The electrical potential causes the atoms on the atmosphere to be attracted towards the base material, forming layers. The

atoms form grains with a few nanometers in size, and the total layer thickness can vary from thin films (1 to 100μm) to bulk materials with several millimeters in thickness. By controlling process variables it is possible to obtain larger or smaller grain sizes, or privilege new grain nucleation instead of growth of the existing grains [Erb, 1995].

The electrodeposition technique has significant advantages over other methods for synthesizing nanocrystalline materials: (1) potential of synthesizing large variety of nanograin materials - pure metals, alloys and composite systems with grain sizes as small as 20 nm - , (2) low investment, (3) high production rates, (4) few size and shape limitations, and (5) high probability of transferring this technology to existing electroplating and electroforming industries.

3.5.2.2. Severe plastic deformation processes – SPD

It has been known that high levels of plastic deformation lead to significant changes in microstructure and texture of metals. Original grain boundaries are added to newly formed sub-grain boundaries, originated by dislocations within the grains [Hughes, Hansen, 1997] [Humphreys *et al*, 1999]. These newly formed grain boundaries have high misorientation angles ($>15^{o}/20^{o}$), leading to the deformation induced reduction in grain size. Severe plastic deformation processes are those which impose a large deformation on a bulk sample, without significant change in its overall dimensions [Valiev, Langdon, 2006].

Imposing large strains to metals can raise operational problems if using conventional processes. For instance, when rolling sheet, there is a limit for the maximum thickness strain to be imposed, since the thickness becomes more and more reduced. Processes using shear strains as the way to impose large deformations have some advantages. It is possible to maintain the overall dimensions of the specimen if only shear strains are imposed. Because of this, very high levels of strain can be imposed without problems. In the 1970-80's, this principle was first applied, and the ECAP - Equal Channel Angular Pressing - process was developed.

ECAP uses a die containing two channels, equal in cross-section, intersecting at an angle U that is generally close to 90^{o}. The test sample is machined to fit within these channels. It is pushed down from the upper die by a piston (as shown by arrow) and is forced around a sharp corner - Figure 23. The strain imposed on the sample in ECAP is dependent upon both the channel angle between the two channels, and the angle defining the outer arc of curvature.

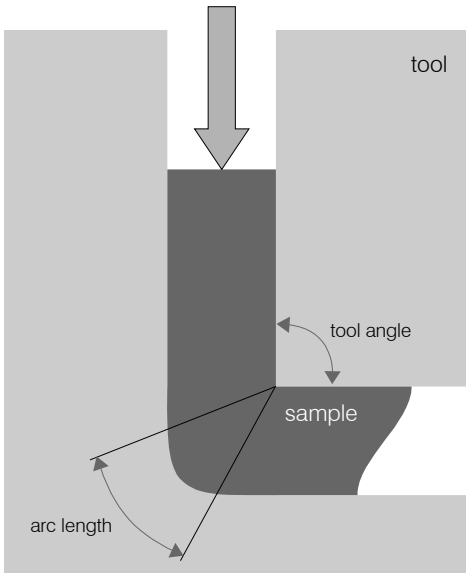

Figure 23: The equal channel angular pressing (ECAP) process.

After its appearance in the 1970's and early 1980's, the ECAP process was not immediately recognized as having the potential for enhancing the material's properties. It was only later that scientists started using ECAP as a tool to obtain unusual mechanical properties, such as superplasticity. A very complete review of the ECAP process was performed by Valiev and Langdon [2006].

An alternative procedure to introduce high plastic strains, illustrated in Figure 24 is called high pressure torsion (HPT). A small sample, in the form of a disk, is held under a high pressure and then subjected to torsional straining. Processing by HPT has the advantage of producing exceptionally small grain sizes, often in the nanometer range (<100 nm), and the ability to process brittle materials such as intermetallics and semiconductors. Nevertheless, HPT has the disadvantage that the specimen dimensions are generally fairly small, with maximum disk diameters of 20 mm and thickness of 1 mm.

As stated, sever plastic deformation processes have the advantages of achieving very high levels of strain without significant change in the specimen's cross sectional area. Therefore, they are best suited for the processing of bulk materials. But there is a disadvantage that limits the practical usage of ECAP in large scale processing of materials. It is, essentially, a discontinuous process. Though some variants being developed aim to overcome this limitation, their implementation in industrial environments is not immediate. Moreover, the processing of sheets is not as straightforward.

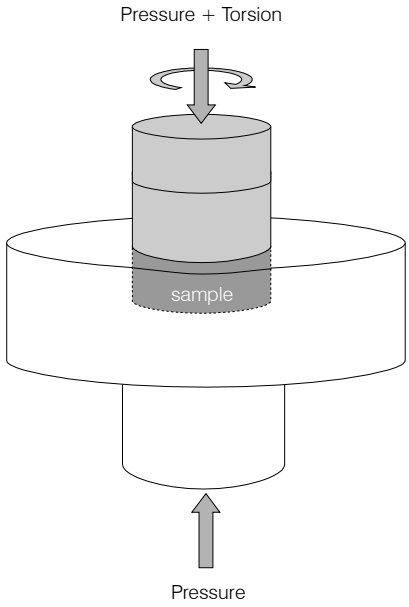

Figure 24: The High Pressure Torsion (HPT) process.

Bearing in mind that rolling is not, by itself, a severe plastic deformation process, as defined earlier, one of its variants may constitute an alternative to the SPD's already presented. By imposing shear strains along with compressive strains, the asymmetrical rolling process has the potential to achieve grain refinement, like other SPD's, but retaining two advantages: adaptation to existent infra-structures in industries; and the suitability for mass production.

3.6. Asymmetrical rolling

Asymmetrical rolling occurs when the rolls have different circumferential speeds relatively to the sheet – see section 2.3. It can either be intentionally imposed, as a mean to obtain curved profiles or rings, or it can occur as a deviation to the normal rolling process, either due to geometric differences between the rolls or, more frequently, due to differences in friction, caused either by uneven lubrication or unequal surface roughness. The second case was the primary reason why asymmetric rolling was first studied, since it lead to undesired sheet curvature and rolling malfunction. But still today there is interest in industrial environments to accurately control conventional rolling processes, and some analytical studies about asymmetry factors can be found [Knight *et al*, 2003].

Later, asymmetrical rolling was recognized as a mean to reduce rolling power and torque, improve sheet surface properties, reduce the number of rolling passes by increasing the reduction in

each pass, and obtain thinner sheets easily in high strength steels [Hwang, 1997]. As the asymmetrical rolling process was further studied, additional potential was recognized. Under proper process conditions, shear stresses imposed on the sheet's surface can be spread along the entire sheet thickness, causing shear strains. These shear strains cause grain rotation and subdivision, leading to grain refinement, for sufficient amounts of deformation. Due to this grain rotation, a change in crystallographic texture also occurs. Typical rolling textures usually found on fcc materials, mainly caused by plane strains, can be modified towards shear texture components, which are said to benefit sheet's properties, especially formability.

Potential advantages of asymmetric rolling are texture optimization and grain refinement. Choi and his co-workers [Choi *et al*, 1998], were the first to study asymmetric rolling aiming to explore this potential. The main challenge is to optimize the asymmetric rolling process in order to achieve these goals.

3.6.1. Influencing parameters

Besides those already considered in conventional rolling (total reduction, reduction in each pass, lubrication, roll speed), there is an additional process parameter in asymmetric rolling: the roll speed ratio. Additionally, rolling can be performed always in the same direction, or the sheet may be rotated between passes around 3 different axes, the normal direction axis, the transverse direction axis and the rolling direction axis. All of the parameters mentioned are to be discussed below.

3.6.1.1. Roll speed

The effect of absolute roll speed is not especially approached in literature reviews. The main focus is almost always the roll speed ratio. Nevertheless, it is possible to find circumferential speeds from 0.045m/s [Cui, Ohori, 2000] to 0.3m/s [Lee, Lee, 2001].

3.6.1.2. Roll peripheral speed ratio

The main difference between asymmetric and conventional rolling is the difference in upper and lower roll speeds. The ratio of these speeds is one of the most important parameters of the process, since it will influence the velocity field along the sheet thickness (together with other parameters, such as friction and reduction per pass).

When studying the influence of speed ratio on asymmetric rolling, Choi [Choi *et al*, 1998] used FEM simulations to access the influence of this parameter on shear strain distribution along sheet thickness and on texture. He used 3 different roll speed ratios, 1.25, 1.5 and 2, and he found

that the optimum value for roll speed ratio was 1.5, since it produced texture components near to the ideal shear. He explained this result based on FEM analysis of shear strain distribution trough thickness. As the roll radius ratio increases from 1.25 up to 2, the amount of shear strain increases at first, but then decreases, due to the decreasing roll pressure when rolling asymmetrically (upper and lower neutral points become more separated). This means that there is an optimum roll radius ratio for which the shear strain imposed is the largest.

3.6.1.3. Roll speed vs roll radius ratio vs single roll drive

As shown on section 2.3, asymmetric rolling can be achieved either by imposing different rotational speeds to the upper and lower rolls, or by using rolls having different diameters while rotating at the same speed. The two methods can be found in literature, but Sang Heon Lee and Dong Nyung Lee [Lee, Lee, 2001] compared both in the case of asymmetric rolling of steel. They also compared another method, single roll drive, when one of the rolls is kept stationary. They have shown that the worst results (in terms of the texture components obtained) arise from single roll drive, and the best are shared identically by roll speed variation / roll radius variation. Hence, they show that identical speed ratios, either obtained by varying the roll radius or the roll speed ratio, yield similar results.

On the other hand, Sakai and co-workers [2001] obtained good results after rolling an AA5052 using single roll drive. But this procedure was performed at 260^{o}C, and thus its results cannot be directly compared with other cold rolling procedures.

3.6.1.4. Total reduction

In order to obtain shear texture components, the total reduction achieved during rolling should be high enough to allow shear strains to develop along the entire sheet thickness. This minimum value for texture development does not seem to be the main concern in literature, since no special attention seems to be given to it. Nevertheless, sheets with 50% in thickness reduction are shown to develop shear texture components.

When considering grain refinement through asymmetric rolling, the presence of shear strains is more important than the maximum level of thickness reduction, as demonstrated by Cui and Ohori [2000]. Grain rotation and subdivision is greatly favored by shear strains, rather than by plane strain compression imposed on conventional rolling.

3.6.1.5. Thickness reduction per pass

One of the most important parameters in asymmetric rolling is the thickness reduction per pass. Increasing the reduction in each pass will increase the necessary rolling power, as demonstrated earlier (see section 2.3). When combined with a difference in roll speeds, increase in thickness reduction per pass imposes larger amounts of shear strains on the sheet surface and, under the appropriate conditions, it is essential to achieve the total propagation of those shear strains along the sheet's thickness. Kim and Lee [2001] studied the influence of the reduction per pass on the shear texture formation. They found that high values of this parameter were necessary to achieve shear textures. Low reductions per pass led to plane strain textures, similar to those found on conventional rolling.

3.6.1.6. Friction

Since the main purpose of asymmetrical rolling is to impose high shear strains on the sheet, in order to obtain shear textures, the friction between the rolls and the sheet has to be kept relatively high. This means that asymmetrical rolling is usually performed with dry rolls. The presence of lubrication would not be favorable for shear stresses.

3.6.1.7. Sheet rotation between passes

Rolling can be performed without any kind of rotation of the sheet between each pass. This is the most usual case in conventional rolling. But in asymmetrical rolling, the purpose of imposing large amounts of shear strains lead to the idea of rotating the sheet between each rolling pass, taking advantage of the difference in roll speeds. Several rotation routes can be performed, as shown on Figure 25.

From the observation of the possible reversal routes, it becomes clear that UD and TD routes do not impose any reversal of strains on the sheet's surface, whereas RD and ND impose strain reversal. In literature, the TD route is one of the most used, but when studying the asymmetrical rolling process in steels, S.H. Lee and D.N. Lee [Lee, Lee, 2001] observed textures closer to the ideal “shear” components on specimens processed by the RD and ND reversing routes.

3.6.2. Literature results

Choi *et al* [1998] first used asymmetrical rolling to produce intense shear deformation throughout the entire sheet thickness, as opposed to superficial shear deformation known to occur on conventional rolling in some conditions. Their main purpose was to obtain shear texture components {001}<110>, {111}<110> and {111}<112>, said to improve sheet's formability. Kim and Lee

[1999] studied the asymmetrical rolling response of pure aluminum and an AA5052. Using a rolling mill having different roll diameters, they studied the influence of the initial textures before asymmetrical rolling of pure aluminum (99.9%). They found that an initial plane strain texture can evolve to a well developed shear texture by imposing large values of shear strains. These can only be produced by high values of thickness reduction per pass – about 50% - 60%. Initial cube textures can also evolve to shear texture components, but in this case the final textures were found to be more diffuse. However, the main conclusion drawn from these experiments was the requirement of high values of thickness reduction per pass in either case, in order to achieve the shear texture components.

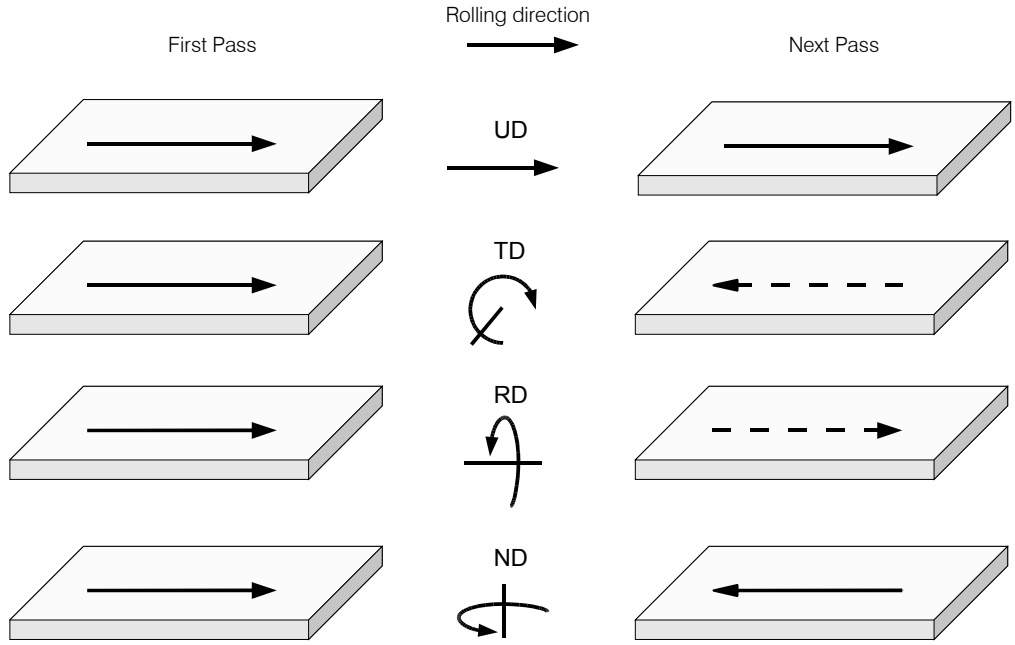

Figure 25: Definition of rolling directions possible to implement in rolling. Unidirectional rolling (UD) does not impose any change in direction; TD, RD and ND impose rotations about the transverse direction, the rolling direction and the normal direction, respectively. [Lee, Lee, 2001]

On the same work, Kim and Lee also studied the effect of asymmetrical rolling on texture and *r* values for AA5052. They were able to obtain a high volume fraction of shear texture components throughout the entire sheet's thickness after asymmetrical rolling, using high values of thickness reduction per pass. Moreover, these shear texture components were found to be retained after annealing at 275^{o}C for 1 hour and almost unchanged after annealing at 400^{o}C for 0.5 hours. Plastic strain ratios were measured on annealed specimens, and compared with conventionally (symmetrically) rolled specimens. Results show an *r* value increase of 1.4 to 1.7 times relatively to

symmetrically rolled specimen - Table 1. Finally, the higher temperature annealing treatment allowed the Δr value to decrease significantly.

Rolling	Annealing conditions	r_0	r_{45}	r_{90}	Average r	Δr
Conventional	400°C, 0,5 hours	0.80	0.86	0.94	0.87	0.01
Asymmetrical	275°C, 1 hour	0.64	2.16	1.04	1.50	1.32
	400°C, 0.5 hours	1.04	1.48	0.90	1.22	0.51

Table 1: r values of AA5052 sheets, after rolling and annealing [Kim, Lee, 1999].

On a later work, Kim and Lee [2001] studied the influence of rolling parameters on shear texture formation, on an AA1050-O. Using experimental and FEM data, they found that there is an optimum roll speed ratio of 1.5, for which the shear deformation distribution throughout the sheet thickness is the most favorable. They also confirmed that a high reduction per pass was a decisive factor. Using FEM simulations, Kim and Lee studied the influence of shear strains evolution on conventional and asymmetrical rolling. They found that on conventional rolling the sheet undergoes positive and negative shear strains, before and after the neutral point, respectively. But during asymmetrical rolling, and since the roll speeds are different, the neutral point moves towards the exit of the sheet, and hence, shear strains are always positive. By imposing the shear strains history, determined for conventional and asymmetrical rolling, to a set of finite elements, Kim and Lee calculated the resulting crystallographic textures. They found that the ideal shear textures were closely related to the shear strain reversal. Hence, they concluded that the ideal shear texture could not be obtained by using unidirectional rolling, but only reversing the rolling direction on each pass.

Sang Heong Lee and Dong Nyung Lee [Lee, Lee, 2001] studied asymmetrical rolling using steel sheets, in order to access the effects of the rolling method – different roll diameters, different roll speeds, one stationary roll – in terms of deformation pattern and consequent textures. Their study also focused the effects of rolling reversal by several routes (RD, TD and ND reversal between each pass, see Figure 25), attempting to achieve the ideal shear texture. Their conclusions are in agreement with those regarding aluminum alloys.

Sakai and co-workers [2001] performed asymmetrical rolling on AA5052 using a single roll drive and 2 passes, each one imposing a 50% reduction in thickness. The rolling process was performed at 260°C, and a conventional route was also performed, for comparison. The friction was maximized by spreading alumina powder in an ethanol solution over the surface of the rolls. They were able to produce a sheet with {001}<110> texture, which spread after annealing, originating a random orientation structure. The resulting r values were close to 1, with little variation, which constituted an improvement relatively to the conventionally rolled specimens - Figure 26.

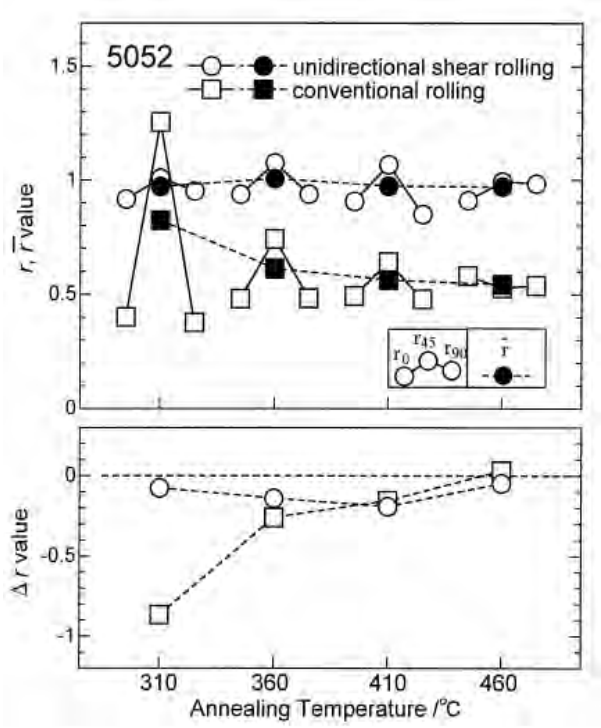

Figure 26: r values of asymmetrically and conventionally rolled AA5052 sheets (performed at 260°C), after different annealing treatments [Sakai et al, 2001].

Jin and Lloyd [2005] performed asymmetrical rolling on an AA5754. A 2.5mm thick sheet, was rolled with two different speed ratios (1.5 and 2), and also with and without reversion between each rolling pass. The total thickness reduction was 56%, obtained in 2 passes. They achieved texture modification especially a reduction in the cube component after reverse asymmetrical rolling, but no shear texture components Their procedure lead to the randomization of texture and reduced planar anisotropy, but the mean *r* value was not improved.

García de Lomana *et al*, [2004] performed asymmetrical rolling on AA1050 and AA5754, using roll speed ratio of 2. Despite having used thickness reductions per pass of 50%, textures were only near to ideal shear texture components. *r* values were calculated from texture data. The mean value of *r* increased after recrystallization (during which texture components were retained) but the Δr value increased as well, indicating undesired anisotropy.

Besides texture modification, asymmetrical rolling is also used as a mean for achieving grain refinement, since it imposes severe plastic deformations on the sheet. Cui and Ohori [2000] used asymmetrical rolling as an alternative to the traditional severe plastic deformation methods as a

mean to obtain grain refinement in pure aluminum. They supported the explanation for the grain refinement mechanism through grain rotation by using EBSD data and measuring the misorientations of grains. They tested several amounts of total thickness reduction, namely 65.2, 85.5 and 92.3%. Asymmetrical rolling was performed using a speed ratio of 1.4 and thickness reduction per pass of 0.2mm. They found that asymmetrical rolling could originate a fine grain structure, even with relatively low values of total thickness reduction, and that the grain size obtained (about 2μm) could be retained for annealing temperatures up to 200°C - Figure 27. Moreover, they compared asymmetrically rolled sheets with conventionally rolled ones having higher reduction in thickness (91.3% vs 65.2%). Despite having gone through a higher amount of strain, the conventionally rolled specimens showed little evidence of high angle boundaries, and hence, grain refinement, when compared to the equiaxed grain structure of asymmetrically rolled specimens. This observation leads to the conclusion that the presence of shear strains is of fundamental importance when seeking to obtain grain refinement, and plane strain compression alone is not the way to achieve this goal.

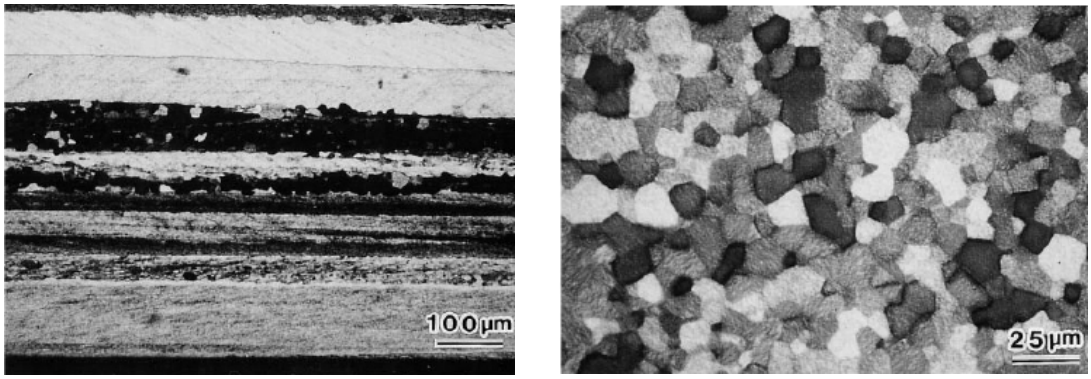

a *b*

Figure 27: Optical microstructures throughout thickness in 91.3% conventionally (a) and asymmetrically (b) rolled 1050 sheets annealed at 250°C for 4hours [Cui, Ohori, 2000].

Kim *et al* [2002] performed asymmetrical rolling on AA1050-O with the dual purpose of texture optimization and grain refinement. He used rolls with different diameters rotating at the same speed and tested several circumferential speed ratios (1.25, 1.5, and 2) aiming to obtain the best shear strain distribution along the sheet's thickness. Moreover, he tested the influence of reversing the rolling route between each pass. He found that, for the conditions considered, he could not obtain shear texture components fully spread along the sheet's thickness, and that the most efficient way of obtaining refined and homogeneous grain structures was to keep the rolling path constant.

Jin and Lloyd [2004a] performed asymmetric rolling (ASR) followed by annealing in order to to produce very fine grain sizes in AA5754. Annealing at 250°C produced grain sizes as small as 1 μm, and the tensile response of this fine-grained material has been compared with that of other fine-

grained alloys produced by alternative methods. The material was demonstrated to obey the Hall-Petch relation for all annealing treatments. Following this work, Jin and Lloyd [2004b] demonstrated that it was possible to achieve a good combination of strength and ductility by producing a duplex grain structure after asymmetrical rolling followed by annealing.

3.7. Chapter conclusions

In the above works, the asymmetrical rolling process is used with two different purposes. The first one is the optimization of crystallographic texture of the sheets towards preferred texture components (shear texture components), in order to improve *r* values and hence, formability. Improved *r* values were obtained by Sakai [Sakai *et al*, 2001] on asymmetrically hot-rolled AA5052 after annealing treatment. However, no information on the actual mechanical response of asymmetrically rolled sheets is available, even though a comparison with conventionally rolled sheets in similar conditions is shown. As for grain refinement, Cui and Ohori [2000] have shown the difference in grain size and morphology when rolling AA1050 by the asymmetrical and conventional methods. But once more, the respective mechanical response is not shown. Therefore it seems important to evaluate the mechanical responses of asymmetrically rolled and annealed aluminum sheets, and compare those with conventionally rolled sheets, as a way to correlate the texture and grain size differences achieved by using asymmetrical rolling.

Chapter 4 - Preliminary experimental tests

The present chapter describes procedures and results obtained when studying the asymmetric rolling and annealing of 1050-O sheets. Preliminary procedures have the purpose to gain knowledge of the rolling process and its variables, as well as establish relations between rolling and annealing procedures and the consequent mechanical response. The rolling variables such as total thickness reduction, thickness reduction per pass and roll speed ratio are discussed. The annealing treatments are introduced as the way to access the impact of the processing conditions on the material's strain hardening and maximum uniform strain, the indicators of formability on a tensile test.

4.1. Material and procedures

The material used for all experiments was an 8mm thick 1050 sheet, subjected to recrystallization treatment performed at 343^{o}C for 1 hour (as proposed by Lopes *et al*, [2003]). The purpose of this procedure was to obtain a high volume fraction of recrystallization texture components, and lower the sheet's flow stress and hardness, thus facilitating the subsequent rolling procedure.

The rolling device was a house-built rolling mill, having two rolls of equal diameter (180mm), each one powered by an electric motor / speed variator assembly and controlled by a computer through specific software, developed at the University of Aveiro. The software offers the possibility of setting the speed of the upper and lower rolls, as well as their rotation direction independently. The controller uses a closed-loop control system, in order to keep the speed at the required values. Speed ranges from 0 to 15 rpm, which corresponds to a maximum circumferential speed of about 0.071m/s – see Appendix C.

Tensile test specimens were cut from the original 8mm thick sheet in three directions, and then recrystallized using the above mentioned parameters. Tensile tests were performed at room

temperature, in order to obtain reference data for the sheet's mechanical response. The results are shown on Figure 28.

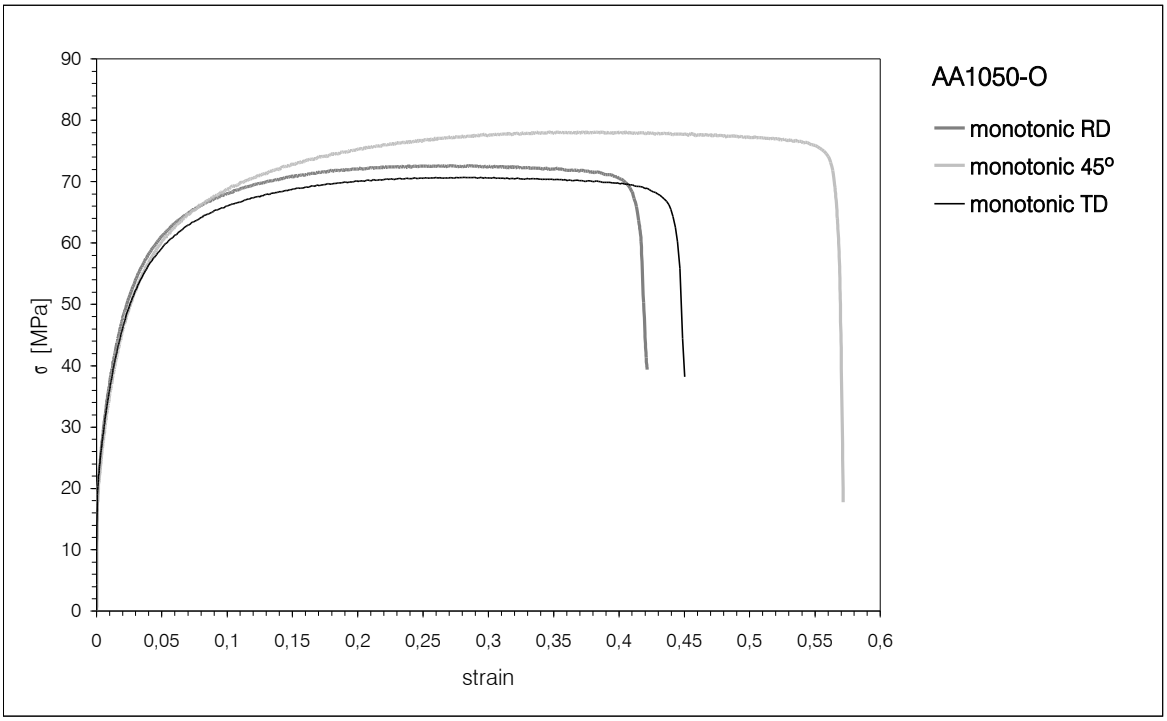

Figure 28: Monotonic tensile tests of the AA1050 8mm thick sheet after heat treatment at 343ºC for 1 hour. Rolling direction (RD), Transverse direction (TD) and 45º from rolling direction.

4.2. Tensile response of rolled and annealed specimens

4.2.1. Objectives

Preliminary rolling experiments had the purpose of accessing the material's and the rolling mill's response to the various rolling process variables, such as rolling speed, lubrication, thickness reduction per pass (RPP), total reduction and roll speed ratio. The first rolling experiment was used to compare the mechanical response of specimens rolled by both asymmetric and conventional procedures, according to a single and fixed set of variables - roll speed, total reduction, RPP.

4.2.2. Material and procedures

Samples of approximately 250mm wide and 300mm long were rolled conventional and asymmetrically rolled using the parameters on Table 2. The parameters were chosen based on rolling

experiments performed previously by the author (roll speed, RPP) as well as on literature data [Kim *et al*, 2002](total reduction). In their work Kim *et al* started with a 6.5mm thick sheet and performed rolling down to ≈0.58mm, which corresponds to a 91% reduction in thickness. When performing asymmetrical rolling, they used a pair of rolls rotating at the same speed but having different diameters. The rolls speed ratio was approximately 2, and the maximum circumferential speed was about 0.045m/s. In these first experiments, a lower circumferential speed was used, about 0.028m/s, since it was observed by the author that this would minimize sheet deviations due to instabilities generated by asymmetric rolling conditions.

Maximum roll speed	Roll speed ratio	Thickness reduction per pass	Total thickness strain	Annealing temperature	Annealing time
6 r.p.m. (0.028m/s peripheral speed)	conventional rolling: 1:1 (6/6 r.p.m.); asymmetrical rolling: 2:1 (6/3 r.p.m.)	0,2 mm	Final thickness = 0,6mm Total thickness strain = 2,7 (thickness reduction=92.5%)	195°C	1h

Table 2: Rolling conditions for first preliminary experiments.

During asymmetrical rolling, the sheet was turned 180° around the TD axis, attempting maximize shear strain in each pass. It would also be possible to choose amongst other reversion methods, as described in Figure 25. This reversion method was thought to promote shear strain more effectively than unidirectional rolling. In the case of conventional rolling, no rotation between each pass was implemented.

After rolling, a set of samples was subjected to an annealing treatment at 195°C for 1 hour. Once more, the annealing treatment was chosen according to Kim *et al* [2002], in order to obtain a first measure of the material's response to the sequence of rolling / annealing. Tensile specimens were cut from the sheet and TD tests were performed in as rolled and annealed specimens, from both asymmetrical and conventional rolling.

4.2.3. First tensile test results

Tensile test results are shown on Figure 29. When analyzing the plot, the first conclusion is that the annealing treatment caused both the flow stress and the extension of asymmetrical and conventional specimens to decrease. If the decrease in flow stress was already expected, the decrease in uniform extension is unexpected, since the annealing treatment has the purpose of restoring some of the material's ductility at the expense of strength. The second observation is related to the small, but consistent difference between asymmetric and conventional specimens. It can be observed that the former have higher flow stress, in both rolled and annealed conditions.

These results show that the asymmetrical rolling procedure is affecting the material's

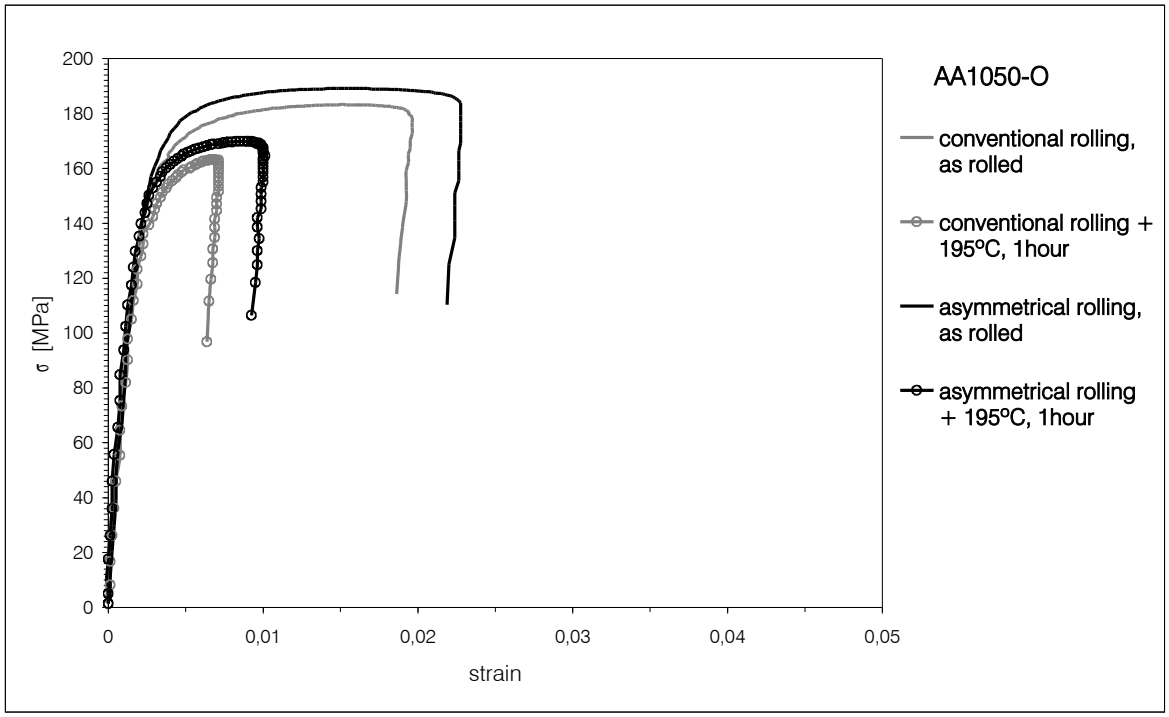

Figure 29: TD tensile test results. Conventional and asymmetrically rolled specimens. As rolled condition and after annealing at 195ºC for 1 hour.

mechanical response, but the decrease in uniform extension cannot be readily explained by current data. Thus, the study of the asymmetrical rolling process must be extended, and the influence of each process variable must be accessed.

4.2.4. Influence of annealing time

Since the tensile tests from the annealed specimens rendered unexpected results, a set of additional rolling experiments was planned, aiming to clarify the influence of the annealing time. Additionally, the total reduction in thickness, or thickness strain, was varied towards smaller values. The purpose of this was to obtain more data on the tensile response of the material as a function of rolling conditions. Specimens were rolled using parameters on Table 3. TD tensile tests were performed on rolled and annealed specimens.

Maximum roll speed	Roll speed ratio	Thickness reduction per pass	Total thickness strain	Annealing temperature	Annealing time
1. 6 r.p.m. (0.028m/s peripheral speed)	conventional rolling: 1:1 (6/6 r.p.m.); asymmetrical rolling: 2:1 (6/3 r.p.m.)	0.2 mm	0.5	195ºC	1h
			1.2		3h

Table 3: Rolling conditions for preliminary tests: influence of annealing time and thickness strain.

Results are shown on Figure 30, for the conventionally rolled, and on Figure 31 for the asymmetrically rolled specimens. As a reference, a monotonic tensile curve for a recrystallized sample is also displayed. The overall trend is similar in both cases. Specimens rolled with lower total reduction (strain=0.5) present lower flow stress when compared with those deformed up to strain=1.2 in thickness, which was already expected. After annealing, 0.5 specimens show a decrease in flow stress, and a small increase in uniform extension. In the case of the 1.2 specimens, there is a decrease in flow stress, but the uniform extension does not increase (it decreases in some cases), for both conventional and asymmetrically rolled specimens. This behavior is similar to the one already observed before (see Figure 29).

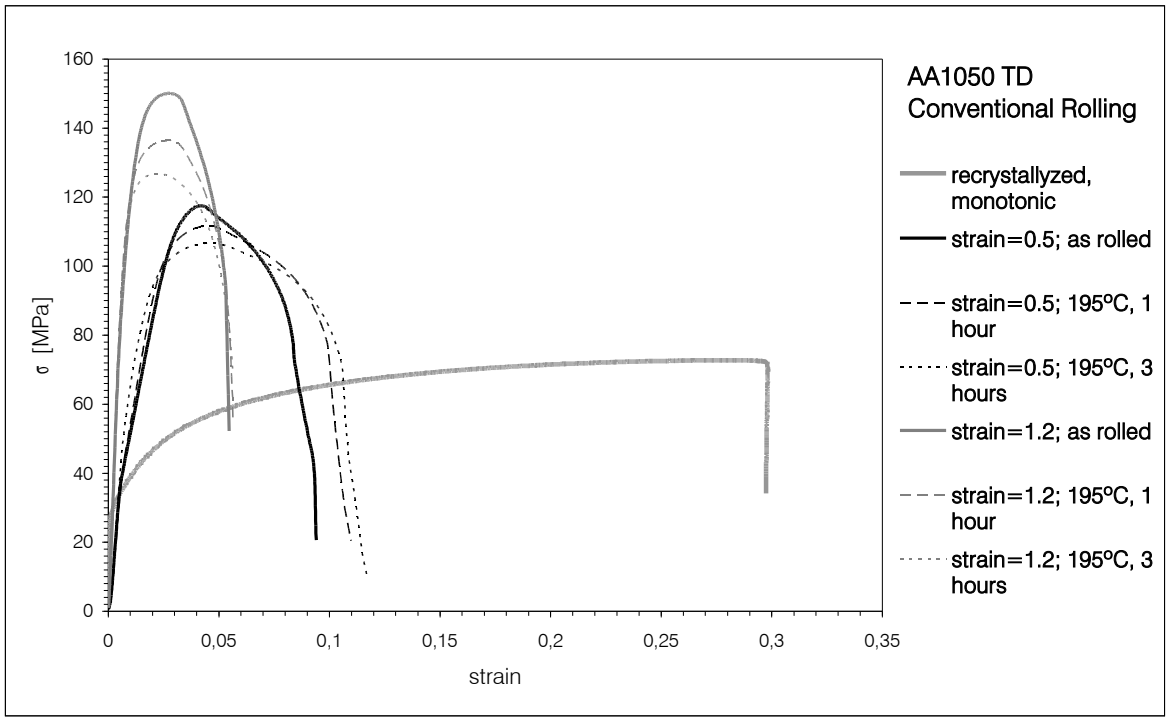

Figure 30: TD tensile tests of rolled and rolled + annealed specimens. Conventional rolling up to 0.5 and 1.2 thickness strain. Annealing treatments performed at 195ºC for 1 hour / 3 hours.

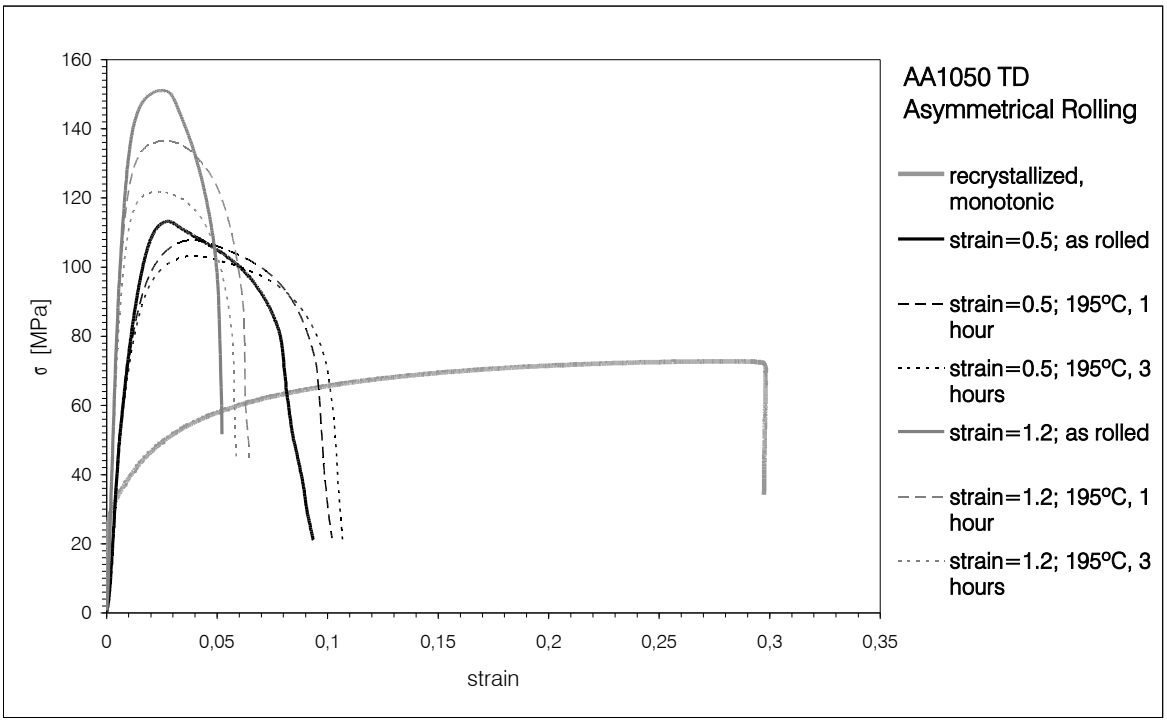

Figure 31: TD tensile tests of rolled and rolled + annealed specimens. Asymmetrical rolling up to 0.5 and 1.2 thickness strain. Annealing treatments performed at 195ºC for 1 hour / 3 hours.

The decrease in uniform extension seems to occur for sufficiently high values of thickness reduction only. For specimens deformed up to strain=0.5 in thickness, such a decrease is not present. Given the current observations, there are two ways to proceed the investigation concerning the influence of rolling parameters on the mechanical behavior:

- consider smaller values of thickness reduction and optimize the remaining parameters (roll speed ratio, thickness reduction per pass);
- consider higher values of thickness reduction and investigate annealing treatments further, trying to reverse the decrease in uniform extension observed.

The second option was chosen because imposing higher strains is one of the means of promoting grain refinement, by grain subdivision mechanisms [Hughes, Hansen, 1997]. Since grain refinement is one of the purposes of this work, along with texture optimization, imposing higher strains seems to be the best way to achieve this goal.

4.2.5. Influence of annealing temperature

The annealing temperature was increased, as an attempt to obtain improved uniform extension. Total thickness strain was also increased, trying to create conditions for grain refinement. Specimens were rolled according to conditions on Table 4. TD tensile tests were performed after annealing and water quenching.

Maximum roll speed	Roll speed ratio	Thickness reduction per pass	Total thickness strain	Annealing temperatures	Annealing time
6 r.p.m. (0.028m/s peripheral speed)	conventional rolling: 1:1 (6/6 r.p.m.); asymmetrical rolling: 2:1 (6/3 r.p.m.)	0.2 mm	≈1.6 up to ≈2.6	225°C 250°C 265°C 275°C	3h

Table 4: Rolling and annealing variables for conventional and asymmetrical processes. Extension of annealing time and temperature.

Figure 32 and Figure 33 compile the data obtained from the tensile tests in two parameters, the ultimate tensile strength (UTS) and the uniform strain, respectively. These two parameters were chosen as indicators of the material's strength and ductility. In the case of the UTS, (Figure 32) the main trend is the decrease of this parameter as the annealing temperature increases. But in the case of specimens annealed at 250°C, a very different trend is observed. There is an strong decrease of UTS as the strain imposed during rolling is increased. Moreover, there are not noticeable differences between asymmetrically and conventionally rolled specimens, even considering the difference observed for 225°C.

In the case of the uniform strain (Figure 33) it is possible to observe the increase of this parameter as the annealing temperature increases. Once more, the thickness strain imposed during rolling seems to have little influence on the sheet's response. It is also interesting to observe the amount of variation of the uniform strain when compared with the variation of annealing temperature. Specimens annealed at 265°C have several times more uniform strain than those annealed at 250°C, despite the relatively low difference in temperature. The rolling and annealing experiments allowed to draw some conclusions regarding the material's response:

- it was possible to access the material's general response to the rolling/annealing experiments;
- the general trend is the decrease in tensile strength and the increase in uniform strain, though in a non-linear fashion;
- the influence of the amount of thickness strain imposed during rolling is not very significant, except in the case of the tensile strength for specimens annealed at 250°C;

- when performing a direct comparison between asymmetric and conventionally rolled specimens, there are little differences in mechanical response.

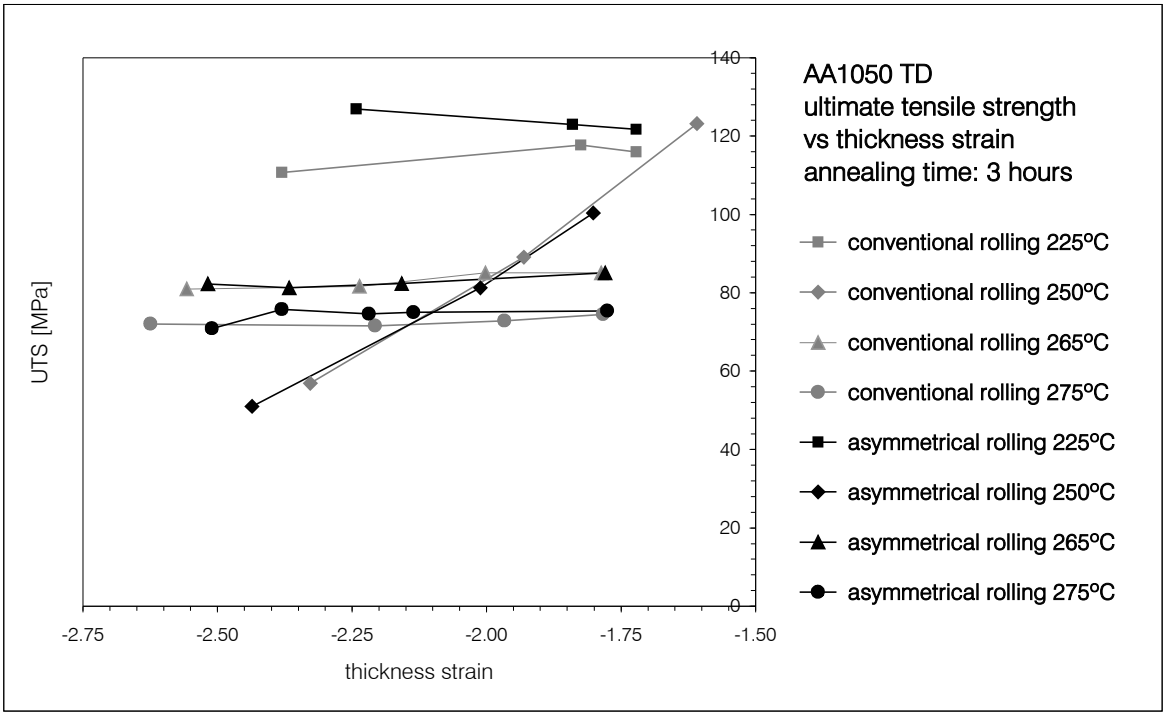

Figure 32: Ultimate tensile strength for specimens rolled and annealed for 3 hours. Conventional and asymmetrical rolling. Thickness strain from 1.6 to 2.6. Annealing temperatures :225ºC, 250ºC, 265ºC and 275ºC.

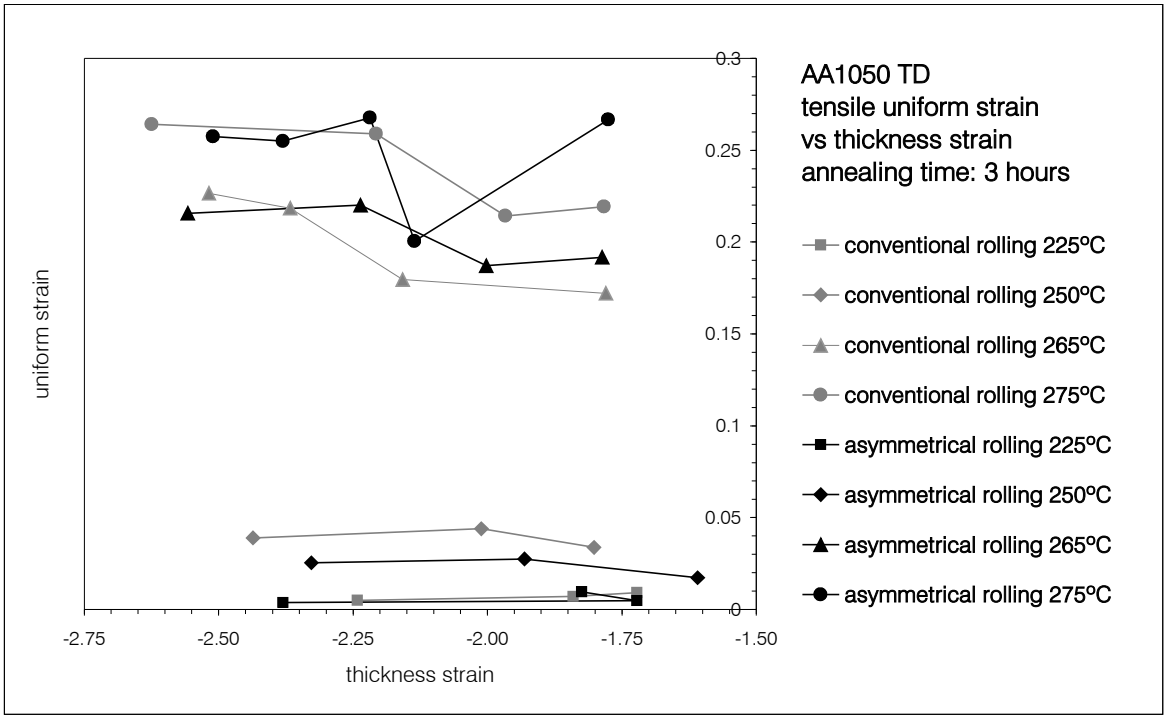

Figure 33: Uniform strain for specimens rolled and annealed for 3 hours. Conventional and asymmetrical rolling. Thickness strain from 1.6 to 2.6. Annealing temperatures :225ºC, 250ºC, 265ºC and 275ºC.

This last conclusion points out that the asymmetrical rolling procedure is probably not optimized. Since the amount of shear strains imposed, as well as their spread throughout the entire sheet thickness during rolling, are the main differences between the asymmetrical and the conventional rolling process, perhaps not enough shear is being imposed to obtain real differences in mechanical behavior. It is, thus necessary to access the influence of rolling parameters on the amount and distribution of shear strains on the sheet.

According to Kim and Lee [1999], the amount of shear strains and their distribution along the sheet's thickness is directly related to the ratio of shear to compression strain imposed to the sheet. This amount is, in turn, directly related to the amount of thickness reduction imposed in each pass. As seen previously, Kim and Lee studied three different rolling schedules, each one with different amounts of thickness reduction in each pass. They found that the best results in terms of texture could only be obtained using the higher reduction per pass.

On the previous rolling procedures, the amount of thickness reduction per pass used was 0.2 mm, a constant and absolute value. Kim and Lee [1999] obtained the best results by using two passes: the first one reduced 1 mm, the second 0.6 mm. The initial sheet was 2 mm thick, so the

percent reductions were 50% and 60%, respectively. For a better analysis of the reduction per pass used in this work and in Kim's work, the following plot was created (Figure 34).

By analyzing the plot, one can reach the conclusion that the amount of RPP used by Kim and Lee, which was told to lead to the best texture results, is much higher than the one used so far on the rolling experiments. However, it is convenient to remember that the initial sheet thickness used was 2mm only, as opposed to the 8mm of the current work.

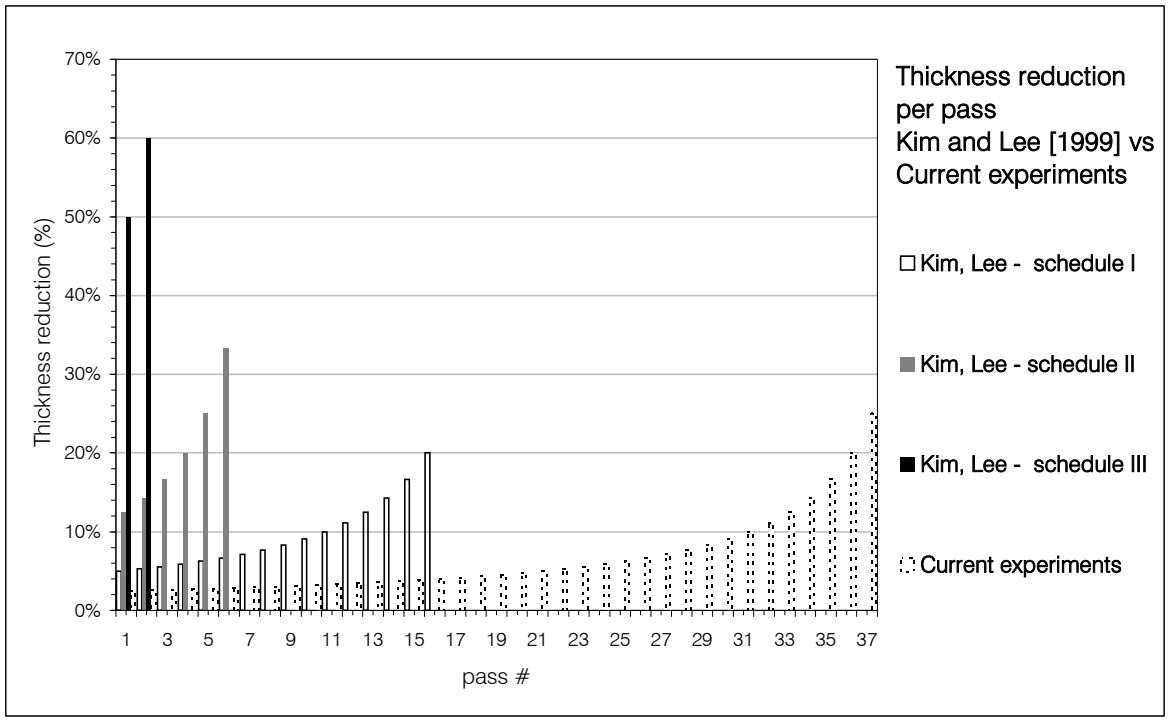

Figure 34: Thickness reduction per pass used on asymmetrical rolling experiments. Comparison among Kim and Lee experiments [1999] and current experiments.

The majority of the rolling passes have a much lower RPP than the one used by Kim and Lee on their “schedule I”, which produced texture results not much different from plane strain textures, typical from conventional rolling, and practically no shear texture components. This analysis seems to confirm the earlier statement that the rolling procedure is not yet optimized. Specifically, the RPP should require an increase, in order to achieve an improvement in the mechanical response of asymmetrically rolled sheets.

4.2.6. Influence of the reduction per pass

In order to access the influence of the amount of RPP on the shear strain distribution along the sheet's thickness, a set of samples having dimensions 50x250x8mm was marked in one of its lateral sides (parallel to rolling direction), with lines perpendicular to the sheet plane. These lines become oblique after asymmetrical rolling, indicating the amount of shear strains. Since shear strains are essential for the formation of shear textures, the shear deformation is a good indicator for the presence of shear texture on the sheet. The inclination angle was observed using an optical microscope.

Several different reductions per pass were used: a constant reduction of 0.2mm; 10%, 25% and 35% in thickness. Initial 8mm thick sheets were machined on the thickness sides parallel to the rolling direction, in order to be traced clearly with vertical marks. These marks evolved from vertical to a different angle, according to rolling conditions. Results are shown on Figure 35.

a) initial sheet tracing

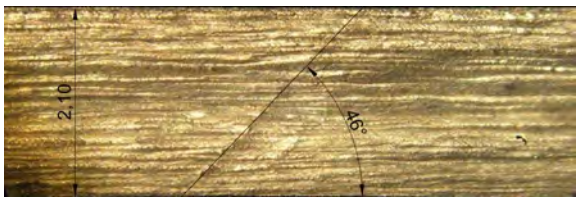

b) 0.2mm RPP

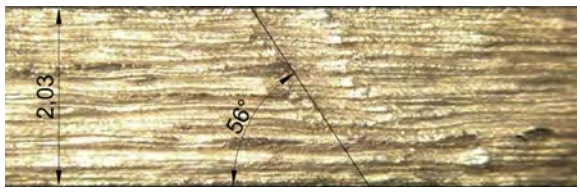

c) 10% RPP

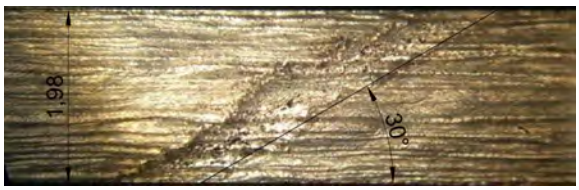

d) 25% RPP

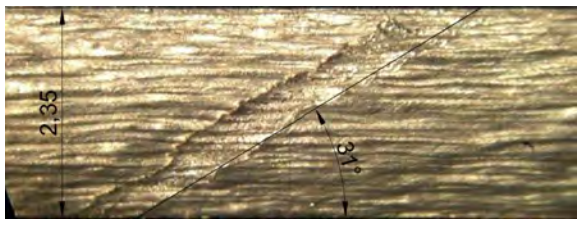

e) 35% RPP

Figure 35: Influence of thickness reduction per pass (RPP) on shear strain distribution through thickness.

It can be observed that shear distribution profiles are affected by the RPP, but not in a linear fashion. For 0.2mm, the profile appears uniform and continuous, with an angle of about 46^{o} from the horizontal. The side of the sheet didn't remain flat, probably due to some compression strain which

caused the appearance of a wavy surface, especially in the center area. For RPP of 10%, the shear profile is irregular. It seems that the down side of the sheet was subjected mainly to compression, whereas the upper side was subjected to shear deformation. For RPP of 25%, the profile observed is regular and the measured angle is about 30°. There is a slight tendency for distortion near the sheet surfaces, which indicates higher shear strain in those areas. For RPP of 35% there is not much difference in the profile angle relatively to 25% RPP (31°) , but it must be noted that the sheet thickness is greater in this case (the total deformation imposed was different), thus affecting the comparison.

Based on these results, new rolling experiments were carried out. Sheets were asymmetrically rolled using approximately 20% thickness reduction per pass, since this value provided a good combination of shear strain and absence of rolling problems. In fact, using higher values of RPP (35%) caused the rolling mill to have difficulties and sometimes even stop because of the excess rolling torque. Thickness values were measured between each pass, and the reduction was then calculated and adjusted in order to achieve values around the desired 20%. After rolling, sheets were annealed at 265°C for 1 hour, 2 hours and 3 hours.

Maximum roll speed	Roll speed ratio	Rolling reduction per pass	Total thickness strain	Annealing temperatures	Annealing time
6 r.p.m. (0.028m/s peripheral speed)	conventional rolling: 1:1 (6/6 r.p.m.); asymmetrical rolling: 2:1 (6/3 r.p.m.)	0.2 mm (conventional rolling) 20% (asymmetrical rolling)	≈1.6 up to ≈2.6	265°C	1h 2h 3h

Table 5: Rolling and annealing variables for conventional and asymmetrical processes. Extension of thickness reduction per rolling pass.

TD tensile tensile tests were performed after annealing. Figure 36 shows the tensile curves of specimens with total thickness strain of about 2.5 after annealing at 265°C for 3 time intervals, 1, 2 and 3 hours. From the observation of the plot, the influence of the amount of RPP becomes evident. Specimens annealed for 1 hour show similar levels of maximum stress, but very different values for uniform strain. ASR specimens have about 6% extension, whereas CR specimens do not go beyond 2%. After 2 hours at 265°C, asymmetrically rolled (ASR) specimens show decreased flow stress, but about two times the amount of uniform strain, when compared to conventionally rolled (CR) specimens. But when the annealing time is increased to 3 hours, the differences in mechanical response are even more obvious. In this case, CR specimens show a strong decrease of flow stress, though the uniform strain improves significantly. But for the same conditions, ASR specimens show a very similar mechanical response to the one observed for 2 hours of annealing time (in fact, there is a slight increase in flow stress and decrease in uniform strain).

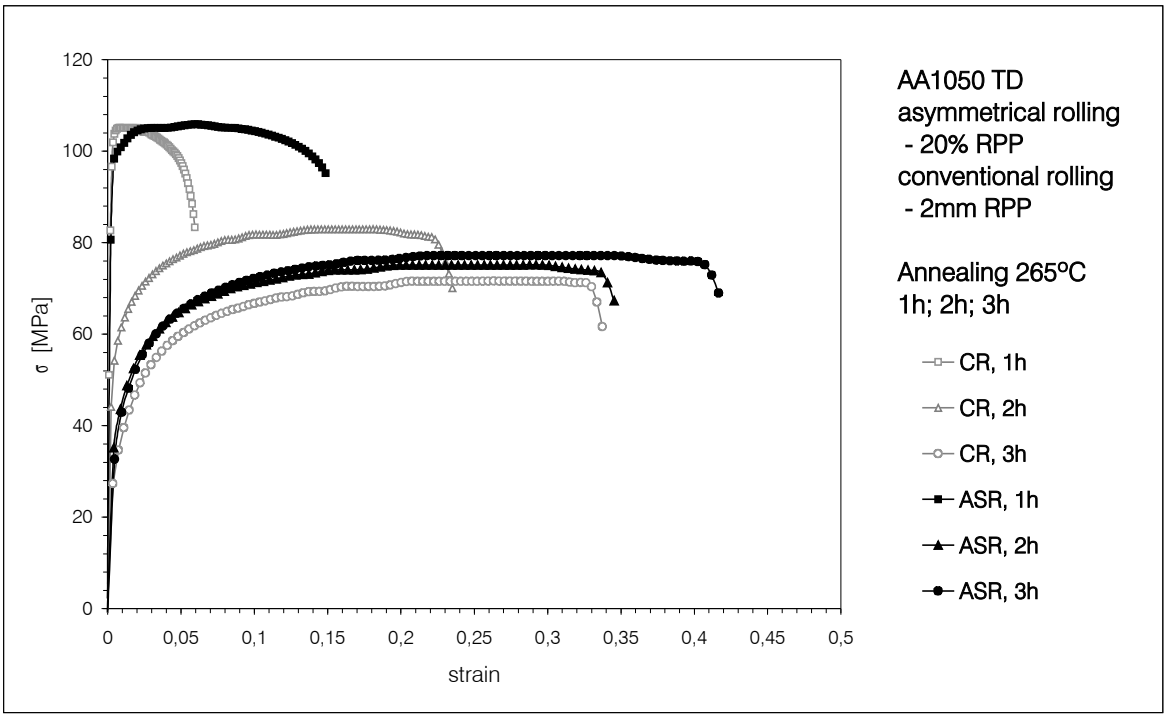

Figure 36: TD tensile tests of rolled and annealed specimens. ASR specimens rolled with 20% RPP (high RPP); CR specimens rolled with 0.2mm RPP (low RPP). Total thickness strain approximately 2.5 for all specimens. Annealing times: 1/2/3 hours.

The explanation for this fact may lie on the nature of textures developed during rolling, and their evolution on annealing. Conventional rolling originates typical deformation texture components – Copper, Brass – on aluminum, which evolve towards recrystallization texture components, such as Cube and Goss, on annealing. Asymmetrical rolling may have generated shear texture components, which have been shown to be retained after annealing treatments, even at higher temperature [Lee, Kim, 2001]. The differences in texture may be, at least partially, the cause of the difference observed.

Though the previous results clearly show the influence of the amount of thickness reduction per pass imposed in the rolling procedure, it must be noted that the high RPP value (20%) was only applied in the asymmetrical rolling procedure. In order to produce valid comparison results between the two processes, the same value of RPP must be used in the conventional process.

Tensile stress strain curves of specimens rolled with RPP values of about 20% (both CR and ASR), and annealed at 265ºC for 2 and 3 hours are shown on Figure 37. For comparison purposes, the tensile curves of specimens with low RPP are also shown. The plot shows that the low RPP specimens have much higher tensile stress relatively to high RPP specimens, but also lower uniform extension. For 2 hours of annealing time, the high RPP ASR specimens display similar response to CR specimens, but there is an obvious curve crossing, which usually indicates differences in texture

[Bacroix *et al*, 2001] (though other microstructural characteristics, such as grain size and morphology may also influence this result). When considering 3 hours of annealing time, it is possible to observe an obvious difference in tensile response between asymmetrically and conventionally rolled specimens. ASR specimens show increased flow stress though slightly less uniform strain relatively to CR specimens.

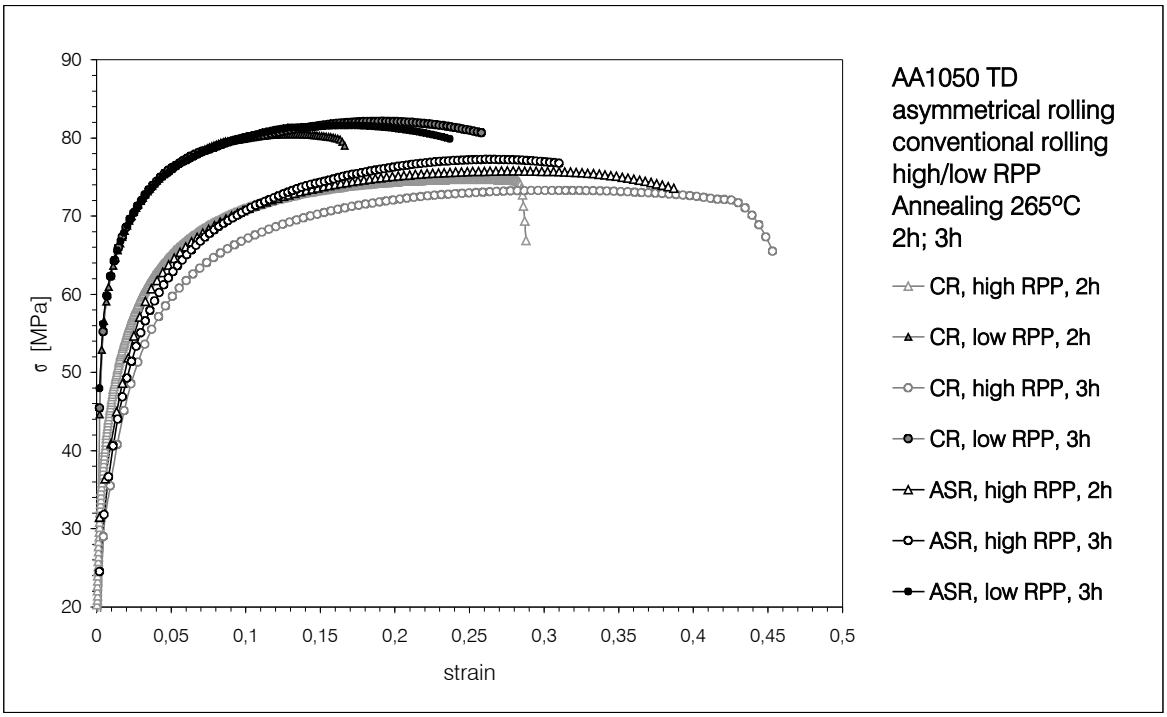

Figure 37: TD tensile tests of rolled and annealed specimens 265ºC, 2h. Comparison between low and high RPP values. Total thickness strain approximately 2.5 for all specimens.

In order to test the hypothesis of crystallographic texture differences, tensile tests were carried out in two additional directions, rolling and 45º from rolling direction. This enabled evaluation of the sheets' anisotropy, and hence obtain clues about possible differences in texture.

Figures 38 to 41 show tensile curves for RD, 45º and TD directions, for ASR and CR specimens after annealing at 265ºC for 2 hours (Figures 38 and 39) and 3 hours (Figures 40 and 41). From the observation of the plots, it is possible to conclude that there are important differences in anisotropy between ASR and CR specimens for the current conditions. In the case of ASR specimens, increasing the annealing time from 2 to 3 hours causes the 45º tensile curve to approach the RD and TD curves, indicating a mechanical response close to isotropic. Yet, the relative position of the curves remains the same. In the case of CR specimens, the increase in annealing time seems to have more impact on the mechanical response. This is especially visible on the TD tensile curve, which was the highest for 2 hours of annealing time, and becomes the lowest for the 3 hour treatment.

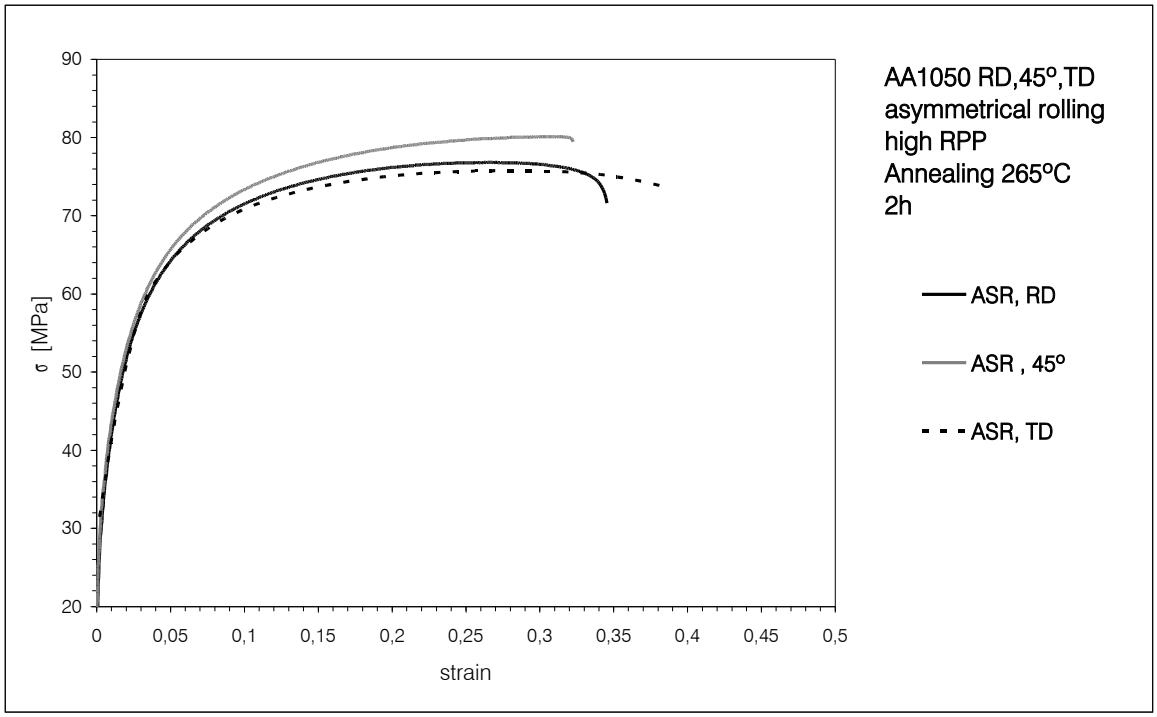

Figure 38: Tensile tests of asymmetrically rolled and annealed specimens at 265ºC for 2h. Comparison between RD, 45º and TD testing directions. High RPP values. Total thickness strain approximately 2.5 for all specimens.

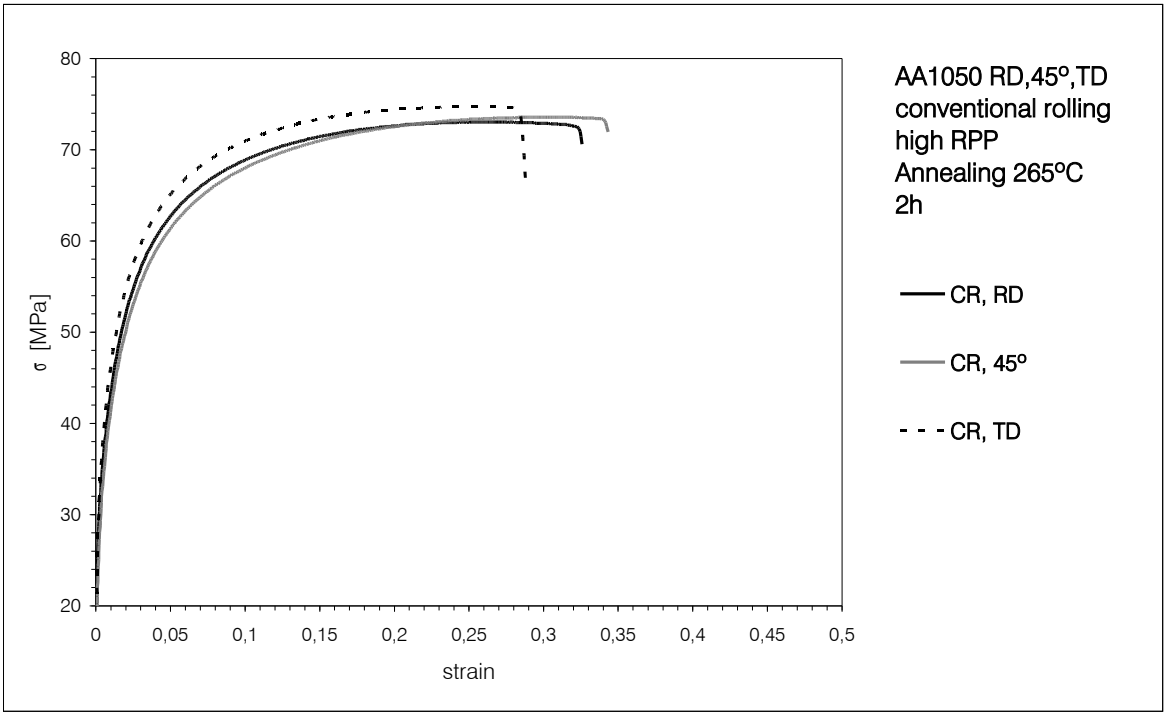

Figure 39: Tensile tests of conventionally rolled and annealed specimens at 265ºC for 2h. Comparison between RD, 45º and TD testing directions. High RPP values. Total thickness strain approximately 2.5 for all specimens.

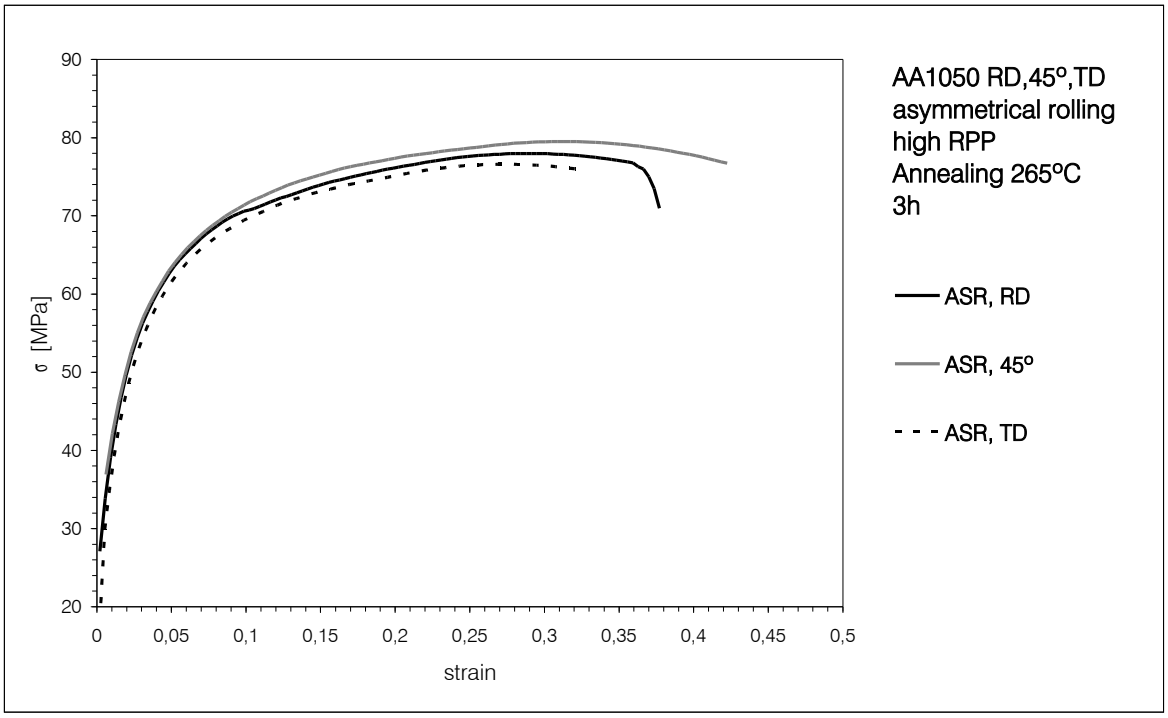

Figure 40: Tensile tests of asymmetrically rolled and annealed specimens at 265ºC for 3h. Comparison between RD, 45º and TD testing directions. High RPP values. Total thickness strain approximately 2.5 for all specimens.

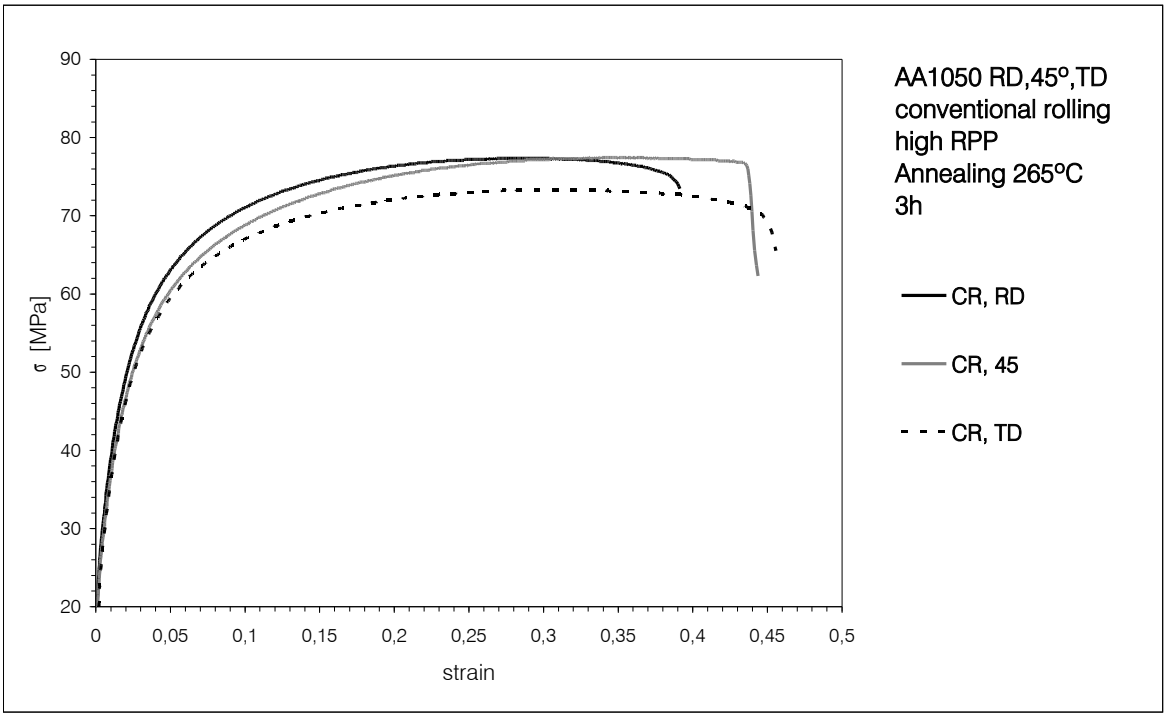

Figure 41: Tensile tests of conventionally rolled and annealed specimens at 265ºC for 3h. Comparison between RD, 45º and TD testing directions. High RPP values. Total thickness strain approximately 2.5 for all specimens.

4.3. Chapter conclusions

The purpose of this chapter was to test the influence of the main rolling and annealing parameters on the mechanical response of the sheets. It was shown that the most influencing parameter is the thickness reduction performed on each rolling pass (RPP). Low values for this parameter cause the mechanical response of asymmetrically and conventionally rolled specimens to become similar. When increasing RPP values, the most noticeable difference between ASR and CR specimens is the evolution of anisotropy for the annealing treatments considered. This difference points towards different crystallographic textures on asymmetrically and conventionally rolled sheets.

It is thus necessary to evaluate the asymmetrical rolling, as well as the annealing parameters in terms of crystallographic texture, and also grain size and morphology.

Chapter 5 - Texture, mechanical response and microstructure

Following the previous experimental tests, this chapter describes the procedures and results obtained when attempting to optimize the asymmetrical rolling procedure. Crystallographic texture data, tensile tests, shear tests and TEM observations are used to evaluate the results. The first step will be the evaluation of the influence of each ideal texture component on the mechanical response of the material, by means of numerical simulations. This will provide data for the correct interpretation of mechanical testing results. After this stage, crystallographic texture measurements are used to access the effectiveness of the asymmetrical rolling process in producing shear texture components. Mechanical testing coupled with crystallographic texture measurements will then be used to access the effects of asymmetrical rolling on strength and ductility of the sheets. These results will be completed with TEM observations, enabling the evaluation of grain size and morphology.

5.1. Effect of texture components – simulation[2]

Since asymmetrical rolling has been studied with the purpose of imposing shear strains through the sheet's thickness, an assessment of the individual impact of those shear texture components on the mechanical response of an AA1050 constitutes valuable data for the interpretation of mechanical tests. The crystallographic texture of real materials is generally spread around variable volume fractions of known orientations, plus a significant amount of random orientations. The assessment of the influence of an individual texture component, even in the case of strongly textured materials, becomes difficult. Numerical simulations provide a valuable tool for modeling the response of theoretical materials having ideal textures. This type of assessment has been performed before (using several types of models, e.g. [Barlat, 1987],[Hu,1998]), but not specifically focused on shear

2 simulations were performed by R.J. Alves de Sousa, see [Alves de Sousa, 2006].

texture components. Since those components are the main scope of this work, it becomes necessary to perform new simulations.

In this case, simulations using a polycrystal plasticity model were carried out. The model is based on the upper bound Taylor assumption and utilizes the notion of interacting slip systems (Gambin and Barlat, 1997) for the single crystal constitutive law. The implementation details are given in Alves de Sousa [2006].

A set of grains having crystal orientations around ideal components (cube ({100}<001>), copper ({112}<111>), and shear texture components ({001}<110>, {111}<110>, {111}<112> and {112}<110>) was subjected to tensile and simple shear boundary conditions. An orientation spread of + /- 15 degrees for each Euler angle was used to generate the grain orientation input data. The spread was generated in a simple linear way, since the main purpose of this procedure was to smooth the simulation curves. A more complex strategy has been used by Barlat [1987] to increase the accuracy in the calculation of yield surfaces for ideal texture components. A spread of orientations following a Gaussian distribution was used. A similar procedure has also been used by Hu *et al* [1998] when performing yield locus calculations for ideal orientations. Then, the simulated yield loci became smoother, approaching the yield loci obtained from experimental (real) textures. The current approach is not the most accurate way to generate the necessary spread around an ideal orientation, but it provides a quicker way to ensure the smoothing of simulation results.

The tensile and shear simulations are shown on Figure 43 and Figure 44, respectively. In the tensile test, the shear 2 component presents the highest stress level, followed by shear 4 and copper. Cube displays the lowest stress response, as well as lower strain hardening. The brass component stress level is similar to the shear 3 and 4 components, but its strain hardening is higher at the beginning and smaller towards the end.

For the case of shear test simulation (Figure 44), it is possible to observe that the Cube component provides the highest shear response, as well as very different strain hardening behavior when compared to other orientations. Nevertheless, its response is not monotonic. This observation is in good agreement with experimental shear tests performed in cube textured AA1050 specimens by Lopes *et al* [2003] and also with the modeling of the same tests performed by Yoon *et al* [2005]. The shear3 and shear2 textures are coincident for shear strains up to 0.15; after the point, shear3 stress response is lower. Copper, brass, shear1 and shear4 textures display similar responses up to 0.35 shear strain; then, the curves diverge and the shear1 texture curve reaches the highest stress value at the end of the simulation.

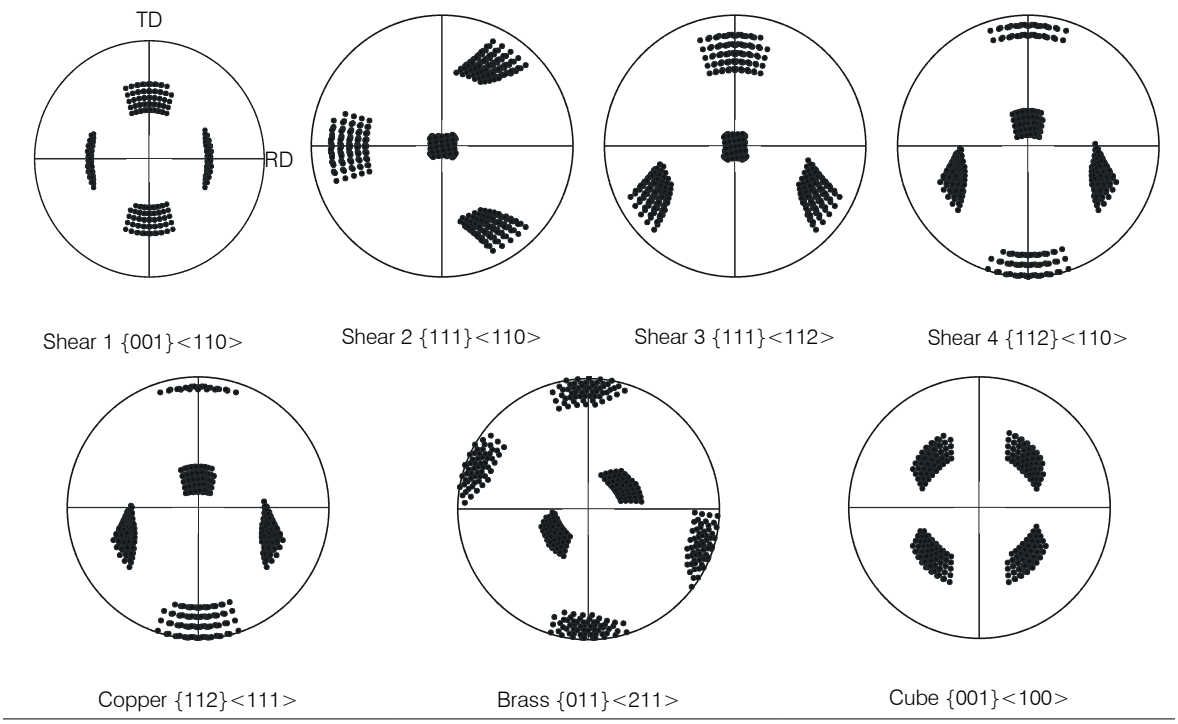

Figure 42: Representation of shear texture orientations (with an orientation spread of +/-15^o on a {111} pole figure.

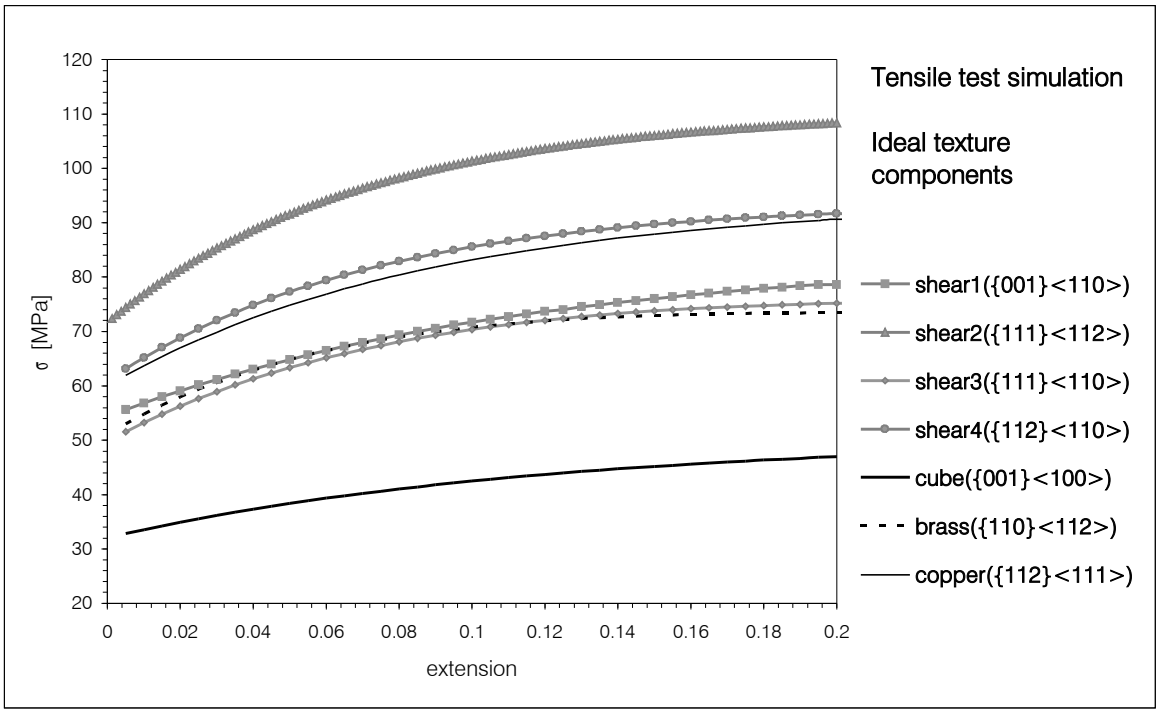

Figure 43: Tensile test simulation using grains having a +/- 15^o spread around ideal orientations.

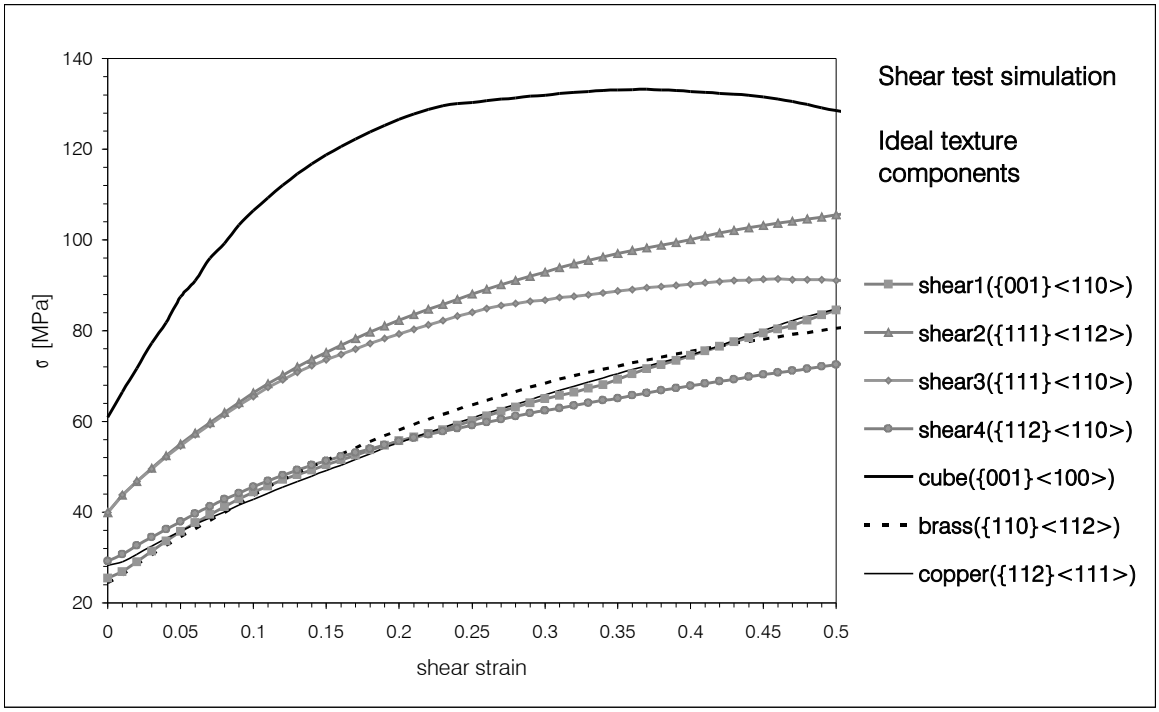

Figure 44: Shear test simulation using grains having a +/- 15º spread around ideal orientations.

5.2. Crystallographic texture evaluation

Since previous mechanical tests (Chapter 4) suggest that rolling parameters might be causing important crystallographic texture changes, a set of experiments was designed to evaluate the current rolling procedures and their actual influence on this material property. Since asymmetrical rolling texture results are available on literature, it was decided to reproduce rolling procedures used by Kim and Lee [1999, 2001], and compare the textures obtained. This would enable the current rolling procedures to be validated.

5.2.1. Experimental procedure

An 8mm thick 1050 sheet was recrystallized for 1 hour at 343ºC. This starting material was then rolled by the conventional method (identical roll speeds) down to 2mm thickness. From this 2mm sheet, two sets of sheet specimens were prepared: one set was directly rolled down to 0.4mm (80% reduction, $\varepsilon=1.6$), using asymmetrical rolling; the other set was previously recrystallized for 1 hour at 343ºC and asymmetrically rolled down to 0.4mm afterwards. This procedure enabled the evaluation of the intermediate annealing on the mechanical behavior and texture.

Kim [1999] proposed three different schedules when rolling asymmetrically each set of sheets, in order to compare the influence of rolling parameters on the final sheet texture. These schedules differ only on the amount of reduction per pass (RPP) used . Schedule 1 consists on using a constant reduction of 0.1mm per pass; schedule 2 consists on using 0.25mm reduction per pass; and schedule 3 uses only two passes, the first with 1mm, the next with 0.6mm. In all tests, the roll speed ratio was 1.5. Table 6 shows the comparison RPP values for each schedule.

Initial Rolling	Set #	Intermediate annealing	Asymmetrical Roll speed ratio	Total thickness strain	Reduction per pass	Schedule name
8mm down to 2mm in thickness (conventional rolling)	1	No	1.5	1.6 (2mm down to 0.4mm)	0.1mm (16 passes)	1
	2	343°C, 1 hour			0.25mm (6 passes)	2
					1mm + 0.6mm	3

Table 6: Rolling procedures used by Kim and Lee [1999, 2001].

5.2.2. Results

Schedule 1 and 2 were performed without major problems, but rolling sheet according to schedule 3 was not possible due to equipment limitations. Thus, the results presented are referred only to sheets rolled according to schedules 1 and 2. After rolling, texture specimens were cutout from the sheets. Texture results are shown on Figure 45 (as a reference, {111} pole figures of the main texture components can be found on Figure 42, or Appendix A). A pole figure for specimens subjected to conventional rolling + recrystallization + asymmetrical rolling through schedule 1 is not shown, since it is similar to the pole figure presented on Figure 45 f). The following observations can be derived:

- Texture on the starting material (8mm sheet, recrystallized at 343°C for 1 hour) does not indicate a fully recrystallized state. In fact, the most intense orientations seem to be near the Brass and S components.
- After conventionally rolled down to 2mm, the sheet shows strong amounts of one of the typical rolling texture components, Copper. After annealing at 343°C for 1 hour, this sheet develops some recrystallization texture components, such as Cube and Goss, but it seems to retain some of the Copper component from the rolling operation.
- The sheet conventionally rolled to 2mm and asymmetrically rolled according to schedule 1 presents typical rolling texture components, Copper, S and Brass. The texture of the sheet rolled according to schedule 2 (after previous conventional rolling down to 2mm) is very similar to the one rolled by schedule 1.
- The intermediate annealing (Figure 45f) does not seem to affect the final texture, when compared to the previous specimen (without annealing), except perhaps for the higher fraction of random orientations.

a) initial sheet (8mm) after recrystallization 343°C 1h

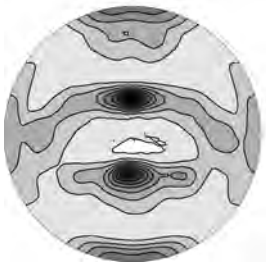

b) recrystallized 343°C 1h + conventionally rolled down to 2mm.

c) recrystallized 343°C 1h +conventionally rolled to 2mm + recrystallized 343°C 1h.

d) recrystallized 343°C 1h + conventionally rolled to 2mm + asymmetrically rolled by schedule 1.

e) conventionally rolled to 2mm + asymmetrically rollled by schedule 2.

f) conventionally rolled to 2mm + recrystallized 343°C 1 hour + asymmetrically rolled by schedule 2

Figure 45: {111} Experimental pole figures for crystallographic texture evaluation experiments.

After observing Figure 45, it became necessary to compare textures with the ones obtained by Kim. Figure 46 shows the experimental pole figures obtained for 1050-O after Asymmetrical rolling by schedules 1, 2 and 3, performed by Kim [1999]. It can be seen that for schedule 1 the texture is near the plane strain, similar to conventional rolling. As the reduction per pass increases, the texture approaches the shear deformation texture ({001}<110> and {111} <110>). Comparing Figures 45 d) and e) with Figures 46 a) and b), similar texture components for schedule 1 can be observed (45d) and 46a)), but for schedule 2 (45e) and 46b)) the textures are different. Kim obtained some shear components using schedule 2, but the best results are for schedule 3. Shear texture components are only obtained by rolling sheet using this schedule.

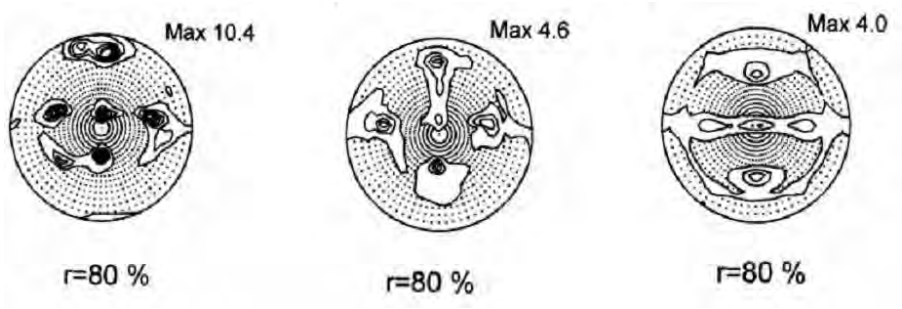

Figure 46: Experimental 111 pole figures obtained by Kim [Kim, Lee, 2001], for asymmetrically rolled specimens by schedules 1 (a), 2(b) and 3(c). Total reduction was 80%.

The importance of the thickness reduction per pass, or RPP, on shear texture development is consistent with the difference in mechanical response already observed in the previous chapter, between low and high RPP rolled specimens. Additional mechanical tests, coupled with texture assessments are necessary, in order to obtain a clear correlation between the shear texture development, the rolling conditions (especially the RPP) and the mechanical response.

At this stage, a change in the way textures are represented becomes necessary. Pole figures have been used so far, since they are also the most frequent representation found in literature on asymmetrical rolling. But the difficulty in identifying shear texture and other components in a pole figure, especially because of the pole multiplicity, lead the author to change texture representation to orientation distribution functions, or ODF. The $\varphi 2=0^{o}$ and $\varphi 2=45^{o}$ sections (see Figure 47 or Appendix A) are the ones where the most part of texture components can be easily identified. Thus, all textures from this point on will be represented by means of $\varphi 2=0^{o}$ and $\varphi 2=45^{o}$ ODF sections.

5.3. Mechanical testing

The mechanical response of sheets was partially addressed on the previous chapter. Now, that mechanical response will be completed with shear tests, and associated with the corresponding crystallographic texture and TEM observations, in order to provide an explanation for the differences in mechanical response already observed. The first step will be the assessment of the influence of the RPP on the production of shear textures on the sheet. Next, tensile and shear tests followed by annealing procedures will evaluate the mechanical response of the sheets. Finally, TEM observations will complement and help to understand the observations. A flowchart showing the planning of experimental tests is shown on Figure 48.

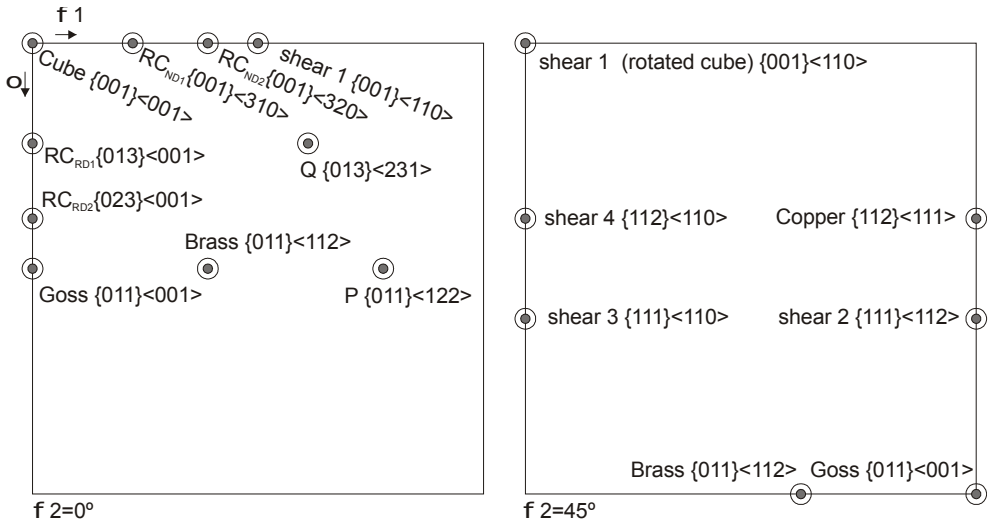

Figure 47: φ2=0° and φ2=45° ODF sections, showing the main texture components for fcc metals.

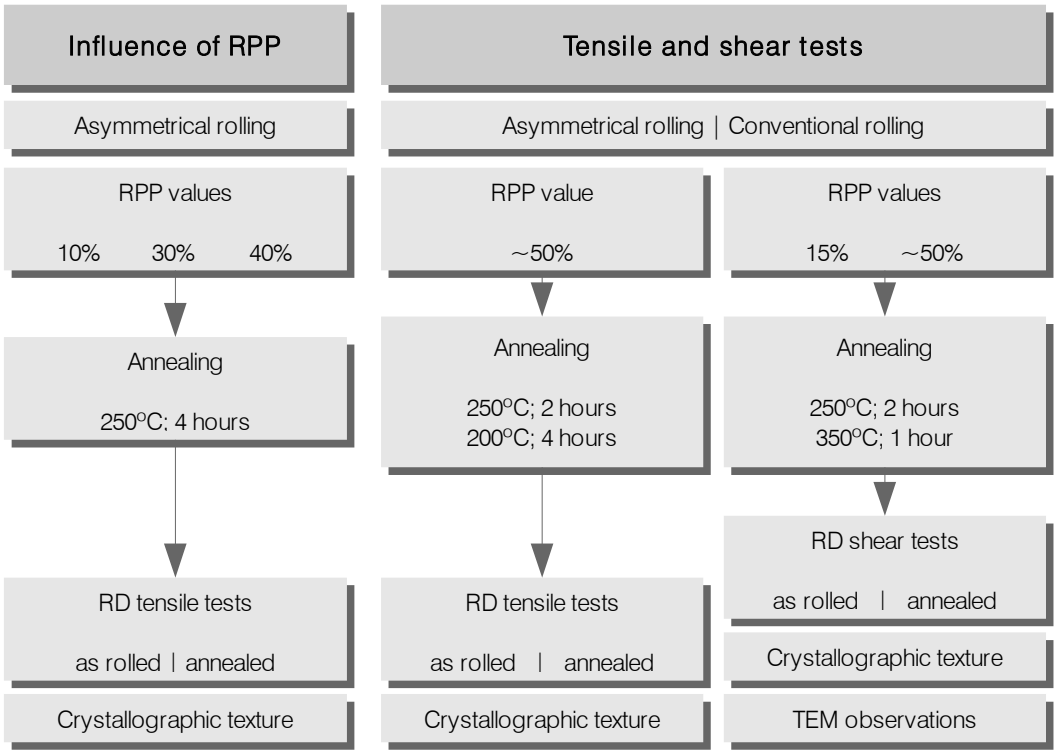

Figure 48: Flowchart of the experimental procedures.

5.3.1. Influence of thickness reduction per pass

Since the reduction per pass used on tests so far was apparently not big enough to cause significant effect on texture, that is, to cause the desired shear texture components to appear, new tests were planned. In order to achieve higher reductions per pass without causing the rolling mill to seize, the sheet width is now reduced, from 75mm to 30mm. This causes the rolling force to decrease as well, thus enabling RPP values to increase. However, specimens cut from these rolled sheets are only suitable for texture analysis, RD tensile tests and shear tests. TD and 45° tensile tests are impossible to perform, and hence an anisotropy assessment is compromised.

1050 sheets were recrystallized at 343°C for 1 hour and then asymmetrically rolled down to 0.5mm using roll speed ratio of 1.36 (an attempt to improve rolling performance) and RPP values of 10%, ~30% and ~40%. These are average values, since experimentally there were some variations. After rolling, specimens were cut from the sheets, for both texture analysis and RD tensile testing. Specimens were tested in as rolled condition and after annealing at 250°C for 4 hours with furnace cooling. Table 7 summarizes rolling conditions. Tensile and texture results are shown on figures 49 to 51. A comparison between all RPP values is shown on Figure 52.

Initial sheet	Type of rolling	Roll speed ratio	Total thickness strain	Thickness Reduction per pass	Annealing
8mm, Annealed 343°C 1h	Asymmetrical (ASR)	1.36	~2.8	10%	250°C, 4h
				30%	
				40%	

Table 7: Rolling conditions for optimization of thickness reduction per pass on asymmetrical rolling.

The choice of annealing temperature is related to literature results about grain refinement using severe plastic deformation processes. According to Humphreys, [Humphreys *et al*, 1999], annealing severely deformed structures on the 150°C~250°C temperature range causes little microstructural changes. Generally, the grains become more equiaxed. Texture is also said not to change significantly. When performing asymmetrical rolling on AA 1050 sheets, Cui and Ohori [2000] used this temperature and time to anneal an asymmetrically rolled sheet, aiming to study the grain size evolution after rolling. They found that grain growth occurs for these conditions, but the final grain size is still of about 10μm. Thus, these conditions may lead to a good compromise between strength an formability. Moreover, results obtained for 265°C and 2 hours, for 20% RPP (roughly 75MPa and 25% uniform extension, see Figure 37), indicate that an increase in RPP tends to lower the stress level, and hence it should be accompanied with a decrease in annealing temperature, in order to optimize the strength / uniform extension ratio.

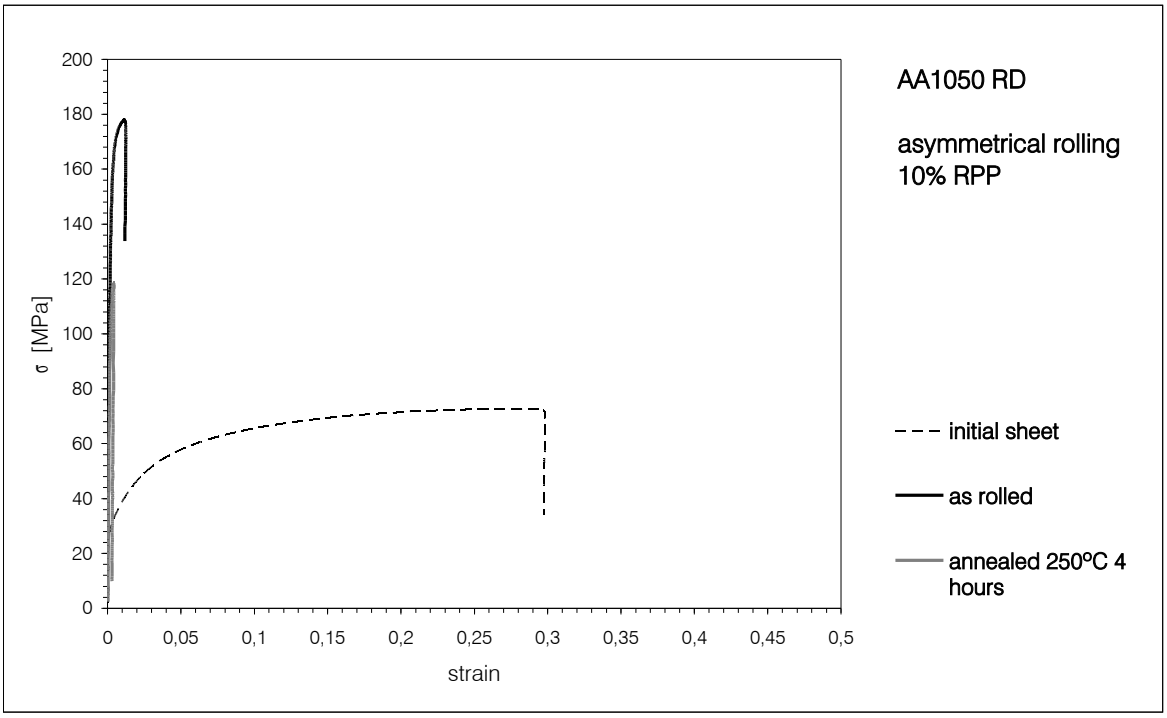

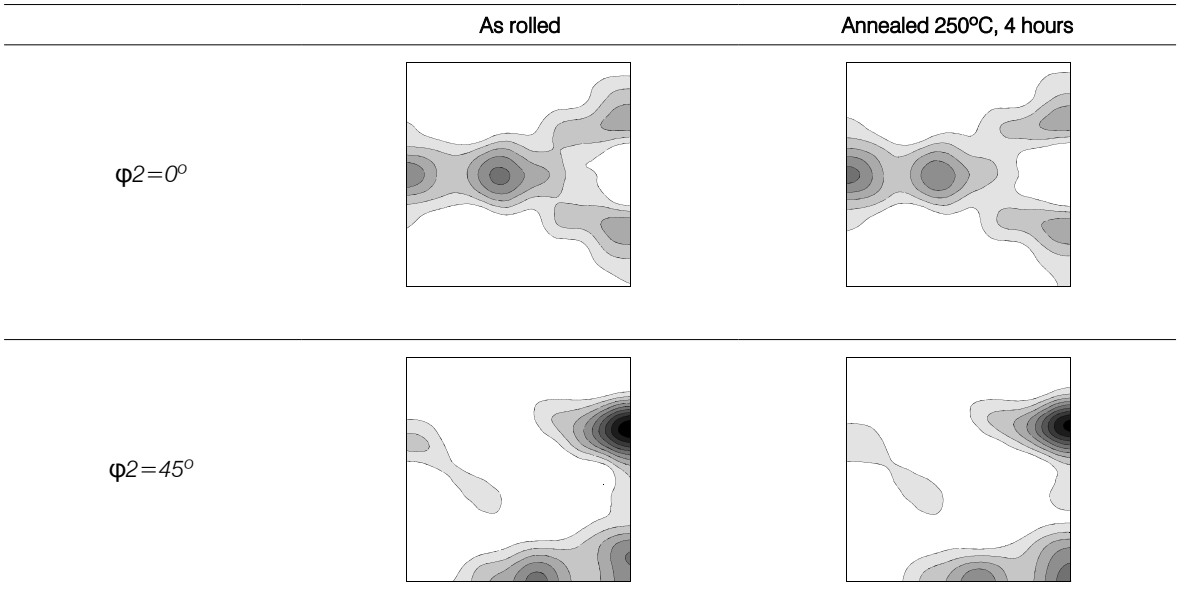

Figure 49: RD tensile test of specimens asymmetrically rolled (10%RPP) and annealed at 250ºC for 4 hours. φ2=0º and φ2=45º ODF sections for texture evaluation.

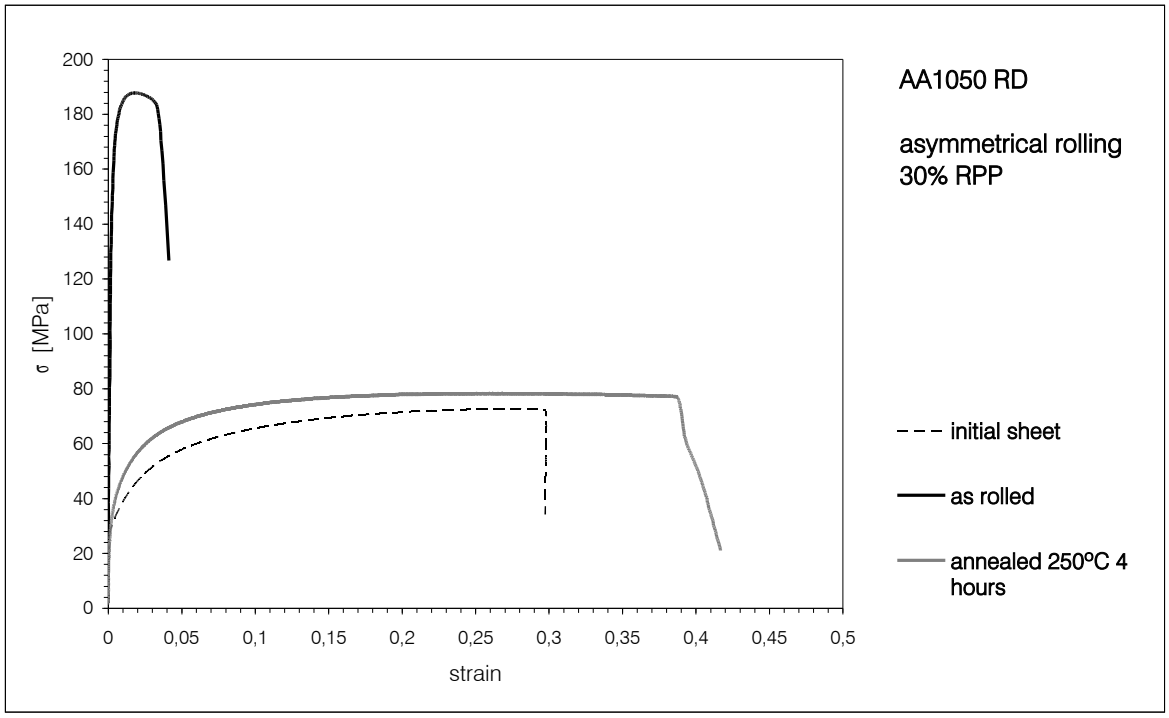

	As rolled	Annealed 250ºC, 4 hours
φ2=0º	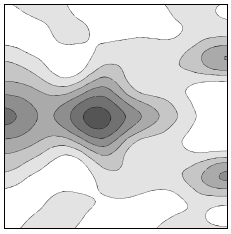	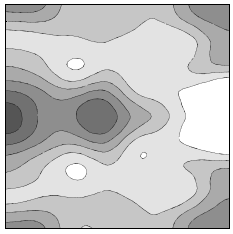
φ2=45º	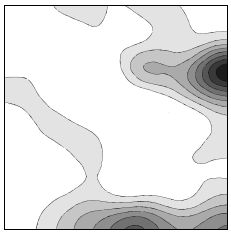	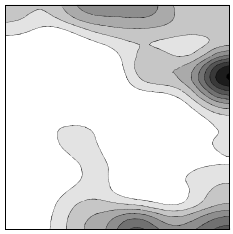

Figure 50: RD tensile test of specimens asymmetrically rolled (30%RPP) and annealed at 250ºC for 4 hours. φ2=0º and φ2=45º ODF sections for texture evaluation.

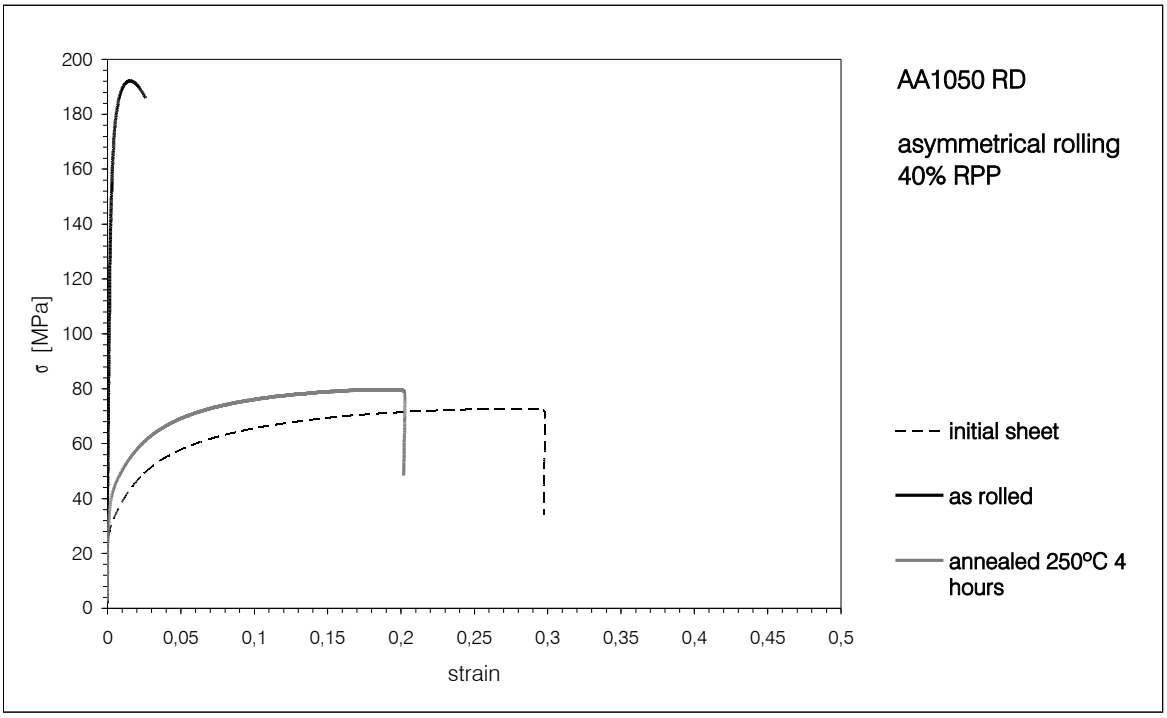

	As rolled	Annealed 250ºC, 4 hours
φ2=0º	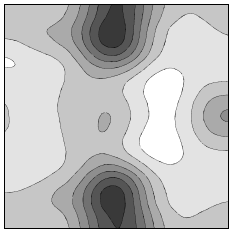	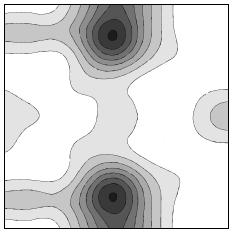
φ2=45º	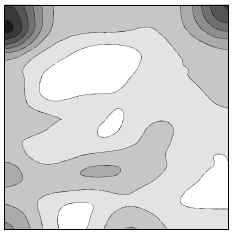	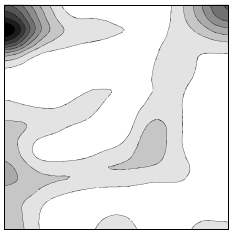

Figure 51: RD tensile test of specimens asymmetrically rolled (40%RPP) and annealed at 250ºC for 4 hours. φ2=0º and φ2=45º ODF sections for texture evaluation.

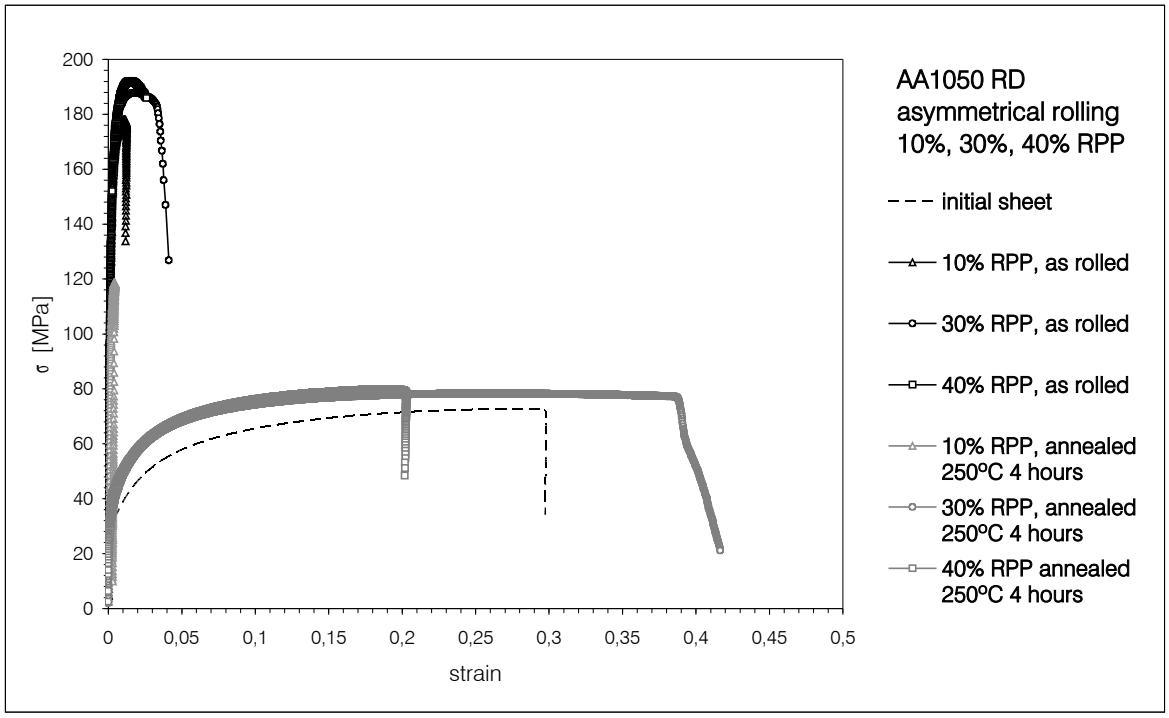

Figure 52: RD tensile tests of specimens asymmetrically rolled and annealed at 250ºC for 4 hours. Comparison among 10%, 30% and 40% RPP procedures.

The use of furnace cooling (as opposed to water quenching used before) is related to the unexpected differences observed on specimens annealed for 2 and 3 hours at 265ºC (Figure 37). The increase in flow stress may have occurred due to the presence of precipitates. By cooling slowly, those precipitates should have time do dissolve.

From the observation of the previous figures, the following observations can be derived:

- *Mechanical response:*
  - As rolled specimens show expected low elongation values and high ultimate tensile stresses. The comparison between each RPP value shows higher values of stress for the higher values of RPP. Uniform extension follows a similar trend, except between the 30% to 40% RPP specimens, where no increase in uniform extension is observed.
  - Annealed specimens show a significant decrease in maximum stress, as well as an increase in uniform extension, as expected. However, the 10% RPP specimens do not follow this trend. The maximum stress decreases relatively to as rolled specimens, but is still much higher than specimens with 30% and 40% RPP. Moreover, the decrease in

maximum stress is not accompanied by the expected increase in uniform extension. This result is unexpected and should be studied further.

- *Texture*
  - After rolling, specimens 10% and 30% RPP specimens show typical deformation texture components, such as Brass and Copper. No shear texture components appear in this case. However, in the case of the 40% RPP specimens, there is a strong shear texture component, namely the shear 1 ({001}<110>).
  - After annealing, 10% RPP specimens show almost no texture evolution. The deformation texture components (Brass, Copper) are retained. 30% RPP specimens show the formation of some Cube component, at the expense of the Brass component. This indicates the recrystallization process has begun. 40% RPP specimens seem to show, once more, a different trend. The initial (as rolled) shear texture components tend to sharpen on annealing.

These results show that high thickness reductions per pass originate the desired shear texture components. Moreover, these components seem to be retained after annealing. Further mechanical tests follow, focusing on higher RPP values, and different conditions for the annealing treatments. Conventionally rolled specimens are added, for comparison purposes.

5.3.2. Tensile tests

New annealing parameters are now introduced, as an attempt to optimize the strength / uniform extension ratio. This is because the tensile curves for specimens annealed at 250°C for 4 hours are already close to the reference curve, from the recrystallized sheet. Hence, two new annealing schedules are introduced (furnace cooling was used once more):

- 250°C, 2h - half the previous time, as a way to increase the maximum stress;
- 200°C, 4h - lower temperature, same time, as an alternative way to increase stress;

Table 8 summarizes the rolling and annealing conditions mentioned. Texture analysis and RD tensile tests were carried out. Results are shown on figures 53 to 55.

Initial sheet	Type of rolling	Roll speed ratio	Total thickness strain	Reduction per pass	Annealing
8mm, Annealed 343°C 1h	Asymmetrical (ASR)	1.36	~2.7	50% max	250°C, 2h 200°C, 4h
	Conventional (CR)	1			

Table 8: Rolling and annealing parameters for the comparison of asymmetrical and conventional rolling using 50% RPP.

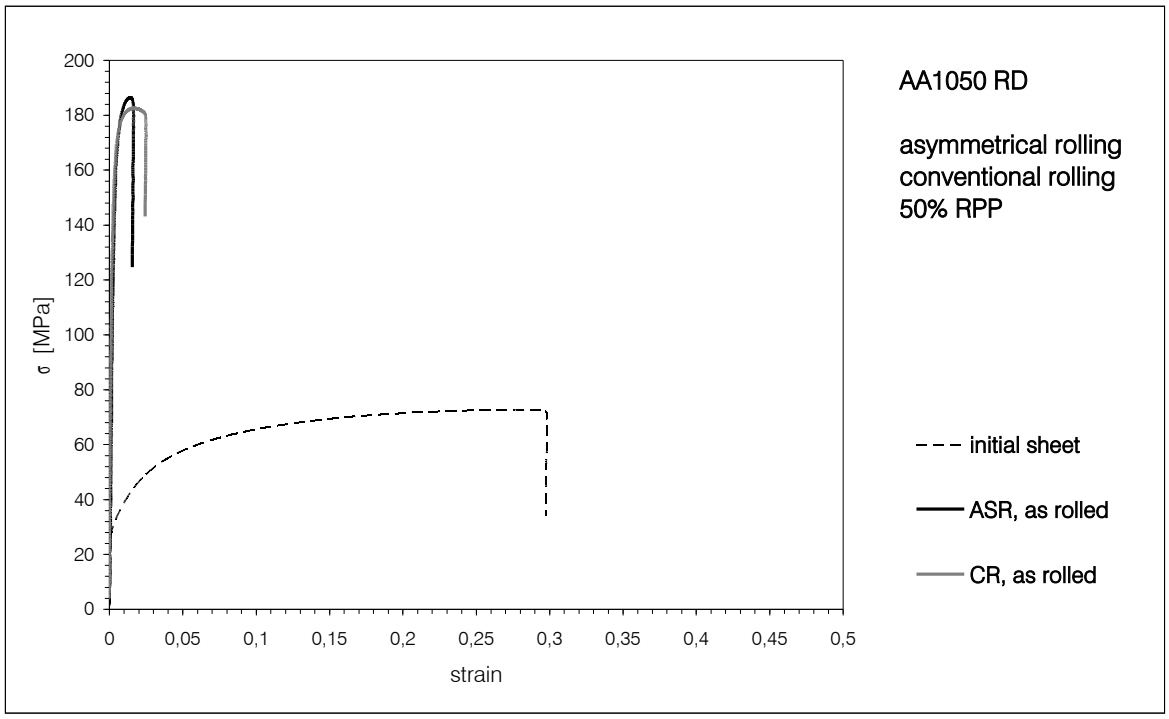

	Asymmetrical rolling (ASR)	Conventional rolling (CR)
$\varphi 2=0^o$	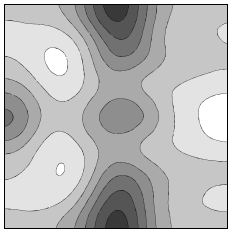	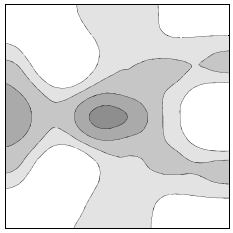
$\varphi 2=45^o$	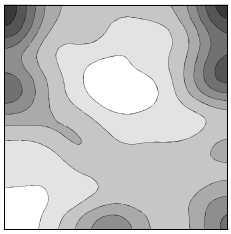	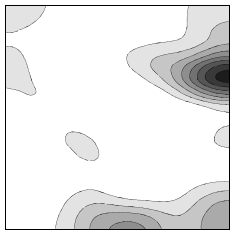

Figure 53: RD tensile test of rolled specimens (50%RPP). Comparison between ASR and CR. $\varphi 2=0^o$ and $\varphi 2=45^o$ ODF sections for texture evaluation.

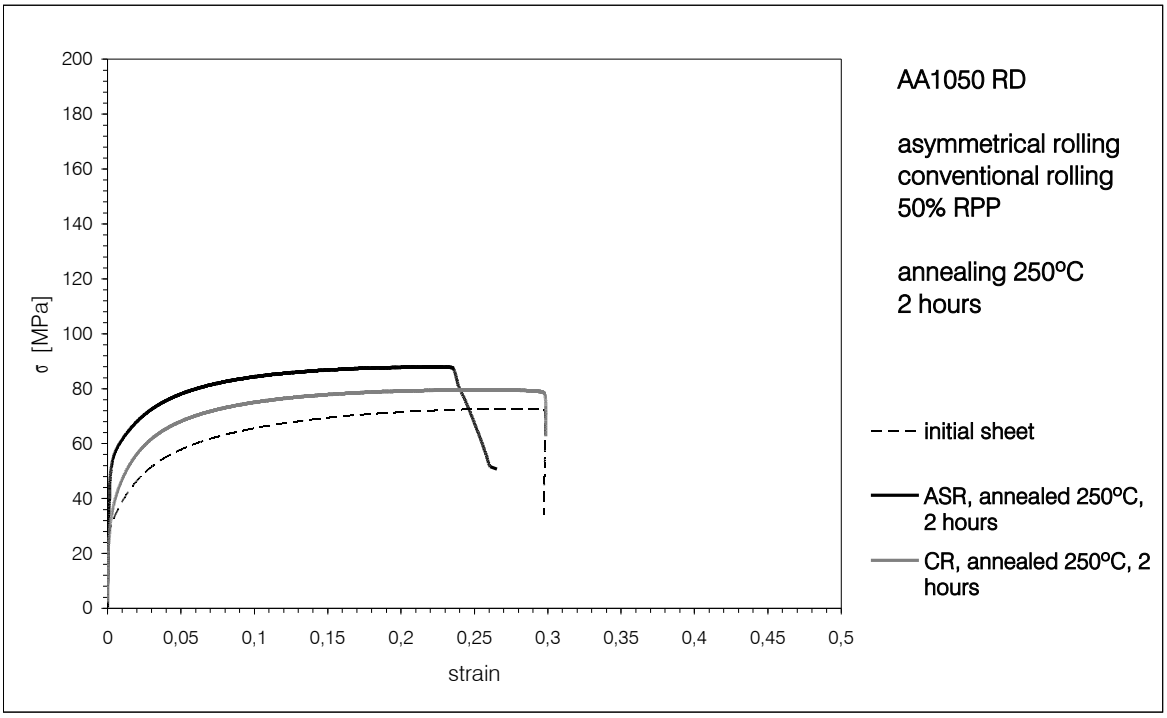

	Asymmetrical rolling (ASR)	Conventional rolling (CR)
φ2=0º	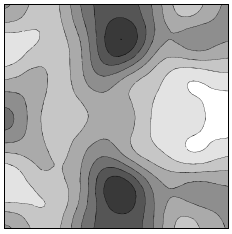	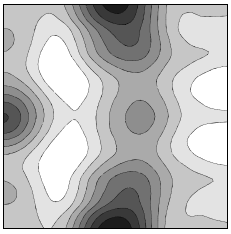
φ2=45º	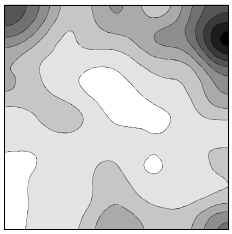	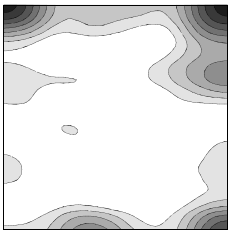

Figure 54: RD tensile test of rolled (50%RPP) and annealed (250ºC for 2 hours) specimens. Comparison between ASR and CR. φ2=0º and φ2=45º ODF sections for texture evaluation.

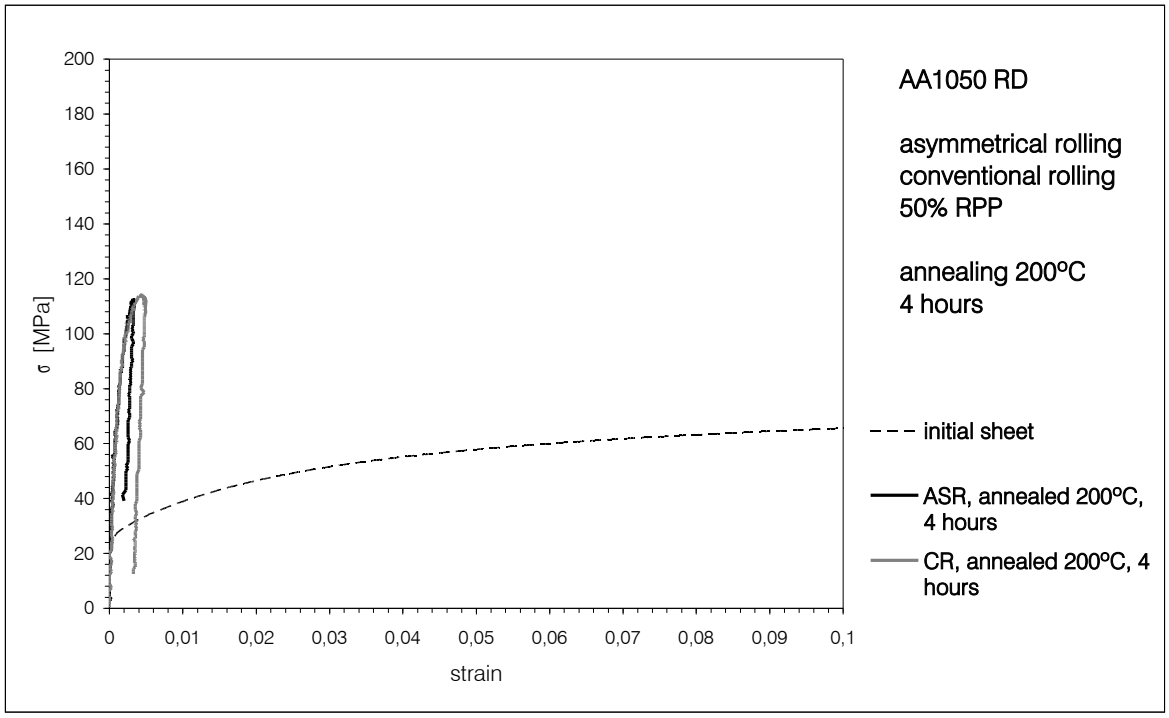

	Asymmetrical rolling (ASR)	Conventional rolling (CR)
$\varphi 2=0^o$	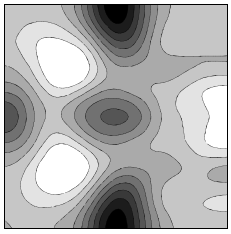	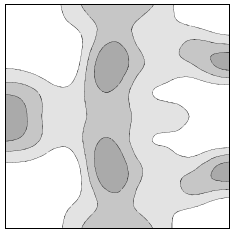
$\varphi 2=45^o$	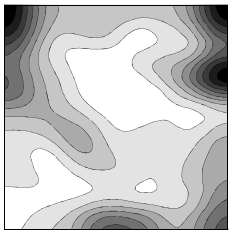	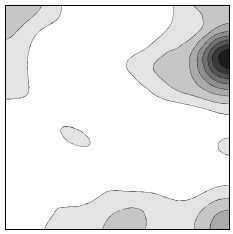

Figure 55: RD tensile test of rolled (50%RPP) and annealed (200ºC for 4 hours) specimens. Comparison between ASR and CR. $\varphi 2=0^o$ and $\varphi 2=45^o$ ODF sections for texture evaluation.

The following conclusions arise from the results:

- *Mechanical response:*
  - as rolled specimens: mechanical responses are similar, though asymmetrically rolled specimens display slightly higher maximum stress.
  - specimens annealed at 250ºC for 2 hours: mechanical response is different among Asymmetrical and conventional specimens. The most noticeable difference is the yield stress, which is more than two times greater for Asymmetrical specimens. Maximum stress is also greater, but uniform strain is lower.
  - specimens annealed at 200ºC for 4 hours: mechanical response results were unexpected. Both Asymmetrical and conventional specimens present very low yield stress (relatively to as rolled specimens), but also very low extension. Further investigation should be focused on these results.
- *Texture*
  - as rolled specimens: Texture is quite different between asymmetrically and conventionally rolled specimens. The latter has typical rolling texture components, especially Brass and Copper, whereas the former has some rolling components as well, but strong shear texture components, mainly shear 1 ({001}<110>), and some amount of shear 4 ({112}<110>).
  - specimens annealed at 250ºC for 2 hours: Texture analysis shows that asymmetrically rolled specimens tend to retain texture components, when compared to “as rolled” specimens. Conventionally rolled specimens present some shear components, especially shear 1 ({001}<110>). This might be a consequence of high shear strains on the sheet surface, already observed by Kim [1999]. This texture result is not in logical agreement with the previous set of specimens (as rolled), because shear textures cannot be generated from typical plane strain textures, such as Brass or Copper, by annealing treatments. It should be emphasized that different specimens were used for each texture analysis (that is, the texture specimen for the “as rolled” condition was not annealed), despite the fact that all specimens of the same type were cutout from the same rolled sheet.
  - specimens annealed at 200ºC for 4 hours: texture results are very similar to the ones observed for “as rolled” specimens. It seems like there was little texture evolution for these annealing conditions.

Results suggest that asymmetrical rolling can give rise to shear texture components, which remain stable even after annealing. High values of RPP seem to be required to achieve this kind of textures. In order to obtain a better understanding of the effects of the RPP, coupled with the effects of the asymmetry of the rolling procedure, a set of additional experiments was carried out. These experiments will also help to clarify the conditions for the appearance of shear texture components even on conventionally rolled specimens.

5.3.3. Shear tests

The starting material was the same 1050-H111 8mm thick sheet. It was first heat treated at 343°C for 1 hour, as on the previous works, then rolled down to 0.65mm by two different procedures: Asymmetrical (ASR) and conventional (CR). Asymmetrical rolling was performed with no lubrication, in order to maximize shear deformation. Roll speed ratio was set to 15/11 r.p.m. (1.36) and the specimen was rotated 180° about the TD axis between each pass. Conventional rolling was carried out with identical upper and lower roll speeds and normal lubrication, keeping specimen position in every pass.

In order to evaluate the influence of RPP in a shear solicitation, the two existing specimen sets (ASR and CR) were subdivided according to RPP values used: 15% and (maximum) 50% of thickness. Note that the lower RPP value was kept constant on every pass, whereas the higher RPP is a maximum value, since variations occurred during rolling (related to difficulties in imposing such large reduction in thickness).

5.3.3.1. Experimental procedure

Shear specimens having dimensions of 30x10 mm were cut from the sheet, along its rolling direction, and divided into three groups, for both Asymmetrical and conventional processes: as rolled (AR), heat treated at 250°C for 2h, followed by furnace cooling (HT1), and heat treated at 350°C for 1h, followed by water quenching (HT2) - Table 9. The first annealing procedure is identical to the previous one, whereas the second (HT2) is different. It was chosen to verify the stability of texture components at higher annealing temperatures. Shear texture components have been reported to remain stable even after annealing at 350°C for 30 min [Lee, Kim, 2001].

Initial sheet	Type of rolling	Roll speed ratio	Total thickness strain	Reduction per pass	Annealing
8mm, Annealed 343°C 1h	Asymmetrical (ASR)	1.36	~2.8	15%	250°C, 2h (HT1)
				50% max	
	Conventional (CR)	1		15%	350°C, 1h (HT2)
				50% max	

Table 9: Rolling conditions for evaluation of the influence of thickness reduction per pass.

Surface and full thickness texture analyses were carried out to access texture gradients along the sheet's thickness. Until now, only surface texture measurements have been used. Information about texture distribution over the sheet's thickness is not available. One of the difficulties of the asymmetrical rolling process is to impose the desired shear texture components throughout the th sheet's thickness, so attention must be paid to this aspect.

For full thickness texture analysis OIM measurements [Krieger-Lassen *et al*, 1992] were conducted over the entire thickness of the sheet sample. In OIM, an electron probe is stepped across a crystalline surface, inclined to the incident beam by 70°. Any sample volume with an undisturbed lattice gives rise to a characteristic diffraction pattern which is a two-dimensional projection of the three-dimensional unit cell. From this diffraction pattern, the three angles relating the crystal coordinate system to the sample system (that is the crystallographic orientation) are calculated, using automated pattern recognition procedures. In this way 5000–10,000 orientations (data points) can be determined per hour. This technique was used to measure the average texture over the entire sheet thickness.

5.3.3.2. Shear test results

Figures 56, 57 and 58 show the shear test results (rolling direction) for ASR and CR specimens, for both 15% and 50% RPP values, for as rolled, after HT1 and after HT2 annealing, respectively. As rolled specimens (Figure 56) show yield stress values around 90MPa and maximum strain of about 0.13. There is little difference between ASR and CR specimens within the same RPP value, but it can be observed that specimens with higher RPP value have higher maximum stress. After HT1, (Figure 57) it can be observed that for the lower RPP value, both ASR and CR specimens show similar response, despite the obvious curve crossing, which may indicate differences in texture [Bacroix *et al*, 1999].

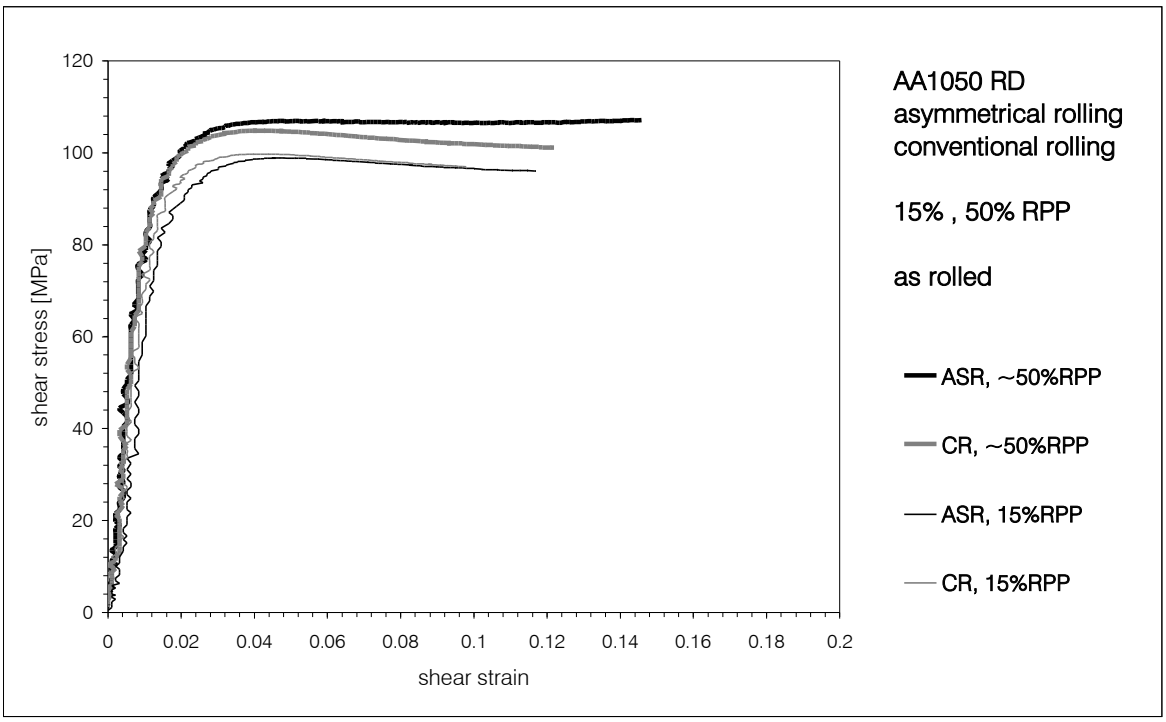

Figure 56: RD Shear test for asymmetrically and conventionally rolled specimens, as rolled. RPP values: 15% and 50%.

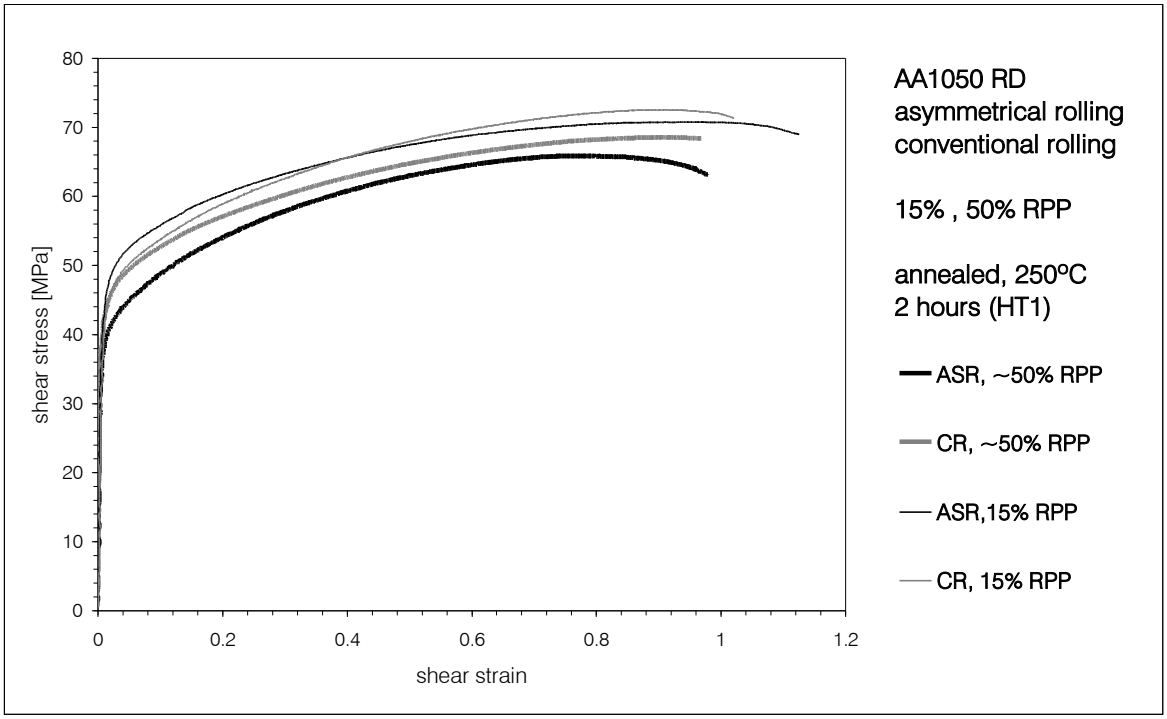

Figure 57: RD Shear test for asymmetrically and conventionally rolled specimens, heat treated 250ºC, 2 hours (HT1). RPP values: 15% and 50%.

When RPP value increases, the flow stress of both ASR and CR specimens decreases relatively to the former set. Within this set, CR specimens show both higher yield and flow stresses. ASR specimens seem to show higher strain hardening rate after yielding. When considering HT2, (Figure 58) specimen response is practically independent of processing conditions. All shear stress – shear strain curves are coincident.

5.3.3.3. Texture results

Figure 59 shows the surface texture evolution for 15% RPP ASR and CR specimens, measured in three states, as rolled, annealed by HT1 and HT2. For the case of “as rolled” state, it is possible to observe that both CR and ASR specimens develop typical rolling deformation textures - Copper, Brass - with no significant difference between them. ASR specimens also develop some Goss component.

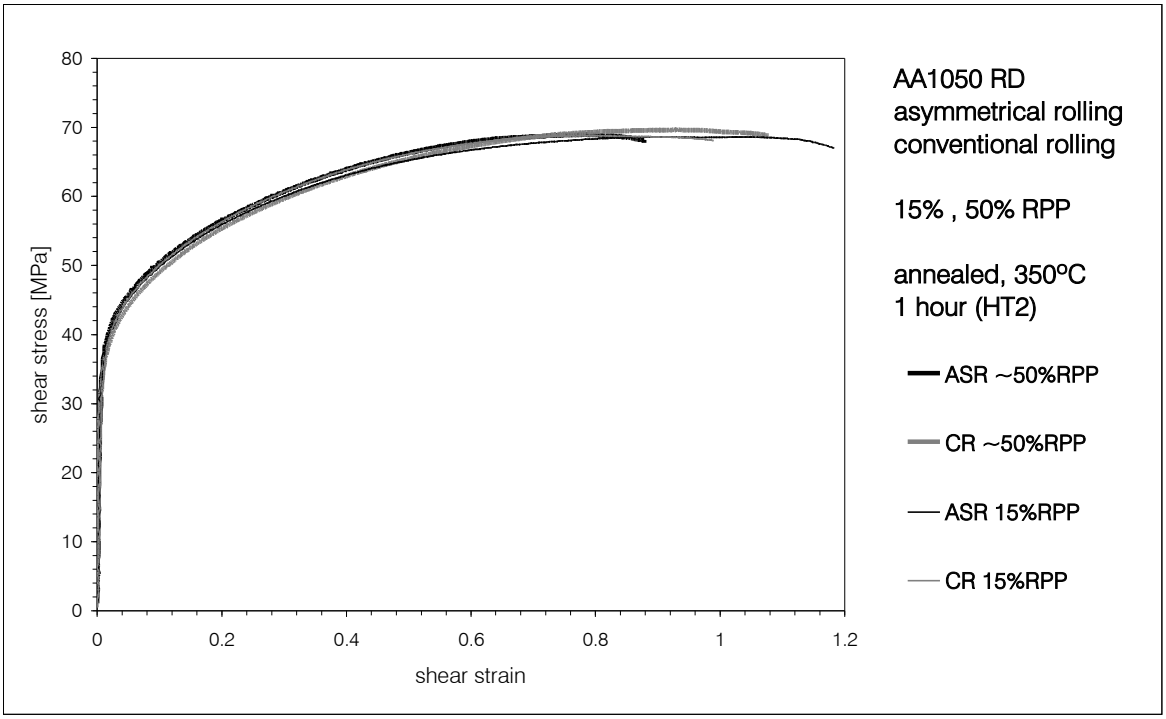

Figure 58: RD Shear test for asymmetrically and conventionally rolled specimens, heat treated 350ºC, 1 hour (HT2).

After HT1, some differences in texture components arise. For these conditions, CR specimens develop mostly recrystallization components, but ASR specimens tend to retain deformation components, though some texture spread can be observed, from Copper components toward Cube and Goss. The $\varphi 2=45^{o}$ ODF section shows no shear texture components for neither CR nor ASR specimens.

Figure 60 shows the ODF sections $\varphi 2=0^{o}$ and $\varphi 2=45^{o}$ obtained by full thickness texture measurements (OIM) on 15% RPP ASR and CR specimens after HT1. This procedure allows accessing the material's average texture, providing an indirect way to identify texture gradients along the sheet thickness, when combined with surface texture measurements.

CR specimens display Copper and Brass texture components, probably retained from the rolling process, as well as some Goss and a significant amount of the Cube orientation, indicating some degree of recrystallization. ASR specimens also show recrystallization components, especially Cube, but less deformation components such as copper. As for shear texture components, very little amount can be observed in either sample in this case.

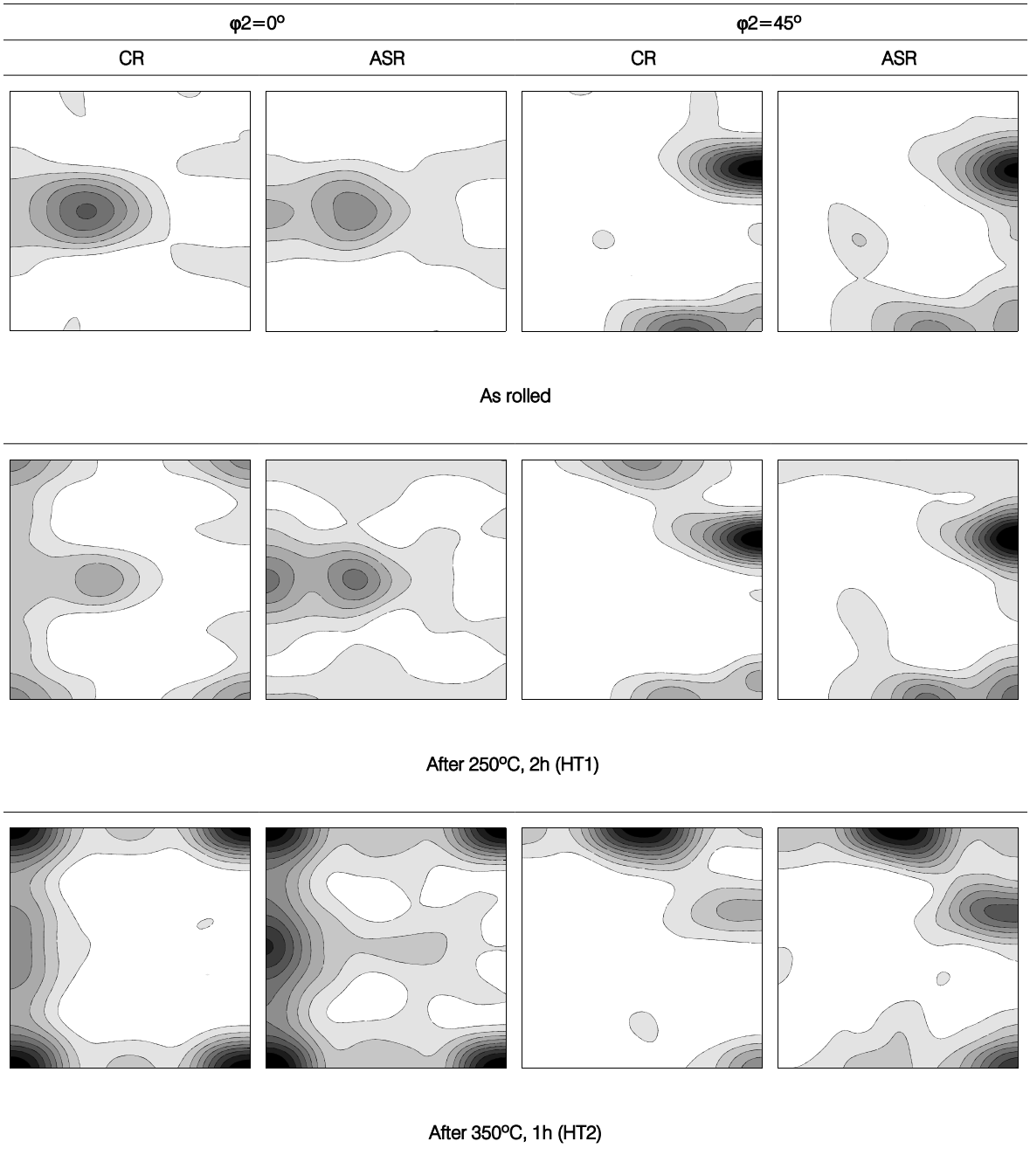

Figure 59: Surface φ2=0º and φ2=45º ODF sections for ASR and CR specimens rolled with 15% RPP. Conditions: as rolled, HT1, HT2.

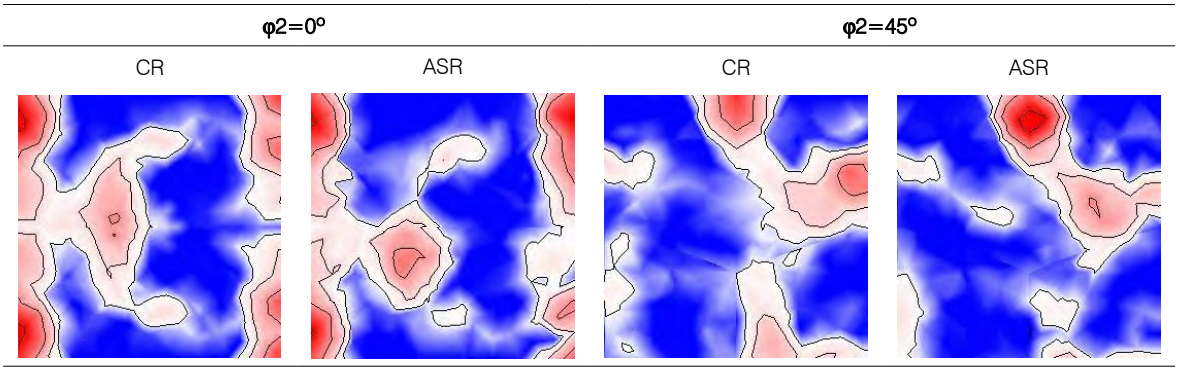

Figure 60: Through thickness ODF's for ASR and CR specimens rolled using 15% RPP, after HT1.

Figure 61 shows the surface texture evolution for 50% RPP ASR and CR specimens, measured in three states, as rolled, annealed by HT1 and HT2. The first major difference between these samples and the former set is the appearance of shear texture components, especially the shear 1 (rotated cube, {001}<110>) component. This is evident on both conventional and asymmetrically rolled specimens. Another important observation is the stability of the shear texture components throughout the thermal treatments performed. Even after HT2, (350ºC, 1h), CR and ASR specimens present amounts of shear texture components similar to as rolled condition. Only a slight difference in texture between CR and ASR specimens can be pointed out: the larger spread observed on ASR specimens, especially toward other shear texture components, such as {111}<110>. In order to complete the information provided by this figure, the trough thickness texture measurement was also performed, for the HT1 specimens.

Figure 62 shows the ODF sections $\varphi 2=0^{o}$ and $\varphi 2=45^{o}$ obtained by full thickness texture measurements (transmission method) on 50% RPP ASR and CR specimens after HT1. The main difference between CR and ASR specimens is the relative amount of cube component, higher on CR specimens. Shear texture components are relatively weak in both specimens, and the {001}<110> component does not appear.

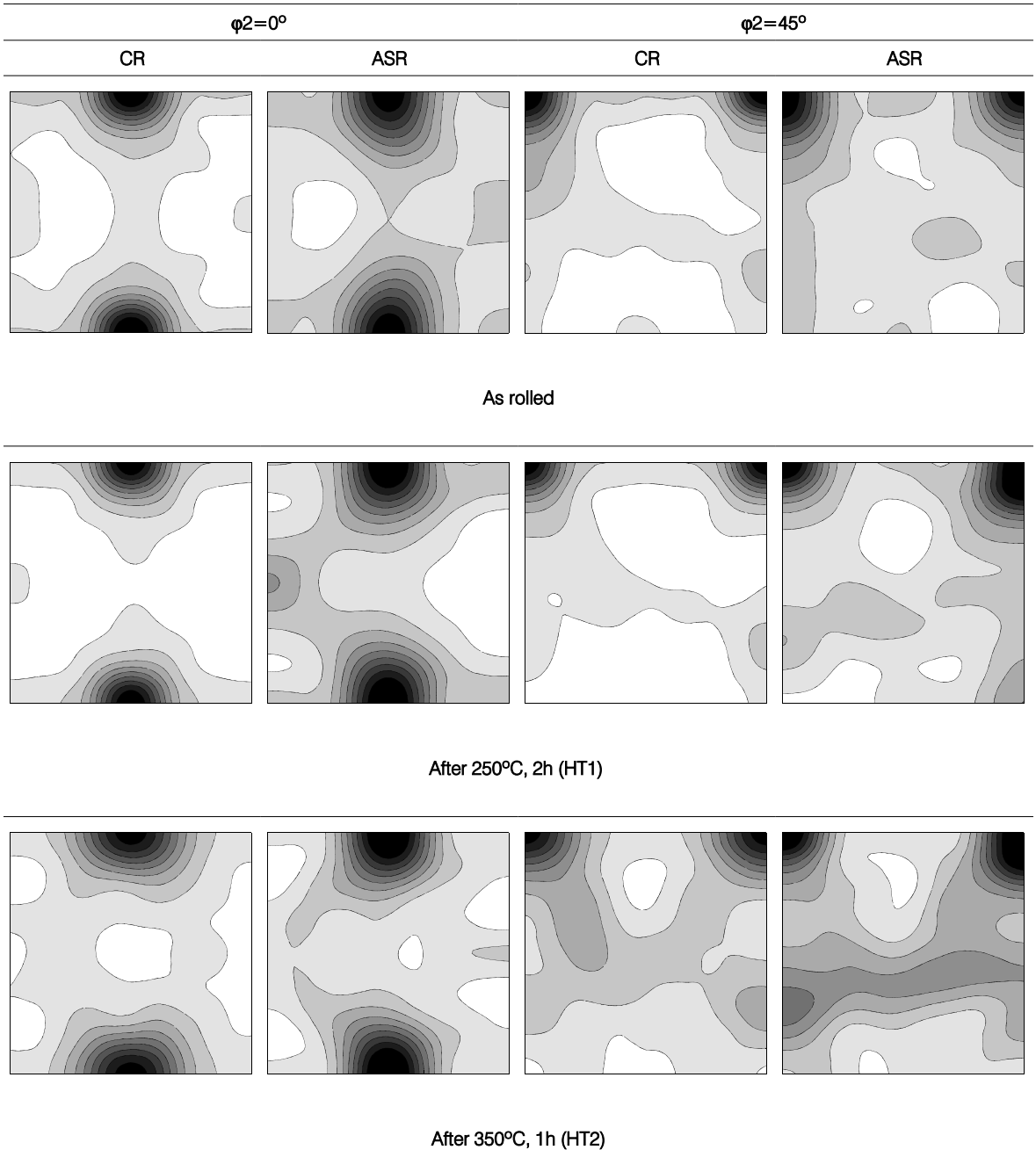

Figure 61: Surface φ2=0º and φ2=45º ODF sections for ASR and CR specimens rolled with 50% RPP. Conditions: as rolled, HT1, HT2.

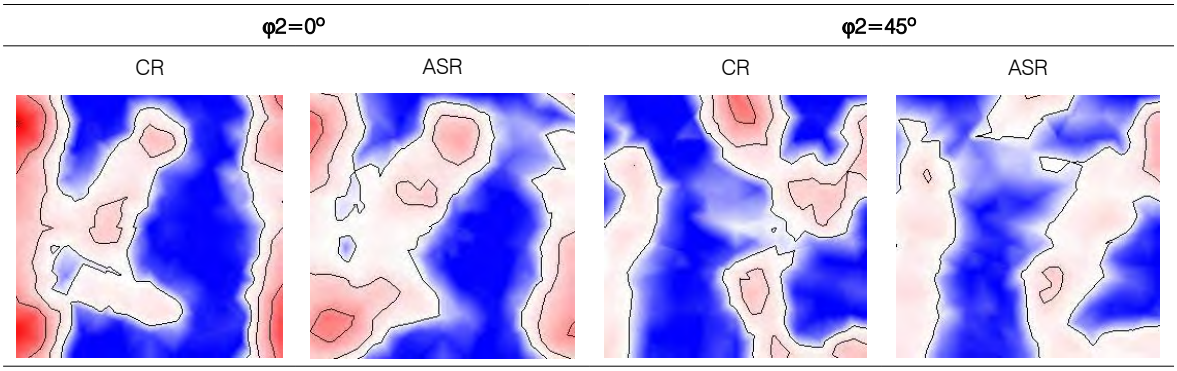

Figure 62: Through thickness ODF's for ASR and CR specimens rolled using 50% RPP, after HT1.

5.3.3.4. TEM observations

Observations of grain structures were performed using a Hitachi H-9000 (300 kV) transmission electron microscope (TEM). The TEM foils were taken parallel to the rolling plane at the sheet mid-thickness location. In order to do this, the samples were mechanically ground on both surfaces, then electropolished using a double-jet thinner with a dilute solution of HNO_3 and methanol under 12 V tension at 20º C until perforation occurred.

Observations were performed on ASR and CR specimens. Figure 63 shows grain structure of ASR specimens with 15% and 50% RPP, as rolled. A structure of what seem to be equiaxed subgrains is visible and their size is estimated to be around 1-2μm. As rolled CR specimens are not shown, due to observation difficulties caused by excessive oxidation on the specimen's surface. Figure 64 shows a comparison between ASR and CR specimens (15% and 50% RPP) after HT1. The subgrain structures observed seem very similar in all cases. The only major difference between this set of samples and the previous one is the obvious subgrain growth (observable in the difference of scales). In this case, the subgrain size is estimated to be around 5-7μm. An attempt of performing an observation of HT2 specimens was performed, but the excessive grain size (over 25-30μm) of the samples prevented an accurate result. Optical microscopy is more appropriate in this case.

5.3.4. Influence of rolling direction reversal

Kim and Lee [2001] noted that the ideal shear texture (the {111}||ND components) could not be obtained by unidirectional rolling. Instead, a reversal in the shear strains imposed was necessary. This was because on conventional rolling using high values of friction, the ideal shear textures could be observed on the sheet's surface. During conventional rolling there is a shear strain reversal on the sheet's surface, because the circumferential speed of the sheet is first lower than the rolls', and higher after a certain point (the neutral point). They found that the way to achieve this shear

reversal on asymmetrical rolling was to perform a rotation of the sheet between each asymmetrical rolling pass.

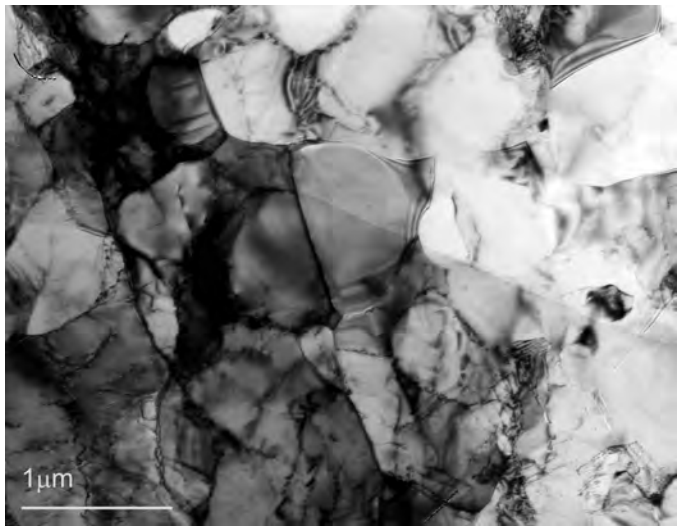

a)

b)

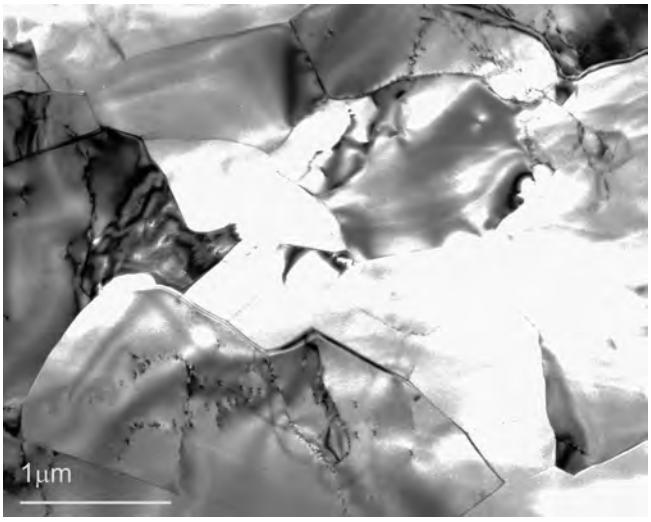

Figure 63: TEM image of an asymmetrically rolled 1050 sheet, after rolling. a) 15%RPP; b)50%RPP.

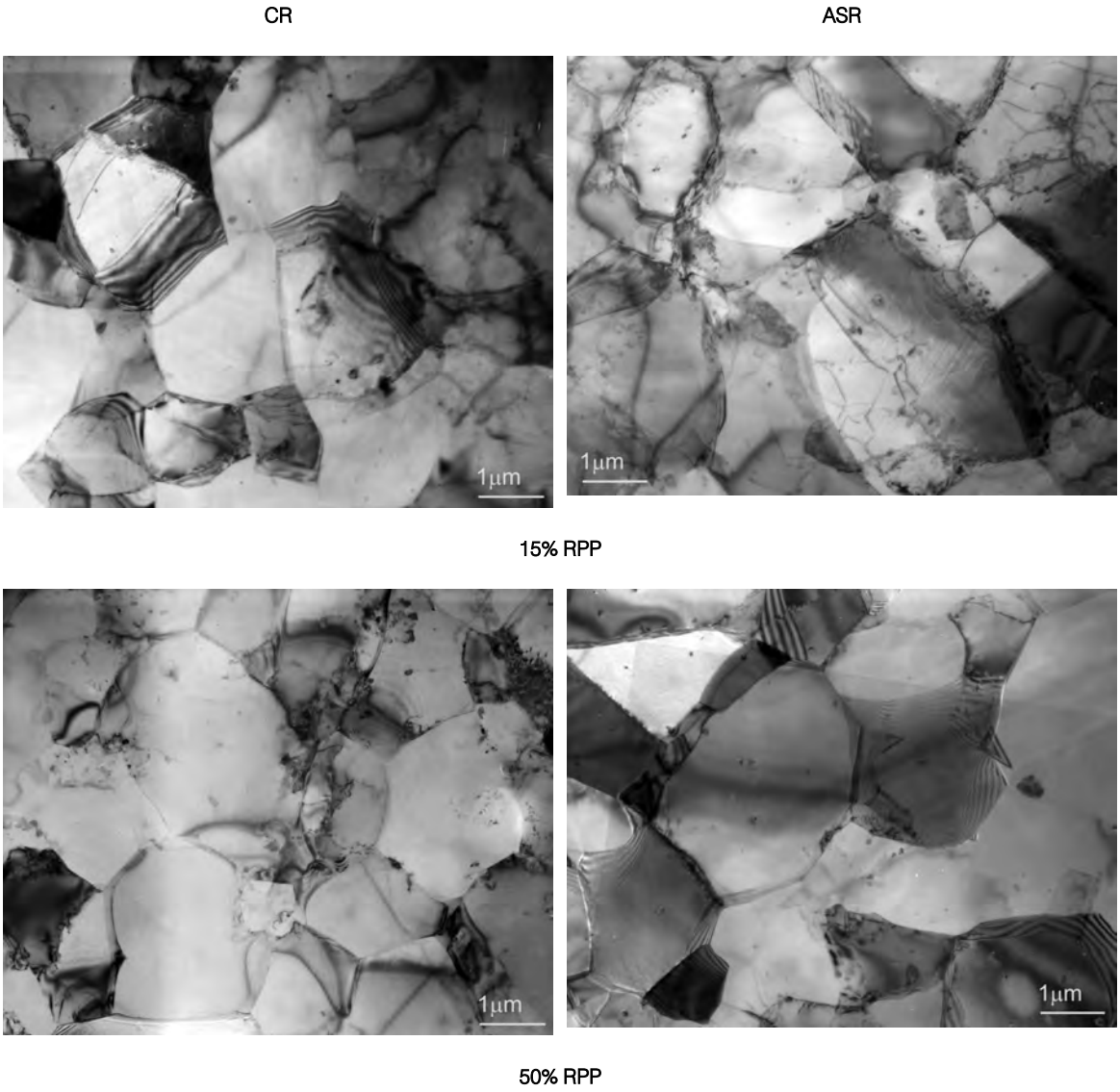

Figure 64: TEM images of asymmetrically and conventionally rolled sheets. Annealing at 250°C, 2h (HT1).

As shown in Figure 25, there are several processing routes possible, concerning rolling direction reversal. In unidirectional rolling (UD) no reversal is imposed; in TD reversal, the sheet is rotated 180° over the transverse direction; in RD, the sheet is rotated 180° over the rolling direction; and in ND the sheet is rotated 180° over its normal direction. In UD and TD reversal, there is no actual reversal of the rolling direction on the sheet's surface. In ND and RD, the sheet's surface is subjected to shear strain reversal between each pass. Lee and Lee [Lee, Lee, 2001] used steel sheets to study the effect of shear reversal on texture formation. They found that RD and ND reversal gave rise to intense shear texture components. Nevertheless, they also stated that amount of strain reversal should be optimized in order to obtain ideal textures.

Kim and Lee [Kim, Lee, 2001] performed a rolling schedule designed to impose shear strain reversal on the sheet, while attempting to produce shear textures along the sheet thickness. Starting from a β fiber textured sheet (conventionally rolled), they performed 2 schedules of unidirectional asymmetrical rolling, followed by a schedule of asymmetrical rolling on the reverse direction. They found the final texture to be close to the ideal shear texture sought.

The current experiments were performed using TD reversal, which may have affected the results in terms of shear texture components. This may also be one of the causes for the lack of texture spreading along the sheet's thickness. In order to study the effects of shear reversal on the sheet, a rolling schedule similar to the one used by Kim and Lee [Kim, Lee, 2001] was performed. The initial 8mm thick sheet was recrystallized at 343°C for 1 hour, and then conventionally rolled down to 2.8mm using 10% RPP. After this, unidirectional asymmetrical rolling was performed, down to a thickness of 0.75mm, using about 50% RPP. Finally, asymmetrical rolling using 30% RPP was performed on the opposite direction, after reversing the sheet around ND. Table 10 summarizes the rolling conditions used.

Initial sheet	Type of rolling	Roll speed ratio	Thickness strain	Reduction per pass	Annealing
8mm, Annealed 343°C 1h	Conventional (CR) followed by Asymmetrical (ASR)	1 / 1.36	CR: ~1	CR - 10%	250°C, 2h
			ASR 1st stage: +~1.4	ASR: 50% max	
			ASR 2nd stage: +~0.35	ASR inverse ND: 30%	

Table 10: Rolling conditions for the reversing direction experiment.

Texture analysis and RD shear tests were performed and compared with previous CR and ASR specimens. Results are shown on Figure 54. The shear response of the ND reversal specimen is similar to the CR specimen, except for the maximum achievable strain, which is lower. Nevertheless its shear response is always above the one of the ASR specimen. Texture measurements show that the shear 1 texture component ({001}<110>) is the most predominant after conventional rolling followed by asymmetrical rolling. When the sheet is further rolled, reversing the initial rolling direction by ND, its surface texture sharpens, as the same shear 1 component is reinforced. After annealing there is little texture change (besides a slight sharpening, once more), as already observed on the previous experiments using this annealing temperature. Though there is a slight difference in shear response between the ND reversal specimen and the previous ones, once more it would be fundamental to analyze the sheet's mid-thickness texture, in order to verify the presence of shear texture components, before reaching a definitive conclusion.

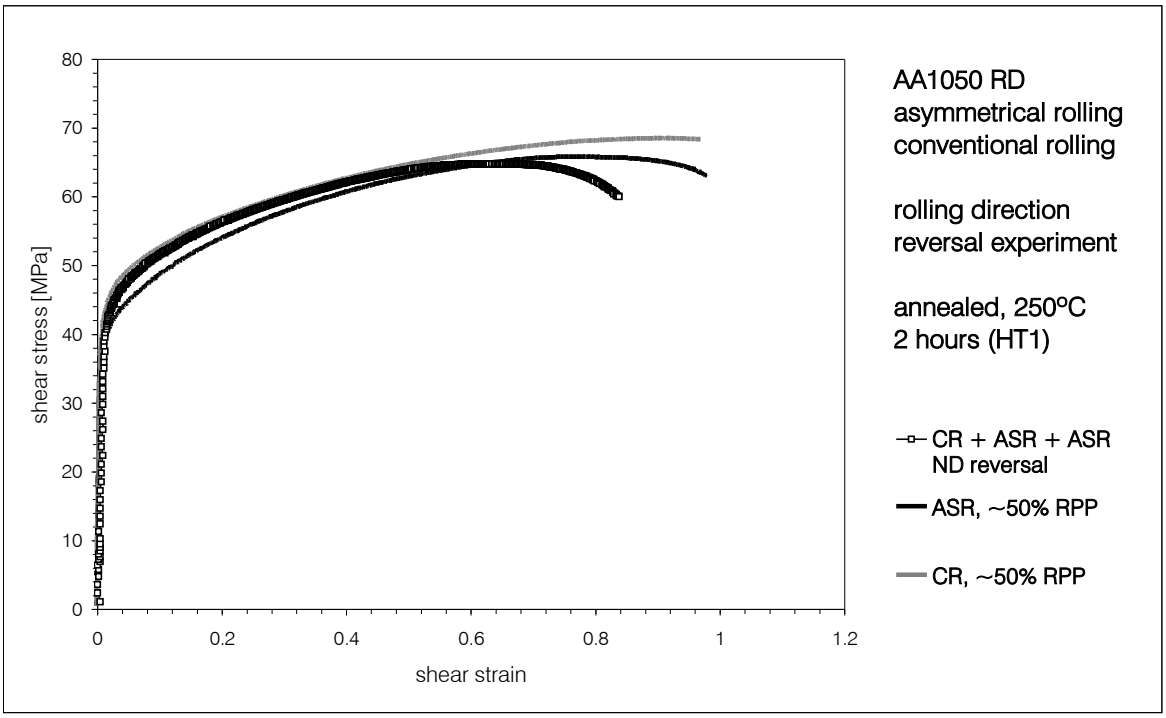

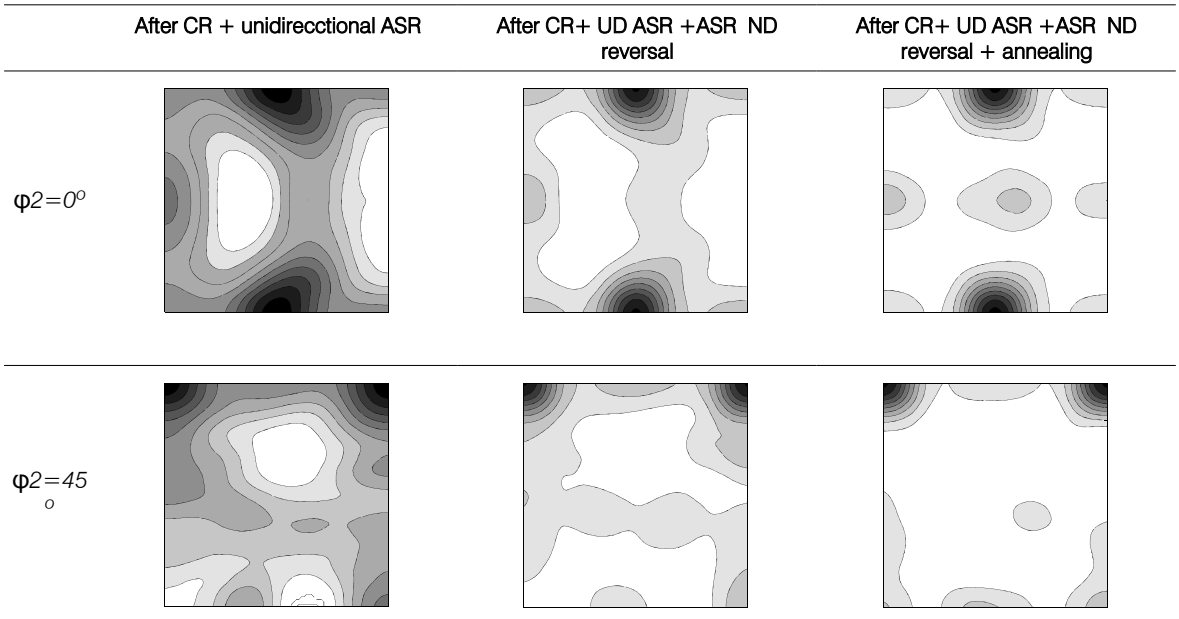

Figure 65: RD shear test of rolled (50%RPP) and annealed (250ºC for 2 hours) specimens. Comparison between ASR, CR and rolling reversal specimens. φ2=0º and φ2=45º ODF sections for texture evaluation.

5.4. Discussion

5.4.1. Shear test results

The direct comparison between the shear response of ASR and CR specimens suggests that there is not a significant difference between both processes. However, some details should be noted. When comparing as rolled specimens, the main differences occur between the two different values of the reduction per pass (15% and 50% RPP), whereas the influence of ASR and CR process is negligible. This result is supported by texture measurements, even if those measurements refer to the sheet surface only. It is possible to observe that the most noticeable differences in texture occur between the two values of RPP, and not between the two rolling processes.

After the first heat treatment, performed at 250^{o}C for 2 hours (HT1), the most obvious differences in mechanical response are still observed when comparing 15% and 50% RPP specimens. CR specimens show similar values of yield stress but different strain hardening response. Texture comparison (full thickness, figures 60 and 62) shows both specimens have strong volume fractions of the cube texture component (probably higher on the 15%RPP specimen), but the 15% RPP specimen has a higher volume fraction of the copper texture component. According to the shear test simulations using ideal orientations (Figure 44), the cube component displays the highest level of stress. This may help to explain the higher stress level observed for the 15% RPP specimen. Also, the 50% RPP specimen has some amount of shear texture components (especially {111}<110>), whereas the 15%RPP specimen does not. According to the simulations performed, shear texture components display lower values of stress (relatively to cube components), which is consistent with the experimental results. At the sheet's surface, the differences in texture are much more evident, especially because of the presence of the {001}<110> shear component on 50% RPP specimens.

ASR specimens show different yield stresses but similar strain hardening behavior. Texture comparison (full thickness, figures 60 and 62) reveals the different volume fractions of the cube component, much higher in 15%RPP, and the absence of shear texture components in these specimens. Once more, these observations are in good agreement with the simulation results.

By comparing among the same RPP value, there is an evident curve crossing for 15% RPP, indicating differences in texture, already mentioned. The differences in volume fraction of the cube and copper components may be responsible for this result. For 50% RPP, there is a significant difference between the two shear curves. The cube component is predominant in CR specimens, and ASR specimens display higher volume fraction of shear orientation (especially {112}<110>). According to the simulations performed, this combination of factors tends to lower the shear stress – shear strain curves, as observed experimentally.

By analyzing the grain structure for HT1 specimens, it was possible to conclude that the grain size and morphology was similar across ASR and CR specimens, for both 15% and 50% RPP. This result means that probably the main factor affecting the material's behavior in these conditions is the crystallographic texture, and not the grain size or morphology.

When considering HT2 specimens behavior, the coincidence observed in the shear stress-shear strain curves for all specimens doesn't fully reflect surface texture results. Even though ASR and CR specimens show similar surface textures within each RPP group, the differences between 15% and 50% RPP sheets are evident. Yet, all HT2 specimens' response is identical. Based on this observation, and since no full texture data was available, it is only possible to propose an explanation: shear texture components were retained after this heat treatment, as shown by surface texture measurements; but considering the entire sheet thickness, the volume fraction of shear texture components is minor, as shown by full thickness texture measurements. So, the deformation texture components already present on the specimens evolved to typical recrystallization (cube) texture components, and at the same time, the cube texture volume fraction already present was reinforced. This caused the sheets to have similar textures (typical recrystallization textures formed from deformation textures) in the majority of their volume, and hence, similar mechanical response. The surface of the sheets may have retained shear texture components after HT2, but their volume fraction is not high enough to control the material's behavior. Grain size is probably not a decisive factor in this case, since all samples presented similar microstructures, even after HT2.

This explanation is reinforced by the previous texture comparisons, showing that the main differences were found between the two values of RPP, and not between the two rolling processes. This means that the asymmetrical rolling process was able to impose shear strains on the sheet surface, but not throughout the entire sheet thickness. If after HT1 there were still some differences in mechanical response, probably due to the presence of deformation texture components, which counterbalanced recrystallization texture components. If shear textures were present throughout the entire sheet thickness they would probably be retained after annealing at HT2 conditions (as observed by Lee and Kim [2001], though using half the annealing time), and a more evident difference in mechanical response would be observed.

5.4.2. Tensile response and shear response

Figure 54 and Figure 57 are plots of, respectively, the tensile and shear response of asymmetrical and conventionally rolled specimens, after heat treated at 250^{o}C for 2 hours. As observed before, the yield strength in tension of asymmetrically rolled sheets is higher than conventionally rolled sheets. Shear tests lead to a different conclusion: in this case, conventionally rolled sheets present higher shear stress when compared with asymmetrically rolled specimens. Taking into account the analysis of the simulated tensile and shear responses for ideal major orientation components (figures 43 and 44), and assuming identical textures in both tensile and shear

specimens (a reasonable assumption, since the processing routes were identical), the difference in mechanical response may be explained by the different responses of individual texture components.

The higher volume fraction of the cube component on conventionally rolled specimens can be one of the factors responsible for their higher stress level, when compared to asymmetrically rolled ones. Simultaneously, the same high volume fraction of the cube component has the opposite effect on the tensile response of the material. Moreover, the shear components, and especially {111}<112> tend to raise the stress level for tensile test. In the case of shear solicitation, their influence is not as important as the cube component.

5.4.3. Asymmetrical rolling optimization strategies

The knowledge obtained on the asymmetrical rolling process and its influencing parameters after the experimental tests performed can now be used to point out ways to optimize the process, and hence, the properties of the processed materials.

- Proper roll speed and roll speed ratio: in literature, roll speed ratio is almost always set to either 1.5 or 2. The value of 1.5 was found by Kim and Lee [2001] to be the one originating the best shear deformation pattern along the sheet's thickness. This result was obtained using rolls having different diameters, rather than having different rotational speeds. The increase of roll diameter causes the decrease of the roll pressure, which does not benefit the formation of shear strains. This is how this result was explained by Kim and Lee. When using rolls having identical diameters, the increase of the roll speed ratio has no effect on roll pressure. In the current experiments, the roll speed ratio was set to 1.36. This value was chosen because it provided better rolling performance, avoiding the rolling mill to seize due to excessive demand of power on the upper roll (the one rotating with the higher velocity). Nevertheless, better results might be obtained if this parameter is increased up to 2.
- Small diameter rolls: using smaller diameter rolls increases roll pressure, and hence, benefits the task of imposing high amounts of shear strains over the sheet's thickness. Higher diameter rolls may cause an excess of compressive strains to superimpose to shear strains, causing the rolling process to approach the conventional rolling. It is possible to find in literature roll diameters ranging from 63mm to 248mm. The current experimental tests were performed using 180mm rolls, which may be excessive.
- Use high reductions per pass: the use of high values of thickness reduction per pass is of key importance in obtaining shear deformations along the sheet's thickness. Values around 50%- 60% were proven to originate the desired shear texture components in literature – see [Kim, Lee, 2001]. Current experiments show that only thickness reduction values of about 50% can originate high volume fractions of shear texture components, even if mainly at the sheet's surface. The spreading of these textures along the entire sheet thickness was not achieved, which indicates that other parameters are also decisive.

- High friction: asymmetrical rolling intends to impose high values of shear strains on the sheet, and hence the friction conditions are of essential importance when attempting to maximize those strains. The use of lubrication will cause friction to decrease, and shear strains to decrease as well. In literature, asymmetrical rolling experiments are generally performed with dry rolls, or even with additional materials to promote friction (alumina powder, see [Sakai et al, 2001]). The current asymmetrical rolling experiments were performed without any lubrication.
- Reversing rolling direction: the works by Kim [Kim, Lee, 2001] and Lee [Lee, Lee, 2001] on the asymmetrical rolling of aluminum alloy and steels have shown that it is important to have shear strain reversal on the sheet's surface, in order to generate shear texture components. In order to achieve such strain reversal, it is necessary to impose ND or RD reversing between each rolling pass. But the optimized conditions for taking advantage of this procedure are not clearly shown. The current experiments were performed with TD rolling reversal, which may have prevented the ideal shear texture components from developing correctly.

Chapter 6 - Conclusions and outlook

Aluminum alloys constitute valid alternative materials for applications involving formed parts. Yet, limitations regarding their strength / formability combination impose restrictions to their widespread use, even if their corrosion resistance and low density are important arguments. Attempts to improve formability are focused in several fields, mainly texture, alloying and grain size optimization. Texture optimization was attempted trough adequate thermo mechanical processing, but conventional procedures haven been shown to have important limitations, rendering insufficient performance. Alloying is already indispensable as the way to achieve proper strength, even if at the cost of some formability. Grain size optimization seems to be another way to provide strength, but once more formability must be taken into account when aiming at very low grain sizes. The present work intended to investigate the potential for an alternative rolling process, asymmetrical rolling, as a mean to produce specific texture components, namely, shear texture components, as well as grain refinement. These shear texture components are sought because they were said to provide very good formability in sheets. Conventional rolling followed by annealing heat treatments cannot produce these textures, but asymmetrical rolling, when properly set, can. Since high shear deformations are also imposed to the sheet, asymmetrical rolling can also be used to produce grain refinement.

The present work intended to perform asymmetrical rolling on an AA1050-O, attempting to optimize the sheet texture and grain size, and observe the corresponding effect on mechanical response. Results were evaluated trough tensile and shear tests, as well as texture analysis and TEM observations. Conclusions after this work are:

- Some of the desired shear texture components were obtained at the surface of asymmetrically rolled sheets, given the proper processing conditions. Their presence affects the material's mechanical response, as observed during tensile and shear tests. Asymmetrically rolled specimens annealed at 250^{o}C for 2 hours show about two times the yield stress relatively to the corresponding conventionally rolled specimens. Shear tests indicate a different trend, as conventionally rolled specimens present higher stress level relatively to asymmetrically rolled ones. Moreover, the strain hardening behavior is also

distinct. An explanation for this result is given based on the influence of individual texture components on tensile and shear solicitations.

- The processing parameters, and especially the thickness reduction between each pass, were shown to have an important influence on the results, especially in terms of crystallographic texture. Low values of this parameter prevent the formation of the desired shear texture components, rendering the process results nearly identical to conventional rolling. Nevertheless, speed ratio and friction must be taken into account, though their specific influence was not the object of the current work.
- The annealing treatments were chosen having the mechanical response, and an adequate strength / formability combination as the main objective. It can be observed that there seems to be a critical value for temperature below which the annealing process produces little results, even for high values of time. This can be observed for treatments performed at 200^{o}C for 2h and 4h, which produced similar, and unexpected results. Further studies should address annealing treatments in order to clarify these observations.
- Grain refinement was achieved down to levels similar to the ones observed in literature, but this doesn't seem to be the main parameter controlling the material's response. Rolled sheets present grain sizes of about 1-2μm, and limited grain growth was observed after annealing treatment at 250^{o}C – 5-7μm.

The results indicate that asymmetrical rolling has the potential to become an important tool to achieve significant improvement in mechanical properties of aluminum alloys. An optimization of process parameters is still necessary, and within this scope, some trends are suggested:

- It is necessary to impose large amounts of thickness reduction between each rolling pass, so a sufficient amount of power should be available on the rolling mill. This power only needs to available on one of the working rolls (the faster), since it will have to compensate the slower roll opposing torque.
- Smaller roll diameters should be studied. This will raise the roll pressure and hence it should promote the formation of shear strain along the entire sheet thickness. This variable should also be taken into account.
- The reversal of rolling direction should be optimized. As stated before, the ideal shear texture cannot be obtained by maintaining the rolling direction. It is necessary to further study the best procedure to reverse the rolling direction, in oder to achieve such texture. Conventional rolling followed by asymmetrical rolling should also be considered.
- Annealing heat treatments are of key importance when optimizing the strength/formability relation. After obtaining the desired shear texture components, and since these components tend to be retained over a wide range of annealing conditions, it will probably be possible to achieve a good solution for the proper annealing parameters.

Appendix A - Crystallographic Texture

A.1 Introduction

A crystal is characterized by the periodic arrangement of its elements (atoms, ions) in space. Because of this, there is a dependence of the crystal properties on the direction considered, which is called anisotropy. Metal alloys contain of many crystals of different size, shape and orientations. In general, the distribution of orientations of the individual crystals in the polycrystal, relatively to a generic macroscopic reference system, is called crystallographic texture. If the orientation distribution was random, i.e., if the total balance of orientations of individual crystals within a polycrystal was null, the material would have no preferred orientation. The material would be isotropic, as its response would not depend on the direction of solicitation. In most cases, though, there is a set of orientations that tend to prevail over others. In metals, this is usually the result of processing routes and / or thermal treatments. Those preferred orientations will cause the material to have anisotropic behavior, much like the individual crystal. Hence, texture is the main source of anisotropy in metals.

A.2 Texture representation

A.2.1 Crystal reference system and sample reference system

The term texture refers to the orientation distribution of crystals relatively to an exterior reference system. It is thus necessary to define such a coordinate system and then a set of parameters to describe the crystal orientation relatively to it. The most usual way to describe the orientation of the crystal reference system relatively to the sample reference system is to relate them by a set of three sequential rotations, named Euler angles. If the crystal reference system is labeled

x,y,z and the macroscopic (exterior) reference system is labeled X, Y, Z, then the sequence of three rotations by the Euler angles is defined as (Bunge convention – see [Kocks et al, 1998]):

- φ1 – rotation of the exterior reference system around the Z axis. The rotated reference system is now labeled X'Y'Z'.

- θ – rotation of the X'Y'Z' reference system around the X' axis. The resulting reference system is X''Y''Z''.

- φ2 - rotation of the X''Y''Z'' reference system around the Z'' axis. The resulting reference system is X'''Y'''Z''', which coincides with the crystal reference system x,y,z.

A better visualization of the rotation sequence is shown on Figure 66.

In practice, one usually refers to the exterior reference system as a set of macroscopic sample orientations. When working with rolled sheet metal samples, the reference system is the set

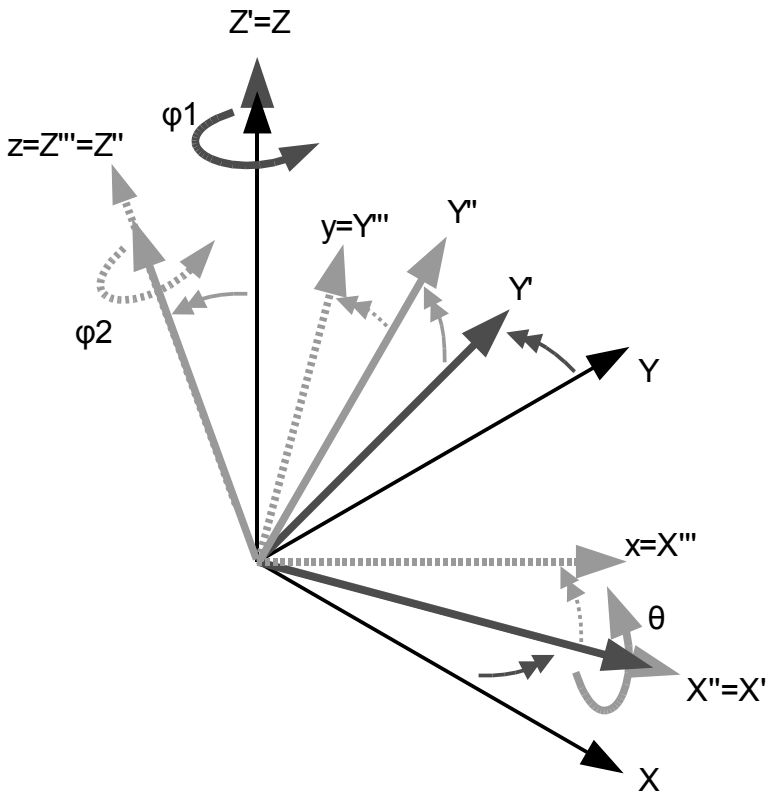

Figure 66: Definition of Euler angles φ1, θ, φ2.

of: Normal direction (ND), Transverse direction (TD), and Rolling direction (RD). Then, the crystal orientations are referred to the ND, TD, RD sample reference system.

On the other hand, the crystal reference system is usually described by lattice planes and directions, using integer indices. A direction is described by a vector:

$$r = u \cdot a + v \cdot b + w \cdot c \tag{20}$$

and denoted by [uvw]. A plane, or set of parallel lattice planes, is described by the following equation:

$$h\frac{x}{a} + k\frac{y}{b} + l\frac{z}{c} = 1 \tag{21}$$

where x, y and z are arbitrary coordinates of a point on the plane, and a,b,c are lengths of the base vectors of the unit cell. The h,k,l indices are called Miller indices of the plane. They represent the reciprocal multiples of the lattice axis (x,y,z) intercepts of the plane. Thus, a lattice plane is usually referred to by its Miller indices in parenthesis, (hkl).

Because of cubic crystal symmetry, it is possible to define families of symmetric planes or directions by a single set u,v,w or h,k,l indices. In the case of directions, one uses angular brackets $<>$ to describe a set of directions, and curly brackets {} to describe a set of planes. For instance, the notation $<100>$ refers to the set of directions $[100], [010], [001], [\bar{1}00], [0\bar{1}0], [00\bar{1}]$.

A.2.2 Orientations

Texture is the distribution of orientations of the set of grains which compose the sample. Usually, to describe the orientation of a crystal relatively to the macroscopic reference system, one uses the following notation:

$$\{hkl\}\langle uvw \rangle \tag{22}$$

which indicates that the sample has its (hkl) plane normal parallel to the Normal direction (ND), and its [uvw] direction parallel to the Rolling direction (RD). This notation is also used to describe slip systems, for instance, $\{111\}<110>$ in fcc metals. This means that slip will occur on (111) planes and along the [110] directions on those planes.

Given an orientation, one can relate the crystal reference system to the sample reference system by determining the set of Euler angles that transform the latter into the former. For instance, in the case of the “cube” texture, described as (100)[001], the crystal (100) plane normal is parallel to

the sample's normal direction (ND), and the crystal's [001] direction is parallel to the sample's rolling direction (RD).

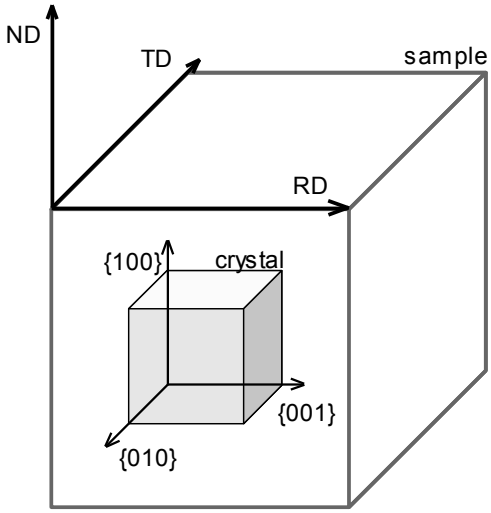

Figure 67: (100)[001] cube orientation.

In this case, the Euler angles describing the relation between the two reference systems would be $\varphi 1 = \theta = \varphi 2 = 0^o$, but given the symmetry of the cubic lattice, they could also be $(\varphi 1, \theta, \varphi 2) = (90^o, 0^o, 0^o)$ for instance, if [100] was parallel to TD, [010]//-RD and [001]//ND. There is a set of equivalent Euler angles for this orientation, as there is for many other orientations, as a result of cubic crystal symmetry. In general, the transformation from the crystal reference system to the sample reference system through three successive rotations by Euler angles can be translated by:

$$[C]=[g][S]$$

$$\begin{bmatrix}(100)\\(010)\\(001)\end{bmatrix}=\begin{bmatrix}\cos\varphi_1\cos\varphi_2-\sin\varphi_1\sin\varphi_2\cos\theta & \sin\varphi_1\cos\varphi_2+\cos\varphi_1\sin\varphi_2\cos\theta & \sin\varphi_2\sin\theta\\ -\cos\varphi_1\sin\varphi_2 & -\sin\varphi_1\sin\varphi_2+\cos\varphi_1\cos\varphi_2\cos\theta & \cos\varphi_2\sin\theta\\ \sin\varphi_1\sin\theta & -\cos\varphi_1\sin\theta & \cos\theta\end{bmatrix}\cdot\begin{bmatrix}RD\\TD\\ND\end{bmatrix}$$

Table 11 presents a list of common deformation and recrystallization textures found on fcc metals, and their respective Euler angles.

Type	Component	{hkl}<uvw>	Euler Angles (Bunge)		
			φ1	θ	φ2
Deformation	Bs (brass)	{011}<211>	35	45	0
	S	{123}<634>	55	35	65
	Cu (copper)	{112}<111>	90	30	45
	Shear1	{001}<110>	0	0	45
	Shear2	{111}<112>	90	55	45
	Shear3	{111}<110>	0	55	45
	Shear4	{112}<110>	0	35	45
Recrystallization	Goss	{011}<001>	0	45	0
	Cube	{001}<100>	0	0	0
	RCRD1	{013}<100>	0	20	0
	RCRD2	{023}<100>	0	35	0
	RCND1	{001}<310>	20	0	0
	RCND2	{001}<320>	35	0	0
	P	{011}<122>	70	45	0
	Q	{013}<231>	55	20	0
	R	{124}<211>	55	75	25

Table 11: Typical deformation and recrystallization texture components in fcc metals.

A.2.3 Stereographic projection. Pole figures

It is possible to represent a vector or direction as a point on the surface of a unit sphere. The first point of the vector coincides with the center of the sphere, and the second point will lie on the sphere's surface. A similar concept can be applied to a direction; in this case, there are two points where the line defining the direction intercepts the sphere.

If one positions a single crystal on the center of the sphere and draw a set of desired plane normals (for instance, the (100) normals), those lines will intercept the sphere and generate points at its surface. Those points can be located trough spherical coordinates, if a reference system is set previously. If the sphere reference system is set as the macroscopic reference system (RD, TD, ND), as seen previously, then one obtains the orientation of the crystal (of it's (100) plane normals in this case) relatively to the sample.

If instead of a single crystal one measures the orientation of a set of crystals, and find the points where their specific plane normals intercept the sphere, one can view the distribution of orientations of the crystals relatively to the sample reference system, and hence, its texture. Since a 3D representation of a sphere is difficult to interpret, there are methods to project the surface of the sphere onto a plane. Stereographic projection and equal-area projection are the two existing

methods. They allow points on the sphere surface to be represented on the plane, as well as measure angular distances between them. The definition of each type of projection is shown on Figure 68.

Stereographic projections are the base for the construction of pole figures. If one chooses to represent the location, or orientation of a set of specific plane normals, for instance, the {100} planes in a given number of grains, the stereographic projection of those locations relatively to the sample coordinate system would be a {100} pole figure. The location of these specific plane normals can be obtained trough X-ray diffraction using a goniometer. In this device, X rays are directed to the sample while it rotates and tilts. According to the x-ray detector setting, several plane normals can be set to diffract, thus detecting their orientation in space, as a function of the rotating and tilting angles. This is one of the most used methods for determining texture. Table 12 shows the {111} pole figures for the most important deformation and recrystallization texture components for aluminum, derived from the orientations described on Table 11.

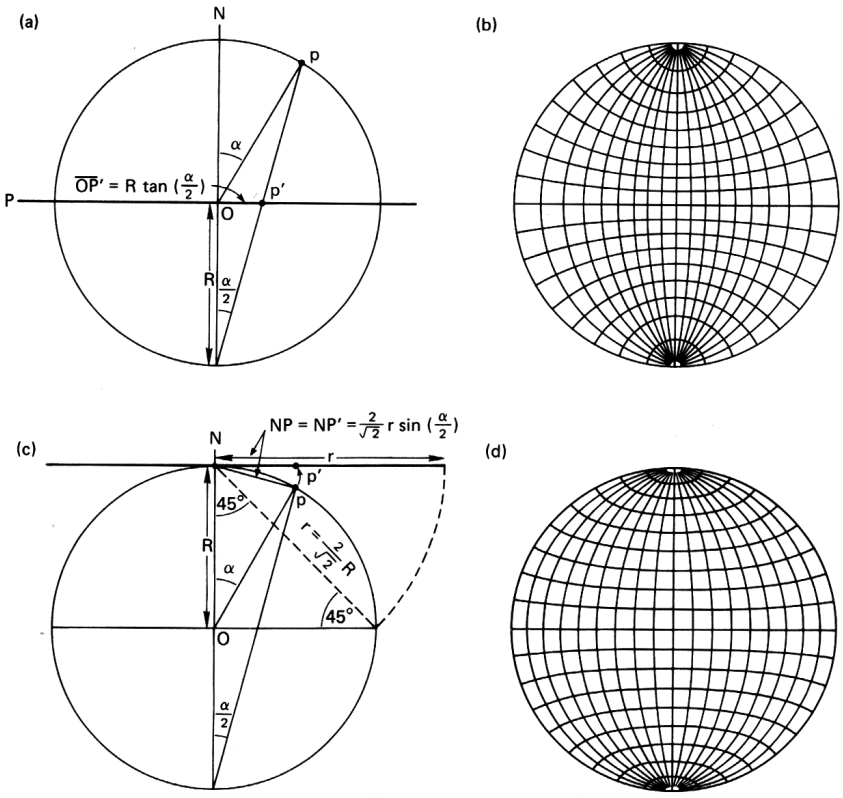

Figure 68: Stereographic (a) and (b) and equal-area projections(c) and (d).

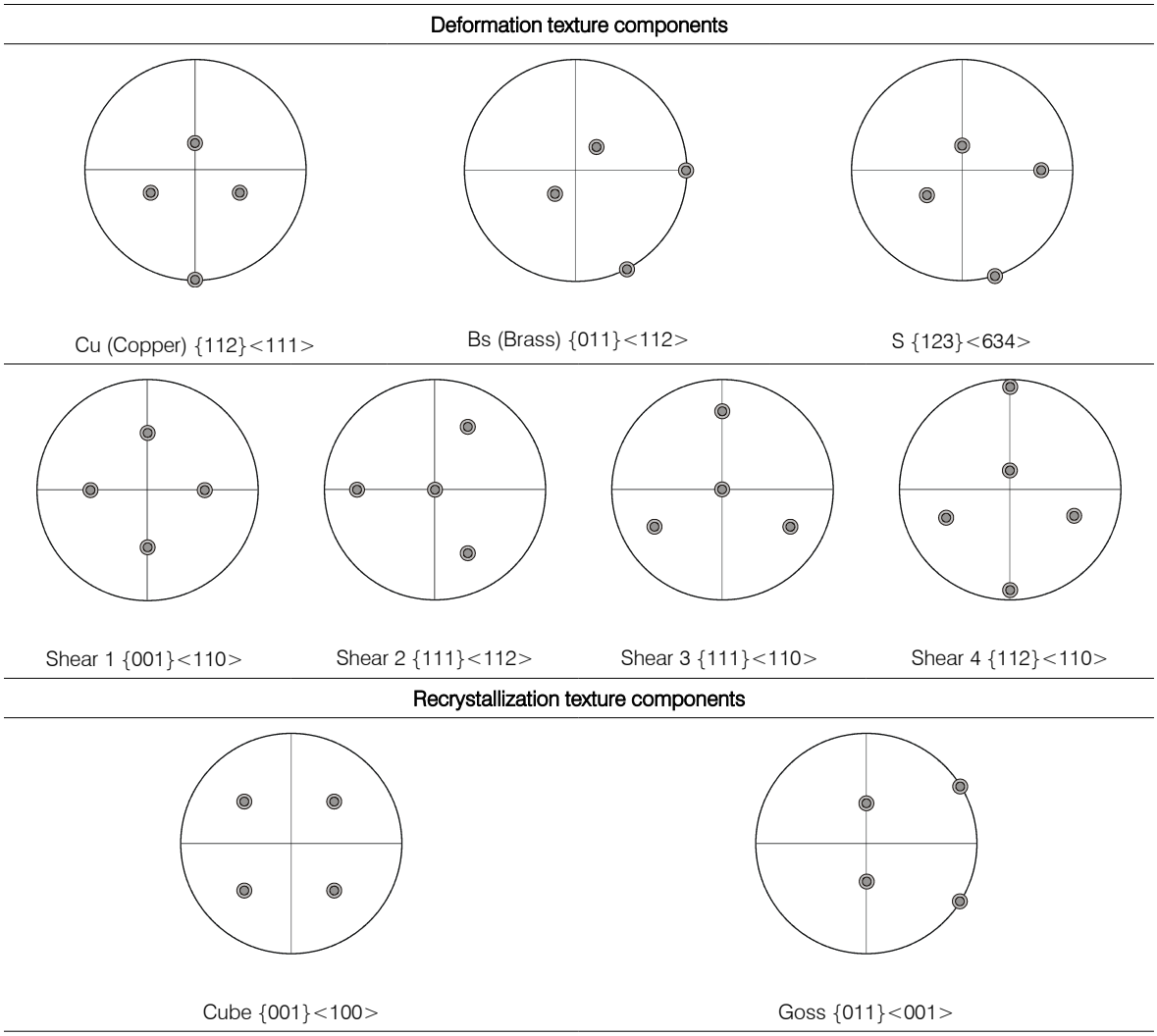

Table 12: {111} pole figures of the main deformation and recrystallization texture components of fcc metals.

A.2.4 Orientation distribution function (ODF)

Pole figures are determined by x-ray diffraction, and their output is the location of specific plane normals relatively to the sample reference system – hence there are {111}, {100}, {110} pole figures. However, pole figures alone do not describe the orientation of the crystal relatively to the sample reference system, since they only measure plane normals, and not directions on the plane.

Using the data from several pole figures, it is possible to determine the relative density or strength of a given orientation relatively to the random orientation distribution, which acts as the reference (random orientations is equivalent to no preferred orientation, and hence, *no texture*). This determination is performed by using spherical harmonics to describe the distribution function, whose

coefficients are then determined through pole figure data. The Orientation Distribution Function *f(g)* can be interpreted as the volume fraction of grains possessing a given orientation *g*:

$$\frac{dV(g)}{V} = f(g)\,dg \tag{23}$$

In order to represent this function, a 3D plot would be necessary, since it is a function of three angles, the Euler angles describing the orientation of the crystal. In order to overcome this difficulty, the ODF is usually represented by sections where one of the Euler angles is kept constant, usually φ2, and the other 2 are plotted on a cartesian frame. Since the ODF is calculated as a continuous function, each section displays areas or lines of equal volume fraction of grains. Typical texture components can be mapped onto an ODF, providing a quick way to identify them when analyzing a new ODF. Figure 69 shows two ODF sections with typical texture components identified. Figure 67 shows an example of an ODF for rolled and annealed AA1050.

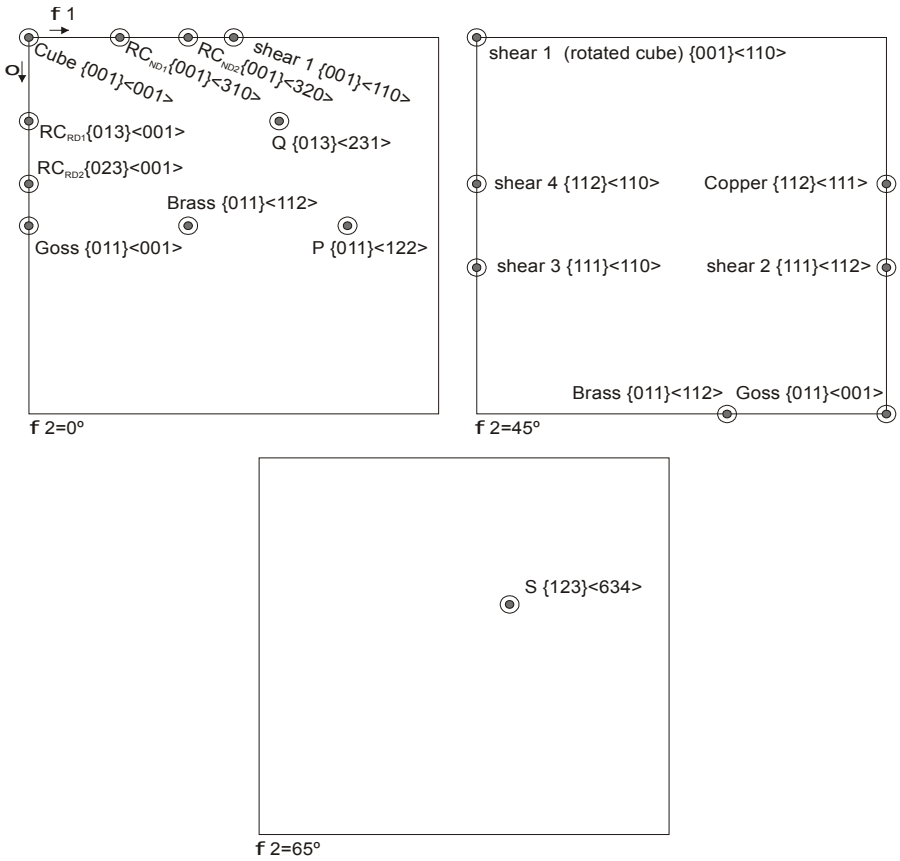

Figure 69: ODF sections showing typical rolling and annealing texture components for fcc metals.

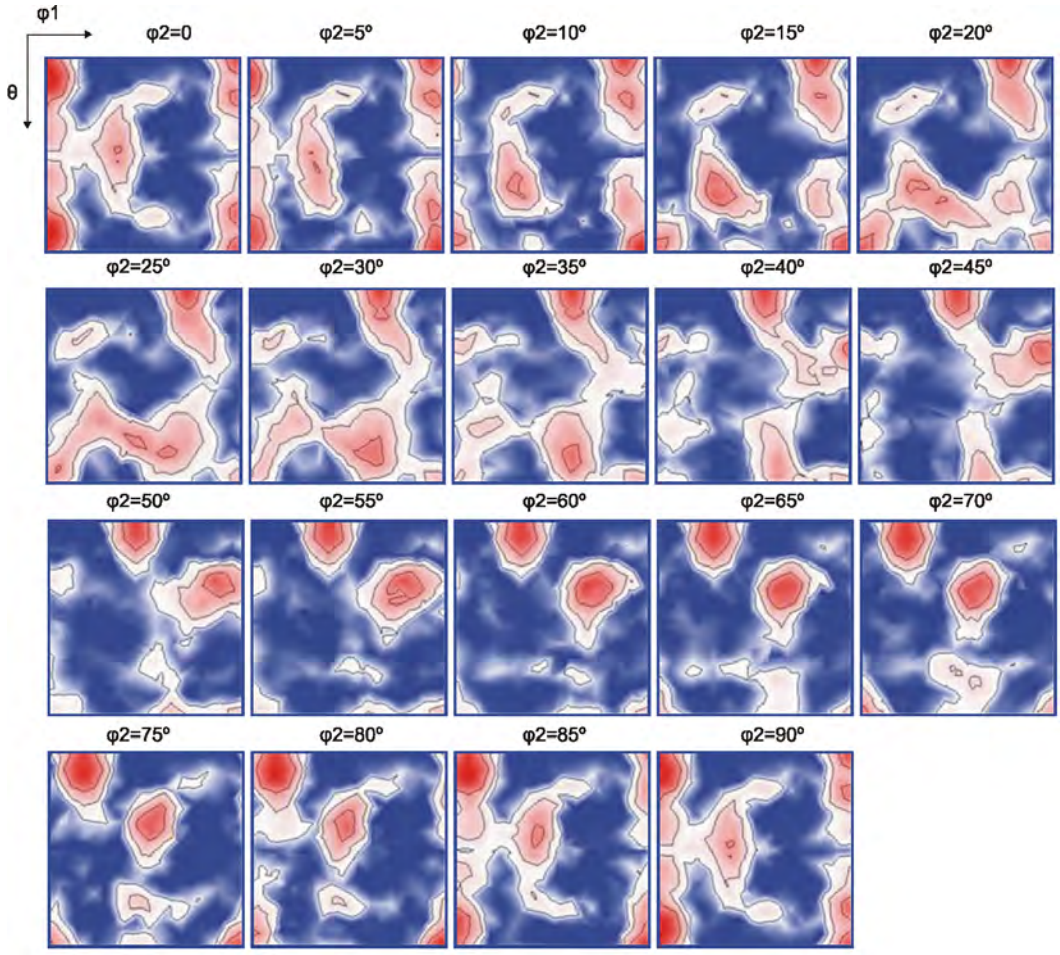

Figure 70: Example of an ODF for AA1050 after rolling and annealing.

Appendix B - Aluminum alloys

This Appendix presents the main groups of wrought aluminum alloys, it's classification according to the EA standards (EN573-1, EN515), as well as their reference mechanical properties (EN485-2).

A.3 Classification of wrought aluminum alloys

Each aluminum alloy is designated by a 4 digit number, which is followed by the temper designation – the state of the alloy, which affects its properties. The first digit indicates the group, or series, according to the major alloying element:

- **1xxx** Aluminum 99.0% minimum;
- **2xxx** Copper (1.9%~6.8%);
- **3xxx** Manganese (0.3%~1.5%);
- **4xxx** Silicon (3.6%.~13.5%);
- **5xxx** Magnesium (0.5%~5.5%);
- **6xxx** Magnesium and Silicon (Mg 0.4%~1.5%, Si 0.2%~1.7%);
- **7xxx** Zinc (1%~8.2%);
- **8xxx** Others.

The second digit indicates modification of the alloy or impurity limits. Original (basic) alloy is designated by “0” as the second digit. Numbers 1…9 indicate various alloy modifications with slight differences in the compositions. In the alloys of the 1xxx series the second digit indicates modifications in impurity limits: 0 means natural impurity limit; 1…9 indicate special control of one or more impurities or alloying element. The last two digits identify aluminum alloy or indicate the alloy purity. In the alloys of the 1xxx series the last two digits indicate the level of purity of the alloy:

- 1070 or 1170 mean minimum 99.70% of aluminum in the alloys;
- 1050 or 1250 mean 99.50% of aluminum in the alloys;
- 1100 or 1200 mean minimum 99.00% of aluminum in the alloys.

In all other groups of aluminum alloys (2xxx through 8xxx) the last two digits signify different alloys in the group. Table 13 presents the chemical composition limits of a typical set of wrought aluminum alloys.

A.4 Temper designations of aluminum alloys

Aluminum alloys can be divided in two groups: heat treatable and non-heat treatable. Alloys of groups 2, 4, 6 and 7 are said to be heat treatable, because they are able to produce precipitates when subjected to specific heat treatments. Alloys of groups 1, 3 and 5 cannot produce precipitates, and hence can only be strengthened by strain hardening.

The temper designation system adopted by the Aluminum Association and used in industry pertains to all forms of wrought and cast aluminum and aluminum alloys except ingot. It is based on the sequences of basic treatments used to produce the various tempers. The temper designation follows the alloy designation, being separated by a dash.

Basic temper designations consist of letters. Subdivisions of the basic tempers, where required, are indicated by one or more digits following the letter. These digits designate specific sequences of basic treatments, but only operations recognized as significantly influencing the characteristics of the product are indicated. Should some other variation of the same sequence of basic operations be applied to the same alloy, resulting in different characteristics, then additional digits are added.

The basic temper designations and subdivisions are as follows:

- F, as fabricated: Applies to products that acquire some temper from shaping processes not having special control over the amount of strain-hardening or thermal treatment. For wrought products, there are no mechanical property limits.
- O, annealed, recrystallized (wrought products only): Applies to the softest temper of wrought products.
- H, strain-hardened (wrought products only): Applies to products that have their strength increased by strain-hardening with or without supplementary thermal treatments to produce partial softening. The -H is always followed by two or more digits. The first digit indicates the specific combination of basic operations, as follows:

ALLOY GROUP	ALLOY DESIGNATION	CHEMICAL COMPOSITION LIMITS(WT%)										
		Cu	Si	Fe	Mn	Mg	Zn	Cr	Ti	Pb,Bi	Al	Others
1000	1050	0.05	0.25	0.4	0.5	0.05	0.05	-	-	-	99.50min	-
	1100	0.05~0.20	Si+Fe1.0max		0.05	-	0.1	-	-	-	99.00min	-
	2011	5.0~6.0	0.4	0.7	-	-	0.3	-	-	0.2~0.6,each	rem	-
2000	2014	3.9~5.0	0.5~1.2	0.7	0.4~1.2	0.2~0.8	0.25	0.1	0.15	-	rem	-
	2017	3.5~4.5	0.2~0.8	0.7	0.4~1.0	0.4~0.8	0.25	0.1	0.15	-	rem	-
	2024	3.8~4.9	0.5	0.5	0.3~0.9	1.2~1.8	0.25	0.1	0.15	-	rem	-
	2218	3.5~4.5	0.9	1	0.2	1.2~1.8	0.25	0.1	-	-	rem	Ni1.7~2.3
	2224	3.8~4.4	0.12	0.15	0.30~0.9	1.2~1.8	0.25	0.1	0.15	-	rem	-
3000	3003	0.05~0.20	0.6	0.7	1.0~1.5	-	0.1	-	-	-	rem	-
4000	4032	0.5~1.3	11.0~13.5	1	-	0.8~1.3	0.25	0.1	-	-	rem	Ni0.5~1.3
5000	5052	0.1	0.25	0.4	0.1	2.2~2.8	0.1	0.15~0.35	-	-	rem	-
	5056	0.1	0.3	0.4	0.05~0.20	4.5~5.6	0.1	0.05~0.20	-	-	rem	-
	5083	0.1	0.4	0.4	0.4~1.0	4.0~4.9	0.25	0.05~0.25	0.15	-	rem	-
	5086	0.1	0.4	0.5	0.20~0.7	3.5~4.5	0.25	0.05~0.25	0.15	-	rem	-
6000	6061	0.15~0.40	0.4~0.8	0.7	0.15	0.8~1.2	0.25	0.04~0.35	0.15	-	rem	-
	6063	0.1	0.2~0.6	0.35	0.1	0.45~0.9	0.1	0.1	0.1	-	rem	-
	6070	0.15~0.40	1.0~1.7	0.5	0.40~1.0	0.50~1.2	0.25	0.1	0.15	-	rem	-
	6151	0.35	0.6~1.2	1	0.2	0.45~0.8	0.25	0.15~0.35	0.15	-	rem	-
	6262	0.15~0.40	0.4~0.8	0.7	0.15	0.8~1.2	0.25	0.04~0.14	0.15	0.40~0.7,each	rem	-
	6351	0.1	0.7~1.3	0.5	0.4~0.8	0.40~0.8	0.2	-	0.2	-	rem	-
	6463	0.2	0.20~0.6	0.15	0.05	0.45~0.9	0.05	-	-	-	rem	-
7000	7001	1.6~2.6	0.35	0.4	0.2	2.6~3.4	6.8~8.0	0.18~0.35	0.2	-	rem	-
	7003	0.2	0.3	0.35	0.3	0.50~1.0	5.0~6.5	0.2	0.2	-	rem	Zr0.05~0.25
	7050	2.0~2.6	0.12	0.15	0.1	1.9~2.6	5.7~6.7	0.04	0.06	-	rem	Zr0.08~0.15
	7075	1.2~2.0	0.4	0.5	0.3	2.1~2.9	5.1~6.1	0.18~0.28	0.2	-	rem	-
	7178	1.6~2.4	0.4	0.5	0.3	2.4~3.1	6.3~7.3	0.18~0.35	0.2	-	rem	-
	7475	1.2~1.9	0.1	0.12	0.06	1.9~2.6	5.2~6.2	0.18~0.25	0.06	-	rem	-
8000	8090	2.4~3.0	1.1	0.12	0.05	0.25	0.1	0.05	0.15	Zr0.08~0.15	rem	Li1.9~2.6

Table 13: Chemical composition limits for typical wrought aluminum alloys.

- H1, strain-hardened only: Applies to products that are strain-hardened to obtain the desired mechanical properties without supplementary thermal treatment. The number following this designation indicates the degree of strain-hardening.
- H2, strain-hardened and then partially annealed: Applies to products that are strain-hardened more than the desired final amount and then reduced in strength to the desired level by partial annealing. For alloys that age-soften at room temperature, the -H2 tempers have approximately the same ultimate strength as the corresponding -H3 tempers. For other alloys, the -H2 tempers have approximately the same ultimate strengths as the corresponding -H1 tempers and slightly higher elongations.The number following this designation indicates the degree of strain-hardening remaining after the product has been partially annealed.
- H3, strain-hardened and then stabilized: Applies to products which are strain-hardened and then stabilized by a low-temperature heating to slightly lower their strength and increase ductility. This designation applies only to the magnesium-containing alloys that, unless stabilized, gradually age-soften at room temperature. The number following this designation indicates the degree of strain-hardening remaining after the product has been strain-hardened a specific amount and then stabilized.
  - The second digit following the designations -H1, -H2, and -H3 indicates the final degree of strain-hardening. Numeral 8 has been assigned to indicate tempers having a final degree of strain-hardening equivalent to that resulting from approximately 75 per cent reduction of area. Tempers between -O (annealed) and 8 (full hard) are designated by numerals 1 through 7. A material having an ultimate strength about midway between that of the -O temper and that of the 8 temper is designated by the numeral 4 (half hard); between -O and 4 by the numeral 2 (quarter hard); and between 4 and 8 by the numeral 6 (three-quarter hard). (Note: For two-digit -H tempers whose second figure is odd, the standard limits for ultimate strength are exactly midway between those for the adjacent two-digit -H tempers whose second figures are even.) Numeral 9 designates extra-hard tempers.
  - The third digit, when used, indicates a variation of a two-digit -H temper, and is used when the degree of control of temper or the mechanical properties are different from but close to those for the two-digit -H temper designation to which it is added. (Note: The minimum ultimate strength of a three-digit -H temper is at least as close to that of the corresponding two-digit -H temper as it is to the adjacent two-digit -H tempers.) Numerals 1 through 9 may be arbitrarily assigned and registered with the Aluminum Association for an alloy and product to indicate a specific degree of control of temper or specific mechanical property limits. Zero has been assigned to indicate degrees of control of temper or mechanical property limits negotiated between the manufacturer and purchaser that are not used widely enough to justify registration with the Aluminum Association.

- The following three-digit -H temper designations have been assigned for wrought products in all alloys:
  - H111: Applies to products that are strain-hardened less than the amount required for a controlled H11 temper.
  - H112: Applies to products that acquire some temper from shaping processes not having special control over the amount of strain-hardening or thermal treatment, but for which there are mechanical property limits, or mechanical property testing is required.
- The following three-digit H temper designations have been assigned for wrought products in alloys containing more than a normal 4 per cent magnesium.
  - H311: Applies to products that are strain-hardened less than the amount required for a controlled H31 temper.
  - H321: Applies to products that are strain-hardened less than the amount required for a controlled H32 temper.
  - H323: Applies to products that are specially fabricated to have acceptable resistance to stress-corrosion cracking.
  - H343: Applies to products that are specially fabricated to have acceptable resistance to stress-corrosion cracking.

- W, solution heat-treated: An unstable temper applicable only to alloys that spontaneously age at room temperature after solution heat treatment. This designation is specific only when the period of natural aging is indicated.
- T, thermally treated to produce stable tempers other than -F, -O, or -H: Applies to products that are thermally treated, with or without supplementary strain-hardening, to produce stable tempers. The -T is always followed by one or more digits. Numerals 2 through 10 have been assigned to indicate specific sequences of basic treatments, as follows:
- T1, naturally aged to a substantially stable condition: Applies to products for which the rate of cooling from an elevated temperature-shaping process, such as casting or extrusion, is such that their strength is increased by room-temperature aging.
- T2, annealed (cast products only): Designates a type of annealing treatment used to improve ductility and increase dimensional stability of castings.
- T3, solution heat-treated and then cold-worked: Applies to products that are cold-worked to improve strength, or in which the effect of cold work in flattening or straightening is recognized in applicable specifications.
- T4, solution heat-treated and naturally aged to a substantially stable condition: Applies to products that are not cold-worked after solution heat treatment, or in which the effect of cold work in flattening or straightening may not be recognized in applicable specifications.

- T5, artificially aged only: Applies to products that are artificially aged after an elevated-temperature rapid-cool fabrication process, such as casting or extrusion, to improve mechanical properties or dimensional stability, or both.
- T6, solution heat-treated and then artificially aged: Applies to products that are not cold-worked after solution heat-treatment, or in which the effect of cold work in flattening or straightening may not be recognized in applicable specifications.
- T7, solution heat-treated and then stabilized: Applies to products that are stabilized to carry them beyond the point of maximum hardness, providing control of growth or residual stress or both.
- T8, solution heat-treated, cold-worked, and then artificially aged: Applies to products that are cold-worked to improve strength, or in which the effect of cold work in flattening or straightening is recognized in applicable specifications.
- T9, solution heat-treated, artificially aged, and then cold-worked: Applies to products that are cold-worked to improve strength.
- T10, artificially aged and then cold-worked: Applies to products that are artificially aged after an elevated-temperature rapid-cool fabrication process, such as casting or extrusion, and then cold-worked to improve strength.

Additional digits may be added to designations -T1 through -T10 to indicate a variation in treatment that significantly alters the characteristics of the product. These may be arbitrarily assigned and registered with The Aluminum Association for an alloy and product to indicate a specific treatment or specific mechanical property limits. These additional digits have been assigned for wrought products in all alloys:

- T__51, stress-relieved by stretching: Applies to products that are stress-relieved by stretching the following amounts after solution heat-treatment:
- Plate - 1.5 to 3% permanent set.
- Rod, Bar and Shapes - 1 to 3% permanent set.
- Drawn tube - 0.5 to 3% permanent set.

Applies directly to plate and rolled or cold-finished rod and bar. These products receive no further straightening after stretching. Applies to extruded rod and bar shapes and tube when designated as follows:

- T__510 : Products that receive no further straightening after stretching.
- T__511: Products that receive minor straightening after stretching to comply with standard tolerances.
- T__52, stress-relieved by compressing: Applies to products that are stress-relieved by compressing after solution heat-treatment, to produce a nominal permanent set of 2½ per cent.

- __54, stress-relieved by combined stretching and compressing: applies to die forgings that are stress relieved by re striking cold in the finish die.

The following two-digit -T temper designations have been assigned for wrought products in all alloys:

- T42: Applies to products solution heat-treated and naturally aged that attain mechanical properties different from those of the -T4 temper.
- T62: Applies to products solution heat-treated and artificially aged that attain mechanical properties different from those of the -T6 temper.

Table 14 presents a list of aluminum alloys and their mechanical properties, as a general indication. Typical applications are also shown.

ALLOY GROUP	ALLOY DESIGNATION	TYPICAL TEMPER	MECHANICAL PROPERTIES UTS (MPa)	YTS (MPa)	ELONGATION (%)	DENSITY (g/cm3)	TYPICAL APPLICATIONS
1000	1050	H14	108	98	10	2.71	Chemical equipment Sheet metal work Coiled tube
	1100	H14	108	98	1~10	2.7	
2000	2011	T3	372	294	15	2.83	Screw machine products Truck frame Aircraft structure jet engine impellers Aircraft engine cylinder heads
	2014	T6	470	412	13	2.8	
	2017	T4	421	274	13	2.79	
	2024	T4	480	363	10	2.78	
	2218	T72	333	255	11	2.8	
	2224		0	0			
3000	3003	H14	147	137	6~16	2.73	Cooking utensils, Chemical equipment
4000	4032	T6	372	314	9	2.68	Pistons
5000	5052	H14 H34	255	206	10	2.68	Architectural Cable Sheating Welded pressure vessels Hydraulic tubes Transportation equipment
	5056	H12 H32	304	147	35	2.64	
	5083	H112	304	186	16	2.66	
	5086	H32 H116	284	206	12	2.66	
6000	6061	T6	304	274	12	2.7	Heavy duty stucture Furniture Architectural Heavy duty welded stucture Pipeline Heat Sink
	6063	T5	186	137	22	2.71	
	6070	T6	314	167	20	2.7	
	6151	T6	304	255	14	2.71	
	6262	T9	392	372	10	2.71	
	6351	T6	304	274	14	2.69	
	6463	T6	235	206	12		
7000	7001	O	676	147	14	2.84	High strength stucture Aircraft structure Bat
	7003	T5	314	255	15		
	7050	T73	460	412	8	2.83	
	7075	T6	539	480	6	2.8	
	7178	T6	608	539	11	2.83	
	7475	T61	549	510	12	2.8	
8000	8090	T8	568	529	7	2.59	

Table 14: Mechanical properties and typical applications of some aluminum alloys.

Appendix C - Testing equipment

A.5 Rolling machine

The rolling machine used in this work was developed at the Centre for Mechanical Engineering and Automation - TEMA - of the University of Aveiro - Figure 71. It has two motors, each one attached to a continuous speed variator, thus allowing to set the rotation speed of each roll separately. Additionally, the speed setting is computer controlled trough software also developed at TEMA. The system is able to maintain the required speed by means of a closed-loop control system. The rolls have both 90mm radius and 300mm length. The power of the motors is 2,2kW (each). The rotation speed can be set between 0 and 15r.p.m., and the rotation direction can be reversed.

A.6 Tensile test machine

The tensile test machine was used to perform standard tensile tests and also shear tests, by means of a special testing apparatus. It is manufactured by Shimadzu®, and it has a maximum loading capacity of 50kN. An clip-on extensometer (manufactured by MF®) having variable reference length from 25mm to 100mm was used to evaluate strain, in both tensile and shear tests. The shear test apparatus was built at TEMA, and it allows to perform shear tests of specimens up to 60mm in length and 3mm in thickness - Figure 72.

A.7 Furnace

The furnace used on the annealing treatments is manufactured by Termolab®. It is equipped with a temperature controller and a thermocouple. It has ceramic walls and no convection capability. The approximate dimensions of the chamber are 250x250x500mm.

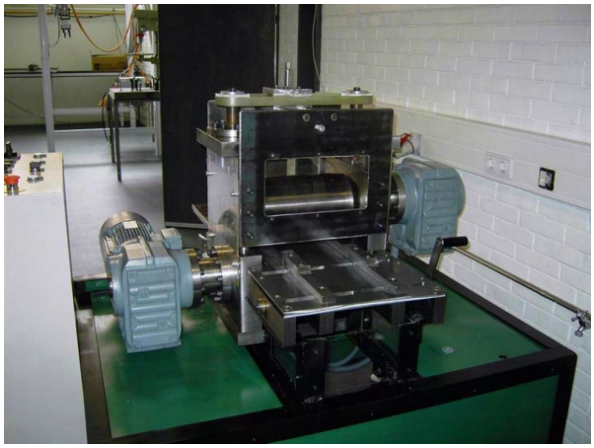

Figure 71: Rolling machine used in the experiments.

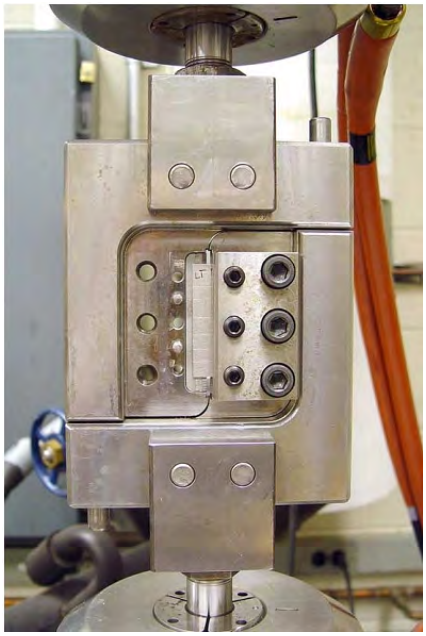

Figure 72: Shear testing apparatus. The assembly is mounted on the tensile test machine.

References

[alumatter, 2007] European Aluminum Association, MATTER – University of Liverpool – AluMATTER, > Processing > Rolling. webpage: http://www.aluminium.matter.org.uk/content/html/eng/default.asp?catid=30&pageid=1006172110

[alumatter, 2007-2] European Aluminum Association, MATTER – University of Liverpool – AluMATTER, Applications > Packaging > Beverage Cans. Webpage: http://www.aluminium.matter.org.uk/content/html/eng/default.asp?catid=84&pageid=-1941055071

[Alves de Sousa, 2006] Alves de Sousa, R. J., PhD Thesis, University of Aveiro.

[Avitzur, 1964] Avitzur, B., *An Upper Bound Approach to Cold Strip Rolling*, J of Eng. for Ind., Trans. ASME, Series B, 86, p31.

[Avitzur, 1983] Avitzur, B., *Handbook of Metal-Forming Processes,* ISBN 0-471-03474-6, Wiley-Interscience Publication, New York, 1983.

[Bacroix *et al*, 2001] Bacroix, B. Chauveau, Th., Ferreira Duarte, J.M.,Barata da Rocha, A., Gracio, J.J., *The respective influences of grain size and texture on the formability of a 1050 aluminium alloy*, International Journal of Engineering Science 37, pp509-526.

[Barlat, 1987] Barlat, F., *Crystallographic texture, anisotropic yield surfaces and forming limits of sheet metals,* Materials Science and Engineering, 91, pp55-72.

[Campos *et al*, 2006] Campos, H.B., Butuc, M. C. Grácio, J. J., Rocha, J. E., Ferreira Duarte, J. M.,*Theorical and experimental determination of the forming limit diagram for*

the AISI 304 stainless steel, Journal of Materials Processing Technology 179, pp55-60.

[Choi *et* al, 1998] Choi, C.-H., Kim, K.-H. and Lee, D. N., *The effect of shear texture development on the formability in rolled aluminum alloy sheets*, Materials Science Forum, 273-275, pp391-396.

[Choi *et al*, 2000] Choi, S. -H., Brem, J. C., Barlat, F, Oh, K. H., *Macroscopic anisotropy in AA5019A sheets*, Acta Materialia 48, pp1853-1863.

[Cui, Ohori, 2000] Cui Q., Ohori K., *Grain refinement of high purity aluminium by asymmetric rolling*, Materials Science and Technology vol. 16, nº10, pp1095-1101.

[Duarte, 1997] Ferreira Duarte, J.M., *Conformacão Plástica de Chapas Metálicas: Simulacão Numérica e Caracterizacão Mecânica*, PhD thesis, Faculty of Engineering of the University of Porto, Mechanical Engineering Department.

[Engler *et al*, 2001] Engler O., Kim H.C., Huh M.Y., *Formation of {111} fibre texture in recrystallised aluminium sheet*, Materials Science and Technology, Volume 17, Nº1, pp75-86.

[Engler, 2007] Engler O, Hirscha J, *Polycrystal-plasticity simulation of six and eight ears in deep-drawn aluminum cups*, Materials Science and Engineering: A, Volumes 452-453, pp640-651.

[Erb, 1995] Erb, U, *Electrodeposited nanocrystals: synthesis, processes and industrial applications*, Nanostructured Materials, 6, pp533-538.

[García de Lomana *et al*, 2004] García de Lomana, M., Rodríguez, A., Tamayo, J., Zubillaga, C., García-Rosales, C., Gil Sevillano, J., *Modificación de las texturas e de los índices de embutibilidad de chapas de aleaciones de aluminio Al 1050 y Al-Mg 5754 mediante laminación asimétrica*, Boletin de la Sociedad Española de Cerámica e Vidrio 43, 2, pp175-178.

[Gleiter, 1989] Gleiter, H., *Nanocrystalline materials*, Progress in Materials Science 33, 4, pp223-315.

[Goodwin, 1968] Goodwin, G.M., *Application of strain analysis to sheet metal forming problems in press shop*, SAE Paper No. 680093.

[Gracio et al, 2004] Gracio, J. J. Barlat, F., Rauch, E. F., Jones, P. T., Neto, V. F., Lopes, A. B., *Artificial aging and shear deformation behaviour of 6022 aluminium alloy,* International Journal of Plasticity Volume 20, Issue 3, pp427-445.

[Hähner, 1997] Hähner, P., *On the critical conditions of the Portevin – Le Châtelier effect*, Acta Materialia 45, 9, pp3695-3707.

[Hall, 1951] Hall, E.O., Proc. Phys. Sot. London, 1951, pp643-747.

[Hong, Lee, 2002] Hong, S.-H., Lee, D.N., *Recrystallization Textures in Cold-Rolled Ti Bearing IF Steel Sheets*, ISIJ International, Vol. 42, No. 11, pp1278–1287.

[Hu *et al*, 1998] Hu, J, Ikeda, K, Murakami, T., *Effect of texture components on the plastic anisotropy and formability of aluminium alloy sheets*, Journal of Materials Processing Technology 73, pp49-56.

[Hughes, Hansen, 1997] Hughes, D. A., Hansen, N, *High angle boundaries formed by grain subdivision mechanisms*, Acta Materialia 45, 9, pp3871-3886.

[Humphreys *et al*, 1999] Humphreys, F.J., Prangnell, P.B., Bowen, J.R., Gholinia, A., Harris, C., *Developing stable fine-grain microstructures by large strain deformation*, Philosophical Transactions A 357, pp1663-1681.

[Hwang, 1997] Hwang, Y-M, Tzou, G-Y, *Analytical and Experimental study of Asymmetrical sheet rolling,* International Journal of Mechanical Sciences 39, 3, p289.7

[Jin, Lloyd, 2004a] Jin H., Lloyd D. J., *The tensile response of a fine-grained AA5754 alloy produced by asymmetric rolling and annealing*, Metallurgical and Materials Transactions A, Vol. 35, n^{o} 3, pp997-1006.

[Jin, Lloyd, 2004b] Jin H., Lloyd D. J., *Effect of a duplex grain size on the tensile ductility of an ultra-fine grained Al–Mg alloy, AA5754, produced by asymmetric rolling and annealing*, Scripta Materialia 50, pp319–1323.

[Jin, Lloyd, 2005] Jin, H., Lloyd, D.J, *The reduction of planar anisotropy by texture modification through asymmetric rolling and annealing in AA5754,* Materials Science and Engineering A 399, Issues 1-2, pp358-367.

[Johnson, 1966] Johnson W, Needham G. *An experimental study of asymmetrical rolling,* Applied Mechanics Convention, Cambridge, UK. Institution of Mechanical Engineering 1966.

[Keller, Backofen, 1964] Keeler, S.P., Backofen, W.A *Plastic instability and fracture in sheets stretched over rigid punches*, ASM Trans. Quart. 56 p25.

[Kim, Lee, 1999] Kim, K.-H. and Lee, D. N., *The deformation textures and lankford values of asymmetrically rolled aluminum alloy sheets*, Proceedings of the 12th ICOTOM (edited. by J.A. Szpunar), NRC-CNRC, Canada, pp755-760.

[Kim, Lee, 2001] Kim, K.-H. and Lee, D. N, *Analysis of Deformation Textures of Asymmetrically Rolled Aluminum Sheets*, Acta Materialia. 49, pp2583–2595.

[Kim *et* al, 2002] Kim, S.-H., Ryu, J.-H., Kim, K.-H., Lee, D.N., *The evolution of deformation texture and grain refinement in asymmetrically rolled aluminum sheets*, Materials Science Research International., vol 8, n°1, pp20-25.

[Knight *et al*, 2003] Knight, C. W. Hardy, S. J., Lees, A.W., Brown, k. J., *Investigations into the influence of asymmetric factors and rolling parameters on strip curvature during hot rolling*, Journal of Materials Processing Technology 134, pp180-189.

[Kocks *et al*, 1998] Kocks, U.F., Tomé, C.N., Wenk, H.-R., *Texture and Anisotropy*, Cambridge University Press, 1998, ISBN 0 521 46516 8.

[Krieger-Lassen *et al* 1992] Krieger-Lassen, N.C., Juul Jensen, D., Conradsen, X., *Image processing procedures for analysis of electron back-scattering patterns,* Scanning Microscopy 6, pp115–121.

[Lee, Lee, 2001] Lee, S. H., Lee, D. N., *Analysis of deformation textures of asymmetrically rolled steel sheets*, International Journal of Mechanical Sciences 43, pp1997–2015.

[Lee, Kim, 2001] Lee, D.N., Kim, K.-H., *Effects of asymmetric rolling parameters on texture development in aluminum sheets,* in "Innovations in processing and manufacturing of sheet materials", edited by Demeri, MY, Warrendale, PA, TMS (The Minerals, Metals & Materials Society), pp 219–235.

[Li, Ghosh, 2003] Li, D, Ghosh, K, *Tensile deformation behavior of aluminum alloys at warm forming temperatures*, Materials Science and Engineering A 352, p279-286.

[Li, Ghosh, 2004] Li, D, Ghosh, K, *Biaxial warm forming behavior of aluminum sheet alloys*, Journal of Materials Processing Technology 145, 3, p281-293.

[Lopes *et al*, 2003] Lopes, A. B., Barlat, F., Gracio, J. J., Ferreira Duarte, J. F., Rauch, E. F., *Effect of texture and microstructure on strain hardening anisotropy for aluminum deformed in uniaxial tension and simple shear*, International Journal of Plasticity 19, 1, pp1-22.

[Mahmudi, 1996] Mahmudi, R., *Post-uniform deformation in uniaxial and equi-biaxial stretching of aluminium alloy sheets*, Journal of Materials Processing Technology 70, pp93-98.

[Miao, Laughlin, 1999] Miao,W.F. Laughlin, D.E., *Precipitation hardening in aluminum alloy 6022*, Scripta Materialia 40, pp873–878.

[Orowan, 1943] Orowan E., *The calculation of roll pressure in hot and cold flat rolling,* Proceeding of Institution of Mechanical Engineers, London,150(4), p140.

[Petch, 1953] Petch, N.J., J. Iron Steel Inst. London, 174, 1953, pp25.

[Picu *et a*l, 2005] Picu, R.C., Vincze, G., Ozturk, F., Gracio, J.J., Barlat, F, Maniatty, A.M., *Strain rate sensitivity of the commercial aluminum alloy AA5182-O*, Materials Science and Engineering A 390, pp334–343.

[Picu *et al*, 2006] Picu, R.C., Vincze, G., Gracio,J.J., Barlat, F., *Effect of solute distribution on the strain rate sensitivity of solid solutions*, Scripta Materialia 54, pp 71–75.

[Preston, 1938] Preston G. D., *The Diffraction of X-Rays by Age-Hardening Aluminium Copper Alloys,* Proceedings of the Royal Society of London. Series A, Mathematical and Physical Sciences (1934-1990), Volume 167, Number 931, pp526-538.

[Richelsen, 1994] Richelsen, A.B., *Numerical analysis of asymmetric rolling accounting for difference in friction,* Journal of Materials Processing Technology 45, p149.

[Richelsen, 1997] Richelsen, A.B., *Elastic–Plastic analysis of the stress and strain distributions in asymmetric rolling,* International Journal of Mechanical Sciences 39, p1199.

[Sachs, 1947] Sachs G, Klingler L.J., *The flow of metals through tools of circular contour,* Journal of Applied Mechanics 14, p88.

[Sakai *et al*, 2001] Sakai, T, Hamada, S, Saito, Y, *Improvement of the r-value in 5052 aluminum alloy sheets having trough-thickness shear texture by 2-pass single-roll drive unidirectional shear rolling*, Scripta materialia. 44, pp2569–2573.

[Salimi, 2002] Salimi, M., Sassani, F., *Modified slab analysis of asymmetrical plate rolling*, International Journal of Mechanical Sciences 44, p1999.

[Segal, 1995] Segal, V.M., *Materials processing by simple shear*, Materials Science and Engineering A, 197, pp157-164.

[Siebel, 1941] Siebel E. *Zur theories des walzvoganges bei ungleich angetriebenen walzen,* Archiv fur das Eisenhuettenwesen 15, p125.

[Shi, Meuleman, 1992] Shi, F. Ming, Meuleman, David J., *Strain rate sensitivity of automotive steels*, SAE paper nº920245.

[Valiev *et al*, 1997] Valiev, R. Z., Salimonenko, D.A., Tsenev, N. K., Berbon, P. B., Langdon, T. G., *Observations of high strain rate superplasticity in commercial aluminum alloys whith ultrafine grain sizes,* Scripta Materialia 37, pp1945-1950.

[Valiev, Langdon, 2006] Valiev, R.Z., Langdon, T.G., *Principles of equal-channel angular pressing as a processing tool for grain refinement*, Progress in Materials Science 51, pp881–981.

[Von Karman, 1925] von Karman, T., *Beitrag zur Theorie des Walzvorganges*, ZAMM, 1925.

Yoon et al [2005] Yoon, J.W., Barlat, F., Gracio, JJ, Rauch, E., *Anisotropic strain hardening behavior in simple shear for cube textured aluminum alloy sheets*, International Journal of Plasticity 21, pp2426–2447.

[Youngdahl et al, 1997]. Youngdahl, Carl J., Sanders, Paul G., Eastman, Jeffrey A., Weertman, Julia R., *Compressive yield strengths of nanocrystalline Cu and Pd,* Scripta Materialia, 37, 6, pp809-813.

[Wang, 2004] Wang, Y.M., Ma, E., *Strain hardening, strain rate sensitivity, and ductility of nanostructured metals*, Materials Science and Engineering A 375–377, pp46–52.